
Electronic Thesis and Dissertation Repository

8-16-2017 12:00 AM

Electrospun collagen nanofibers for tissue engineering

Nisha Sharma

The University of Western Ontario

Supervisor

Dr. Wankie Wan

The University of Western Ontario Joint Supervisor

Dr. Derek Boughner

The University of Western Ontario

Graduate Program in Biomedical Engineering

A thesis submitted in partial fulfillment of the requirements for the degree in Doctor of Philosophy

© Nisha Sharma 2017

Follow this and additional works at: <https://ir.lib.uwo.ca/etd>



Part of the [Amino Acids, Peptides, and Proteins Commons](#), [Medical Biochemistry Commons](#), [Medical Biophysics Commons](#), [Medical Biotechnology Commons](#), [Nanomedicine Commons](#), and the [Other Medical Sciences Commons](#)

Recommended Citation

Sharma, Nisha, "Electrospun collagen nanofibers for tissue engineering" (2017). *Electronic Thesis and Dissertation Repository*. 5044.

<https://ir.lib.uwo.ca/etd/5044>

This Dissertation/Thesis is brought to you for free and open access by Scholarship@Western. It has been accepted for inclusion in Electronic Thesis and Dissertation Repository by an authorized administrator of Scholarship@Western. For more information, please contact wlsadmin@uwo.ca.

Abstract

Design and fabrication of the scaffold is an important part of the tissue engineering process. Nanofibrous scaffolds based on proteins are gaining increasing acceptance due to its structural similarity to the extracellular matrix. Making use of the electrospinning technique, rat tail collagen type I nanofibers were produced using a collagen in hexafluoroisopropanol (HFIP) solution. In addition to optimizing the electrospinning process parameters, the effect of humidity on fiber morphology and diameter was investigated for fiber size control for particular tissue engineering applications. A generalized humidity effect on polymer fiber diameter of the polymer solution electrospinning process was developed. The as spun collagen type I fibers were unstable in aqueous solutions. To impart stability these fibers, the technique of ion implantation was used. Both helium (He^+) and nitrogen (N^+) ions were used. Polychromatic ion beam of energies of 0 – 100 MeV (He^+) and 0 – 300 MeV (N^+) with doses varied from 4×10^{15} ions / cm^2 - 1.2×10^{16} ions/ cm^2 were used. The effect of the ion implantation process on collagen fiber stability was investigated as a function of ion dosages. While all implantation conditions gave stable fibers, their swelling characteristics vary. The structural and chemical compositional changes in the stabilized collagen type I fibers were investigated using the X-ray photoelectron spectroscopy (XPS). The results indicated that the lowest dose of both the ion species implanted had the highest degree of crosslinking and retained the largest amount of nitrogen which is essential for cell adhesion and important for tissue engineering.

Keywords

Ion implantation; collagen type I; helium ions (He^+); nitrogen ions (N^+); nanofibrous scaffold; humidity effect on electrospinning; x-ray photoelectron spectroscopy

Co-Authorship Statement

In the chapter 4 author acknowledges Ying Li one of Dr. Wan's group member. Ying Li, has fabricated PCL fibers data set and is used in my thesis for comparing the effect of humidity with different polymers and solvent.

Acknowledgments

Foremost, I would like to express my sincere gratitude to my supervisors Dr. Wankei Wan and Dr. Derek Boughner for the continuous support. Especially Dr. Wan for his patience, motivation, enthusiasm, and immense knowledge, his guidance has always been valuable and assuring in all the time of research and writing of this thesis.

I would also like to thank the rest of my advisory committee: Dr. Jeff Hutter, Dr. John R. De Bruyn for their encouragement, insightful comments, and willingness to train me to achieve my goals. I would like to express my gratitude to Dr. Lyudmila Goncharova, for taking time out, to guide me, as and when required during this journey. My sincere thanks also go to Dr. James Johnson, for offering me the BME student - social representative position for three years, which leads me working on diverse exciting projects. Special thanks to Dr. Jian Liu, Jack Hendriks and Mark Biesinger for their technical support and assistance. I would like to acknowledge Ying Li to fabricate PCL fibers as this data set and is used in my thesis for comparing the effect of humidity with different polymers and solvent.

Some full-hearted thanks go to my friends and lab members, for their love and care, which was the fuel that kept me going through my Ph.D. degree. I would also like to thank my sources of funding: the Canadian Institute of Health Research, the Ontario government and The Natural Sciences and Engineering Research Council of Canada (NSERC). Finally, I will like to thank my parents, my husband, Shailesh Nene and my Son, Rishi Nene (Hrishikesh). For their unconditional love and encouragement during my graduate school.

Table of Contents

Abstract	
Co-Authorship Statement.....	ii
Acknowledgments.....	iii
Table of Contents	iv
List of Tables	viii
List of Figures (where applicable)	ix
Chapter 1	1
1 Introduction	1
Chapter 2.....	8
2 Background and literature review	8
2.1 Tissue engineering	8
2.2 Requirements for tissue engineering.....	9
2.3 Role of scaffolds for tissue engineering.....	10
2.4 Properties requirements of tissue engineering scaffolds.....	11
2.4.1 Bio-and cell compatibility.....	11
2.4.2 Cell Adhesion, migration and proliferation	12
2.4.3 Diffusion of nutrients and metabolites.....	12
2.4.4 Controlled degradability	13
2.4.5 Mechanics	13
2.4.6 Organization of the ECM generated	14
2.5 Material	15
2.5.1 Polymers for soft tissues regeneration	15
2.5.2 Synthetic polymers.....	15
2.5.3 Natural polymers.....	18

2.6	Structure	23
2.6.1	Choice of structure	24
2.7	Fibrous scaffold fabrication	24
2.8	Electrospinning	25
2.8.1	History.....	26
2.8.2	Experimental setup and the electrospinning process	26
2.8.3	Electrospinning parameters.....	31
2.9	Stabilization of electrospun collagen fiber	39
2.9.1	Chemical methods.....	40
2.9.2	Physical stabilization	41
	Chapter 3.....	66
3	Materials and Methods	66
3.1	Materials	66
3.2	Method	66
3.2.1	Isolation and purification of type I collagen from rat tails	66
3.2.2	Electrospinning	67
3.2.3	Ion implantation	68
3.3	Characterization	73
3.3.1	Fiber stability	73
3.3.2	Scanning electron microscopy (SEM)	74
3.3.3	Fiber diameters.....	75
3.3.4	Fiber stability in aqueous media	75
3.3.5	X-ray photoelectron Spectroscopy (XPS).....	76
3.4	Fiber degradation of crosslinked collagen nanofibers	78
3.5	Statistical Analysis.....	80
	Chapter 4.....	82

4	Effect of humidity on electrospun polymer fibers	82
4.1	Introduction.....	82
4.2	Experimental.....	84
4.3	Results and Discussion	87
4.4	Conclusions.....	102
Chapter 5.....		110
5	Preparation and ion beam stabilization of electrospun rat tail collagen type I fibers	110
5.1	Introduction.....	110
5.2	Experimental.....	114
5.2.1	Materials	114
5.2.2	Fiber fabrication.....	114
5.2.3	Ion implantation	115
5.2.4	Effect of ion implantation	117
5.2.5	Effect of exposure to aqueous solutions	117
5.2.6	Scanning electron microscopy (SEM)	118
5.2.7	Fiber diameters.....	118
5.2.8	X-ray photoelectron spectroscopy (XPS)	119
5.2.9	Fiber degradation of crosslinked collagen nanofibers	120
5.2.10	Statistical analysis.....	122
5.3	Results & Discussion	122
5.4	Physical effect of ion implantation on electrospun collagen fibers	122
5.5	Effect of ion implantation on fiber diameters	124
5.6	Stability of the ion implanted electrospun collagen fibers in water and DMEM	134
5.6.1	Discussion.....	134
5.7	Quantify in terms of diameter changes as a proxy for stability – as spun (control) vs. ion implanted.....	136

5.7.1	Physical effect of exposure of the ion implanted electrospun collagen fibers to DMEM.....	138
5.7.2	Fiber diameter changes as a measure of fiber stability	139
5.8	Chemical effects of ion implantation on electrospun collagen fibers.....	143
5.8.1	Effect of Ion Implantation on Chemical Structure.....	147
5.9	Fiber degradation	152
Chapter 6	158
6	Conclusions.....	158
6.1	Application.....	159
6.2	Future work.....	160
Appendices	162
Curriculum Vitae	186

List of Tables

Table 1 Melting point T_m ($^{\circ}$ C) and glass transition temperature T_g ($^{\circ}$ C) (71).....	16
Table 2 The specification of two different ion species used to crosslink the collagen fibers with two different energies, and three different doses.....	72
Table 3 Ion beam treatment was performed with these energies.....	115
Table 5 Diameter change for before and after ion implantation for two different species for all three doses.....	131
Table 6 Diameter change for after soaking in water and cell culture medial DMEM for seven days for two different species for all three doses.....	140
Table 7 Amount of nitrogen, carbon and oxygen present in the ion implanted sample for both the species at different doses.....	145
Table 8 Amide and amine ratio for helium ion implantation ratio	149
Table 9 Amide and amine ratio for nitrogen ion implantation ratio	149

List of Figures (where applicable)

Figure 1 Schematic diagram illustrating the tissue engineering paradigm (Adapted from (1))	9
Figure 2 Collagen type 1 sequence could be further explained by opting one of the following patterns as, Gly-Pro-X or Gly-X-Hyp Adapted from (95).....	23
Figure 3 A standard electrospinning set consist of a syringe pump, with a metal needle tip, a high voltage power supply and a grounded collector.	27
Figure 4 A: Vertical set-ups for electrospinning B: Horizontal set-ups for electrospinning	28
Figure 5 Types of collectors used to align electrospun fibers:	30
Figure 6 Factors effecting electrospinning	31
Figure 7 Screen shot of Stopping and Range of Ions in Matter (SRIM), is a computer simulation software package.....	44
Figure 8 The screen shot of Transport of Ion in Matter (TRIM), is a software that is included in the SRIM program package.	45
Figure 9 : The electrospinning setup with a collector.....	68
Figure 10 Image: Courtesy of Tandetron Lab at University of Western Ontario.	69
Figure 11 Implantation stage Image: Courtesy of Tandetron Lab at University of Western Ontario	70
Figure 12 A: Design of sample holder B: Sample holder.....	72
Figure 13 : A: As-spun in water for 1min B: Electrospun scaffolds	73
Figure 14 Effect of humidity on average fiber diameter of electrospun collagen fibers using collagen in HFIP solutions (a) collagen concentration at 5 wt%; (b) collagen concentration at 5.5 wt%	89

Figure 15 SEM images of electrospun collagen fibers at a humidity of $45 \pm 5\%$ (a) collagen concentration of 5 wt%; (b) collagen concentration of 5.5 wt%	92
Figure 16 Effect of humidity on average fiber diameter of electrospun polycaprolactone (PCL) fibers using a 12 wt% PCL in trifluoroethanol solution	93
Figure 17 SEM micrographs of electrospun PCL nanofibers prepared using a 12 wt% PCL in trifluoroethanol solution at different relative humidity levels (a) 20%; (b) 25%; (c) 30%; (d) 35%; (e) 40%; (f) 45%; (g) 50%; (h) 55%; (i) 60%. The scale bar (500 nm) at the 1	94
Figure 18 A summary plot of the effect of humidity on average fiber diameter of electrospun polymer fibers produced using polymer solutions (a) data for fibers with maximum diameters up to 1 μm (b) data for fibers with maximum diameters above 1 μm	97
Figure 19 Nitrogen- ion implantation at 4×10^{15} ions/cm ² on collagen type-1 nanofibrous scaffold.....	125
Figure 20 Nitrogen- ion implantation at 8×10^{15} ions/cm ² on collagen type-1 nanofibrous scaffold A: Before ion implantation (as- spun fibers) B: After N ⁺ ion implantation	126
Figure 21 Nitrogen- ion implantation at 12×10^{15} ions/cm ² on collagen type-1 nanofibrous scaffold A: Before ion implantation (as- spun fibers) B: After N ⁺ ion implantation	127
Figure 22 Helium- Ion Implantation at 4×10^{15} ions/cm ² on collagen type-1 nanofibrous scaffold A: Before ion implantation (as- spun fibers) B: After He ⁺ ion implantation.....	128
Figure 23 Helium- Ion Implantation at 8×10^{15} ions/cm ² on collagen type-1 nanofibrous scaffold on collagen type-1 nanofibrous scaffold.....	129
Figure 24 Helium- Ion Implantation at 12×10^{15} ions/cm ² on collagen type-1 nanofibrous scaffold.....	130
Figure 25 Error propagation on the results of before and after ion implantation on two different species at different energies and doses.....	132
Figure 26 Overlapping formula for Nitrogen ion and Helium ion implant at for after ion implantation for all three doses.	133

Figure 27 Applying error propagation on water – treatment	136
Figure 28 Applying over lapping law on water - treatment of the percentage change in the diameter of crosslinked collagen nanofibers, when soaked in water for seven days (for two different species at different energies and doses).	138
Figure 29 Applying lapping law on cell culture media – treatment	141
Figure 30 Applying over lapping law on cell culture media - treatment the percentage change in the diameter of crosslinked collagen nanofibers, when soaked in cell culture media for seven days (for two different species at different energies and dose	142
Figure 31 Un-crosslinked collagen sample full scan	144
Figure 32 Atomic percentage (at%) of average of nitrogen for both the ion species at different energies and all the different doses. It gives us a comparative edge with the control, which is as spun collagen nanofibers with the helium and nitrogen ion implanted samples at different dose.	146
Figure 33 High resolution scan of nitrogen at the binding energy of 399.9 eV. It displays comparison of as spun sample with helium ion and nitrogen ion implanted sample.	148
Figure 34 The test reaction will proceed only for a free amino acid	152
Figure 35 %Degree of crosslinking of the crosslinked samples with respect to the control for all the conditions of crosslinking.	154
Figure 36 Histogram of $N^+ 1.2 \times 10^{15}$ ions/cm ²	163
Figure 37 Histogram of $N^+ 8 \times 10^{15}$ ions/cm ²	164
Figure 38 Histogram of $N^+ 4 \times 10^{15}$ ions/cm ²	165
Figure 39 Histogram of helium 1.2×10^{16} ions/cm ²	166
Figure 40 Histogram of helium 8×10^{16} ions/cm ²	167
Figure 41 Histogram of helium 4×10^{16} ions/cm ²	168

Figure 42 plots a full X-ray photoelectron spectroscopy scan that was after nitrogen ion implantation with a dose at 8×10^{15} ions per cm^2 172

Figure 43 high resolution nitrogen scan that was after nitrogen ion implantation with a dose of at 8×10^{15} ions per cm^2 173

Figure 44 plots a full X-ray photoelectron spectroscopy scan that was after helium ion implantation with a dose of 12×10^{15} ions per cm^2 174

Figure 45 high resolution scan of nitrogen that was after helium ion implantation with a dose of 12×10^{15} ions per cm^2 175

Figure 46 plots a full X-ray photoelectron spectroscopy scan that was after nitrogen (N+) ion implantation with a dose of 4×10^{15} ions per cm^2 176

Figure 47 high resolution scan of nitrogen that was after nitrogen (N+) ion implantation with a dose of 4×10^{15} ions per cm^2 177

Figure 48 plots a full X-ray photoelectron spectroscopy scan that was after helium ion implantation with a dose of 8×10^{15} ions per cm^2 178

Figure 49 high resolution scan of nitrogen that was after helium ion implantation with a dose of 8×10^{15} ions per cm^2 179

Figure 50 plots a full X-ray photoelectron spectroscopy scan that was after helium ion implantation with a dose of 4×10^{15} ions per cm^2 180

Figure 51 high resolution scan of nitrogen that was after helium ion implantation with a dose of 4×10^{15} ions per cm^2 181

Figure 52 plots a full X-ray photoelectron spectroscopy scan that was after nitrogen ion implantation with a dose of 4×10^{15} ions per cm^2 182

Figure 53 high resolution scan of X-ray photoelectron spectroscopy scan that was after nitrogen ion implantation with a dose of 4×10^{15} ions per cm^2 183

Figure 54 plots a full X-ray photoelectron spectroscopy scan of an implantation as control	184
Figure 55 high resolution scan of nitrogen of an implantation as control	185

Chapter 1

1 Introduction

The loss or failure of a tissue or organ is devastating to human health. There are limited options available other than tissue or organ transplantation (2). Tissue engineered replacements have the potential to overcome limitations of the traditional solution (3). This technique involves harvesting healthy cells from the patient's body, culturing these cells with 3D porous support structure known as a scaffold (4, 5). The design and fabrication of the scaffold is an important factor to ensure its success as it provides the environment for cells to survive and perform the necessary regeneration. An ideal scaffold should be biocompatible, biodegradable to produce nontoxic by-products after degradation (6, 7). Scaffold, should be highly porous and have a large surface to volume ratio, in order to promote uniform cell distribution, diffusion of nutrients, and to organized cell communities (8). Along, with all these properties, the scaffold should be degradable, mechanically strong and malleable to withstand physiological stress during the tissue regeneration process (9).

Numerous techniques have been developed to fabricate fibrous scaffold. Among the techniques investigated, electrospinning has emerged to be one of the most popular technique. Electrospinning involves the use of an electric field to draw fibers from the polymer solution. A voltage is applied to the polymer solution, which causes a jet of the polymer solution to be drawn toward a grounded collector. The electrospinning process

has been studied using a variety of polymers (including protein such as collagen) with the use of a broad range of solvent (10-12).

Collagen is ubiquitously available in mammalian species (13) and has been an attractive biomaterial of choice as a tissue engineering scaffold material. It possesses properties that meet the requirements of an attractive scaffold material for tissue engineering applications and offers the unique advantage of being a component of the extracellular matrix.

Collagen fiber fabrication by electrospinning has been extensively studied. By controlling the fiber spinning process parameters, reproducible fiber size and morphology can be obtained (14-17). Although the process parameters have been quite extensively studied, however, there have been only several studies on the impact of environmental parameters including temperature and humidity on electrospinning (15, 18). Knowledge of the impact of humidity on electrospun fiber fabrication including collagen fibers would be a significant contribution towards tissue engineering scaffold fabrication.

Collagen fiber in its native state is stable in the aqueous environment. However, collagen nanofibers produced by electrospinning are not stable in water as the native collagen structure is not conserved in the regeneration process. The regenerated fibers disintegrate readily upon exposure to water or any aqueous media. In order to make use of these fibers in the fabrication of scaffold for tissue engineering, they need to be stabilized.

One of the most commonly used technique is to enhance aqueous stability of collagen fibers is use of chemical crosslinking. One of the commonest chemical crosslinking agent is glutaraldehyde. Glutaraldehyde vapor had been used to crosslink electrospun collagen nanofibers (19). The resulting fibers had poor swelling properties and released the highly cytotoxic crosslinking agent over time (20-22). Alternatives chemical crosslinking agents including 1-ethyl-3-(3-dimethylaminopropyl) carbodiimide (EDC) and N-hydroxysuccinimide (NHS) had also been studied. But, they result in fibers with the significant degree of swelling and loss of the nanofibrous morphology and porosity (23, 24). Another less cytotoxic chemical crosslinking agent investigated is genipin. It has achieved varying degrees of success on electrospun collagen fiber scaffold. But it also led to significant swelling and resulted in the loss of fiber structure (25, 26).

Ion beam treatment is a unique physical processing technique based on transfer of energy from accelerating ions to the target material. Contrast to the conventional ion implantation process which is regarded as a surface treatment technique for bulk materials, its use on nanomaterials such as fibers is a bulk modification technique as ions penetrate through the fiber cross-section. This method of energy transfer offers the opportunity to be investigated as a new and novel approach to crosslinking of electrospun collagen fibers.

Early study on ion implantation in polymer fibers was the use of oxygen ions on electrospun polyurethane (PU) fibers (27). This is a unique approach to modification

without damaging the surface morphology of the polymer fiber with ion species of own choice. This technique of ion treatment was later on applied to collagen thin sheets with helium ions for enhanced stabilization (28). Thus, ion beam implantation as one of the suitable ways to stabilize fibers in an aqueous environment by modifying their chemical properties is of particular interest in scaffold fabrication (29). In addition to improvement in aqueous stability, ion implantation has also be found to have an effect on polymer stiffness. A study on electrospun poly(vinyl alcohol) (PVA) fibers using nitrogen and helium ion implantation found that fiber stiffness is a function of ion used and ion doses (29, 30).

The objectives of the current research are to:

- To fabricate collagen type I nanofibers by electrospinning using HFIP as the solvent.
- To study the effect of humidity on electrospun collagen type I fiber diameter and morphology.
- To impart aqueous stability to the electrospun collagen type I fiber using ion implantation using helium ion (He^+) and nitrogen ion (N^+)
- To delineate the chemical changes taking place in the collagen type I fiber using x ray photoelectron spectroscopy (XPS)

Reference:

1. Ikada Y. Challenges in tissue engineering. *Journal of the Royal Society Interface*. 2006;3(10):589-601.
2. Lee S, Henthorn D. *Materials in biology and medicine*: CRC press; 2012.
3. Dvir T, Timko BP, Kohane DS, Langer R. Nanotechnological strategies for engineering complex tissues. *Nature nanotechnology*. 2011;6(1):13-22.
4. Weiss LE, Calvert JW. Assembled scaffolds for three dimensional cell culturing and tissue generation. *Google Patents*; 2000.
5. Li Y, Liu C. Nanomaterial-based bone regeneration. *Nanoscale*. 2017;9(15):4862-74.
6. Gong T, Xie J, Liao J, Zhang T, Lin S, Lin Y. Nanomaterials and bone regeneration. *Bone research*. 2015;3:15029.
7. Dhandayuthapani B, Yoshida Y, Maekawa T, Kumar DS. Polymeric scaffolds in tissue engineering application: a review. *International Journal of Polymer Science*. 2011;2011.
8. Yang Y, El Haj AJ. Biodegradable scaffolds–delivery systems for cell therapies. *Expert opinion on biological therapy*. 2006;6(5):485-98.
9. Reneker DH, Yarin AL, Fong H, Koombhongse S. Bending instability of electrically charged liquid jets of polymer solutions in electrospinning. *Journal of Applied physics*. 2000;87(9):4531-47.
10. Matthews JA, Wnek GE, Simpson DG, Bowlin GL. Electrospinning of collagen nanofibers. *Biomacromolecules*. 2002;3(2):232-8.
11. Frenot A, Chronakis IS. Polymer nanofibers assembled by electrospinning. *Current opinion in colloid & interface science*. 2003;8(1):64-75.
12. Prum RO, Torres RH. Structural colouration of mammalian skin: convergent evolution of coherently scattering dermal collagen arrays. *Journal of Experimental Biology*. 2004;207(12):2157-72.
13. Bhardwaj N, Kundu SC. Electrospinning: a fascinating fiber fabrication technique. *Biotechnology Advances*. 2010;28(3):325-47.
14. Thompson C, Chase GG, Yarin A, Reneker D. Effects of parameters on nanofiber diameter determined from electrospinning model. *Polymer*. 2007;48(23):6913-22.

15. Lannutti J, Reneker D, Ma T, Tomasko D, Farson DF. Electrospinning for tissue engineering scaffolds. *Materials Science & Engineering C-Biomimetic and Supramolecular Systems*. 2007 Apr;27(3):504-9.
16. Reneker DH, Yarin AL. Electrospinning jets and polymer nanofibers. *Polymer*. 2008;49(10):2387-425.
17. Saehana S, Iskandar F, Abdullah M. Optimization of electrospinning parameter by employing genetic algorithm in order to produce desired nanofiber diameter. *World Academy of Science, Engineering and Technology, International Journal of Chemical, Molecular, Nuclear, Materials and Metallurgical Engineering*. 2013;7(1):86-91.
18. Wu H, Fan J, Chu C-C, Wu J. Electrospinning of small diameter 3-D nanofibrous tubular scaffolds with controllable nanofiber orientations for vascular grafts. *Journal of Materials Science: Materials in Medicine*. 2010;21(12):3207-15.
19. Gendler E, Gendler S, Nimni M. Toxic reactions evoked by glutaraldehyde-fixed pericardium and cardiac valve tissue bioprosthesis. *Journal of Biomedical Materials Research Part A*. 1984;18(7):727-36.
20. Gough JE, Scotchford CA, Downes S. Cytotoxicity of glutaraldehyde crosslinked collagen/poly (vinyl alcohol) films is by the mechanism of apoptosis. *Journal of Biomedical Materials Research Part A*. 2002;61(1):121-30.
21. Huang-Lee LL, Cheung DT, Nimni ME. Biochemical changes and cytotoxicity associated with the degradation of polymeric glutaraldehyde derived crosslinks. *Journal of Biomedical Materials Research Part A*. 1990;24(9):1185-201.
22. Wang Y, Yang C, Chen X, Zhao N. Development and Characterization of Novel Biomimetic Composite Scaffolds Based on Bioglass-Collagen-Hyaluronic Acid-Phosphatidylserine for Tissue Engineering Applications. *Macromolecular Materials and Engineering*. 2006;291(3):254-62.
23. Sarkar SD, Farrugia BL, Dargaville TR, Dhara S. Chitosan-collagen scaffolds with nano/microfibrous architecture for skin tissue engineering. *Journal of Biomedical Materials Research Part A*. 2013;101(12):3482-92.
24. Delgado LM, Bayon Y, Pandit A, Zeugolis DI. To cross-link or not to cross-link? Cross-linking associated foreign body response of collagen-based devices. *Tissue Engineering Part B: Reviews*. 2015;21(3):298-313.
25. Huang GP, Shanmugasundaram S, Masih P, Pandya D, Amara S, Collins G, et al. An investigation of common crosslinking agents on the stability of electrospun collagen scaffolds. *Journal of Biomedical Materials Research Part A*. 2015;103(2):762-71.
26. Wong K, Zinke-Allmang M, Wan W, Zhang J, Hu P. Low energy oxygen ion beam modification of the surface morphology and chemical structure of polyurethane

- fibers. Nuclear Instruments and Methods in Physics Research Section B: Beam Interactions with Materials and Atoms. 2006;243(1):63-74.
27. Sugita Y, Suzuki Y, Someya K, Ogawa A, Furuhashi H, Miyoshi S, et al. Experimental evaluation of a new antithrombogenic stent using ion beam surface modification. Artificial organs. 2009;33(6):456-63.
28. Wong KKH, Hutter JL, Zinke-Allmang M, Wan W. Physical properties of ion beam treated electrospun poly (vinyl alcohol) nanofibers. European Polymer Journal. 2009;45(5):1349-58.
29. Wong KKH, Zinke-Allmang M, Wan W. N⁺ surface doping on nanoscale polymer fabrics via ion implantation. Nuclear Instruments and Methods in Physics Research Section B: Beam Interactions with Materials and Atoms. 2006;249(1):362-5.

Chapter 2

2 Background and literature review

The loss or failure of a tissue or organ is one of the devastating and expensive problems in human health care. There are very few options other than organ transplantation (2). Although organ transplant therapy have saved and improved countless lives, however, immune rejection, patient-donor matching and especially the shortage of available organs are the limitations of the organ transplant therapy. Statistics of organ transplants in the United State of America have shown an increase of 20% over five years (2010 – 2015) (31). Signifying that the demand of the organ transplant has grown every year. Over the same period, organ donation has only increased by 10% (32). One of the approaches to overcome this problem is to engineer and construct living biological substitutes. This approach is known as tissue engineering (33).

2.1 Tissue engineering

Tissue engineering crosses the traditional boundaries of engineering and medicine. It has been recognized as a promising alternative for reconstruction and regeneration damaged or lost tissue/organs (33). The field of tissue engineering requires intensive research and knowledge in many areas of sciences and engineering (34). The general concept of tissue engineering leading to a living tissue replacement is shown in Figure 1. It is a multistep process involving the harvesting of cell from the patient's own body and seeding the cells onto a scaffold. By incorporating biochemical signalling molecules such as growth factors into the culturing the cells in a controlled

environment such as a bioreactor, tissue can be regenerated for implantation into the patient's body.

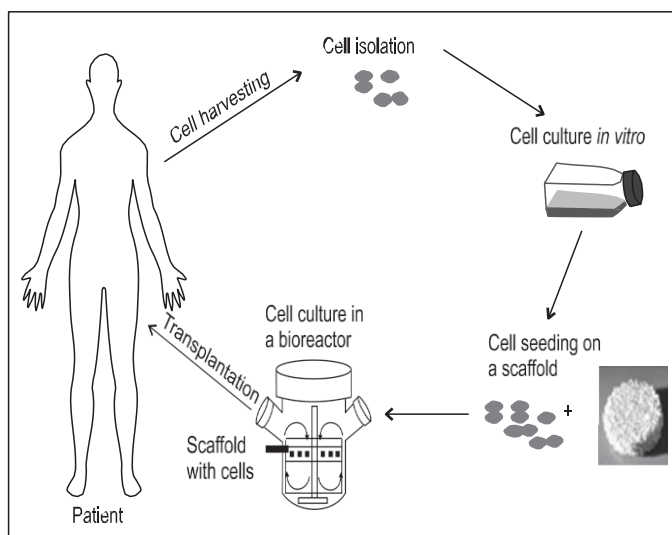


Figure 1 Schematic diagram illustrating the tissue engineering paradigm (Adapted from (1))

2.2 Requirements for tissue engineering

Among the many components involved in tissue engineering, the design and fabrication of the scaffold is an important factor to ensure its success as it provides the environment for cells to survive and perform the necessary regeneration.

2.3 Role of scaffolds for tissue engineering

The success of tissue engineering depends on carriers, which are designed as scaffolds.

One of the best approaches is to design scaffolds that mimick the native extracellular matrix.

The native extracellular matrix usually has a tissue specific composition and cells in human tissues are anchored onto these matrices (35). The extracellular matrix functions are classified into five categories below (4, 36-38) :

1. The extracellular matrix provides structural support and an environment to which cells can attach and then proliferation and migration while responding to cell signals, and so the design of the scaffold should allow for this same support and environment.
2. The extracellular matrix provides structure to the tissue and thus mechanical properties like rigidity and elasticity are associated with its function. For example, randomly organized collagen and elastin fibers are responsible for the elasticity of skin, whereas in tendon collagetype-1 enables high tensile strength. The designed scaffold should therefore provide a defined shape for the tissue, while giving mechanical stability to the engineered tissue.
3. The extracellular matrix regulates the activities of cells by providing bioactive cues. For example, binding events are triggered by the RGD sequence on fibronectin. The scaffold should be designed to provide bioactive cues for cells to interact with other cells to facilitate activities such as adhesion, proliferation and differentiation.

4. The extracellular matrix acts as a bank that supplies growth factors to cells for their bioactivities. The scaffold should be designed as a vehicle that can deliver these growth factors to stimulate the bioactivities of cells.
5. The extracellular matrix facilitates wound healing by degrading and remodeling itself in response to tissues. The scaffold matrix should be designed with controlled degradation mechanisms so that it can respond to tissue remodeling processes.

2.4 Properties requirements of tissue engineering scaffolds

2.4.1 Bio-and cell compatibility

Biocompatibility is the key criterion of the scaffold employed for tissue regeneration. The biomaterial to provide biological cues for cell attachment and migration onto the surface and then eventually through the scaffold laying down a new matrix. To speed up the regeneration process, the scaffold should serve as a delivery vehicle to provide growth stimulating signals, such as growth factors (39). Tissue engineering Scaffolds should cause a negligible immune rejection after implantation so as to prevent inflammatory response caused by rejection by the body.

The important factor that determines the scaffold's biocompatibility is its structural chemistry (40). Thus, the behavior of mammalian cells, such as adhesion, proliferation and migration, depends on the surface characteristics of the material. Numerous physical and chemical surface modification methods are available to optimize the biocompatibility of the material (8)

2.4.2 Cell Adhesion, migration and proliferation

The initial and primary site of cell interaction is the surface of the scaffold and anchoring these cells on the scaffold is one of the major phases towards tissue engineering (41). The surface properties of the scaffolds can be selectively modified to enhance cell adhesion to the biomaterials. Scaffolds with large and accessible surface areas are favorable for tissue regeneration (42). Hence, surface modification of the biomaterial has become an increasingly popular method for cell adhesion, migration and proliferation. Most of this surface modification is performed to improve the biocompatibility of the scaffold, so that the cell can perform its bioactivity on the scaffold.

2.4.3 Diffusion of nutrients and metabolites

The design of the structure of the scaffold is a critical step for tissue engineering because it ensures the diffusion of nutrients to the cell. The scaffold should have an interconnected pore structure that cells can penetrate, allowing for oxygen and nutrient supply to diffuse in and waste removal. The porosity also allows the degraded scaffold to exit without meddling with the newly fabricated extracellular matrix (43).

Mean pore size of the scaffold also plays an important role in the cells' interaction with the scaffold and allows migration throughout the scaffold. Cells connect with the scaffold via ligands, a chemical group on the material surface of the scaffold (44). The density of ligands is influenced by the available surface area within a pore to which cells adhere, thus the pore size within a scaffold plays a critical role in tissue engineering.

2.4.4 Controlled degradability

Scaffolds are not permanent implants, but are meant to degrade. When cells fabricate a new extracellular matrix, the scaffold should degrade, allowing the cells to complete their bioactivity (45). The degraded scaffold by-products should be non-toxic and should not invoke any adverse immune responses.

The intrinsic properties of the polymer play a vital role in the rate at which the scaffold degrades. Among all the intrinsic properties of the polymer, its chemical structure and level of hydrophilicity or hydrophobicity can be changed to control the degradation rate of the scaffold (46). Most importantly the degradation rate should match the rate at which the tissue is regenerated.

2.4.5 Mechanics

The native extracellular matrix provides the mechanical integrity of the tissue (46) and thus the extracellular matrix mimicking scaffolds are anticipated to provide temporary mechanical support to withstand the loads and stress of regenerative tissue.

Also, these mechanical properties intensely impact cells and their functionality and have been shown to regulate many cellular behaviors, including cell-matrix adhesions (47, 48), motility (49), propagation(50), differentiation (51), viability (52), phenotype (51, 53) and apoptosis (54).

These properties have also been tested on mesenchymal stem cells and were able to differentiate into neural, myogenic or osteogenic tissues when cultured on 3D collagen hydrogel with a stiffness of 0.1, 11, or 34 kPa, respectively (55, 56). Thus, the choice of a

biomaterial is an important parameter for tissue engineering, as each tissue in the body has a different stiffness ranging from brain tissue (1 kPa) to calcified bone (100 kPa) (54). Additionally, it is essential to understand how cells sense forces and how these forces are transduced into biochemical signals.

2.4.6 Organization of the ECM generated

The success rate of tissue engineering depends on the fabrication of the scaffolds that mimic the native extracellular matrix (ECM). The ECM is the native fibrillar network composed of GAGs, proteoglycans and proteins used to support cell growth and influence cell behavior (57). Apart from providing support to the cells, ECM also releases the signaling molecules that regulate cell behavior (58). Several synthetic polymers promote properties like degradation and cell adhesion, yet do not adequately provide biochemical signals to control cell behavior (59). The ideal scaffold material would imitate the ECM by properly guiding gene expression, cell migration and differentiation (60). The goal of imitating the ECM can be achieved by incorporating natural polymers, which are present in multicellular components like collagen (61). This step would help us to achieve our goals of imitating ECM and help us incorporate bioactive molecules like RGD peptides as a surface functionalization at the later step while the tissue regenerates.

2.5 Material

2.5.1 Polymers for soft tissues regeneration

In the tissue engineering of soft tissues such as cardiovascular tissues, the scaffold material would need to have mechanical properties similar to that of the tissue. Polymer possesses many of the properties required and is therefore an attractive choice for scaffold fabrication. Many polymeric materials, both natural and synthetic, had been investigated for suitability as scaffold material. Although there is a very wide range of polymers available in the literature, the requirement of degradability and biocompatibility place constraints that limit the choice of suitable candidate polymers.

2.5.2 Synthetic polymers

Synthetic polymers are man-made polymers and are very useful in biomedical applications as their physical and chemical properties like flexibility, degradation and mechanical properties can be tailored by chemical modifications (62). However, they have many advantages when used as the scaffolding material, there is always a risk of rejection for in vivo applications (63).

Some of the more popular synthetic polymers that have been investigated extensively for scaffold fabrication include poly (glycolic acid) (*PGA*), poly(lactic acid) (*PLA*), polycaprolactone (*PCL*), polyethylene glycol (*PEG*), poly(ethylene oxide) (*PEO*), polylactide-co-glycolide (*PLGA*) and polydioxanone (*PDO*).

2.5.2.1 Poly (glycolic acid) (PGA)

PGA is one of the very first degradable polymer investigated for biomedical applications. Most of the PGA material are used as filler material, they often mesh in a scaffold for bone (64, 65), cartilage (66), tendon (67), tooth (68), intestinal (69) and spinal regeneration (70). Due to its rapid degradation, it loses its mechanical strength and is not by itself an attractive biomaterial for scaffold fabrication.

2.5.2.2 Poly (lactic acid) (PLA)

Poly (lactic acid) (PLA) has been FDA approved and thus, widely used in medical applications as implants in the human body. As polylactide has chiral molecules, thus it can be arranged as four forms, and they are poly(L-lactic acid) (PLLA), poly(D-lactic acid) (PDLA), poly(D,L-lactic acid) (PDLLA) and meso-poly(lactic acid) (68). Each of the four forms of PLA, has different properties such as melting point and glass transition temperature, which as specified in the table 1.

Table 1 Melting point T_m ($^{\circ}$ C) and glass transition temperature T_g ($^{\circ}$ C) (71)

Transition temperature	mesoPLA	PDLA	PLLA	PLA
T_g ($^{\circ}$ C)	40-45/34	50-50	53-63	43
T_m ($^{\circ}$ C)	-/153	Around 180	Around 180	153

PLA is primarily used as a non-woven mesh for tissue engineering applications such as scaffolds for bone(72), cartilage(73), tendon(74), neural (75) and vascular(76) regeneration.

Co-polymers of PLA (both L- and D,L-lactide forms) and PGA, known as poly(lactide-co-glycolide) (PLGA), are the most investigated degradable polymers for biomedical applications and has been extensively used in drug delivery applications such as chemotherapeutics (77), proteins (78), vaccines (79) and antibiotics (80). They have also been investigated for scaffold applications (81).

2.5.2.3 Polycaprolactone (PCL)

PCL is biocompatible, degradable and with mechanical strength that are suitable for orthopaedic applications (82). Additionally, PCL has low degradation rate for in vivo applications, thus it is favored as a long-term implantation device. For example, Capronor[®] is a PCL based commercial contraceptive product that is used to deliver levonorgestrel *and has* been on the market for over 25 years (83). PCL has been used to fabricate tissue engineering scaffolds. One of the studies on PCL electrospun fibrous scaffold demonstrated extracellular matrix formation when seeded with mesenchymal stem cells (84). PCL scaffolds have also been used for cartilage (85) and vascular tissue engineering applications (86).

2.5.2.4 Polyethylene glycol (*PEG*):

PEG is a well-known biomaterial and is also known as polyethylene oxide (PEO). As it is hydrophilic in nature, it is difficult to attach antibodies and other proteins to the PEG scaffolds (87). By using PEG in a co-polymer, cell attachment to the scaffold is possible. Additionally, investigations have been done on PEG co-polymers including PEG–PLA constructs, PEG–PPF, which have better degradation characteristics than PEG alone (14).

2.5.3 Natural polymers

Natural polymers are derived from the renewable resources such as plants and animals. Scaffolds fabricated using the natural polymer has the advantage of excellent biocompatibility and are biodegradable (88). Natural polymers that have been investigated for scaffold fabrication are protein and polysaccharide. If they are derived from the extracellular matrix, they would provide a cell friendly environment and allow cells to adhere (89). Degradation of the original polymer while processing and possessing poor mechanical strength are the two major drawbacks of natural polymer (8, 90). Some of the commonly used natural polymers for scaffold fabrication include gelatin, elastin, fibrinogen, collagen, silk protein and chitosan (91).

2.5.3.1 Elastin

Elastin plays a critical role in connective tissues and is a vital protein in the native extracellular matrix (92). Electrospun elastin scaffolds (93) have been fabricated and studied with stem cells to demonstrate the regulation of cell functionality such as proliferation, migration, and differentiation (94, 95). On the other hand, elastin can be used

in the gel form (96) or as a component in copolymers (97). Additionally, numerous studies have been reported that employ elastin scaffolds for cardiovascular tissue engineering purposes (98-100).

2.5.3.2 Fibrinogen

Fibrinogen plays a vital role in blood clotting and is one of the major factors in wound healing (101-103). A naturally occurring plasma protein, fibrinogen scaffolds have been fabricated using the electrospinning technique. These fibrin-based scaffolds have demonstrated mechanical properties mimicking extra cellular matrix and promoting cell migration (101, 102).

2.5.3.3 Silk

Silk protein is a versatile natural polymer for biomedical applications because of its natural strength, biocompatibility and slow degradation rate (104). Silk scaffolds have been fabricated using a solvent system consisting of formic acid, HFIP (Hexafluoroisopropanol) and water as a solvent. Water and formic acid was used to enhance the mechanical properties of the silk scaffolds (105, 106). Electrospun silk fiber was first patented in the year 2000 (107, 108). Silk protein concentration in the fiber spinning solution plays an important role in the fabrication of uniform fibers (109, 110). The addition of PEO to the silk solution increase the solution viscosity (111) and aids cell attachment and proliferation on the scaffold fabricated (112). Studies show that mesenchymal stem cells grow well on silk scaffolds as well as on silk sponges for ligament tissue engineering (113-115).

2.5.3.4 Chitin and Chitosan

Chitin, a carbohydrate polymer, is found naturally in the shell of crustacean and have been widely used in the biomedical field as it has demonstrated to be biodegradable and non-toxic (116). Chitosan is prepared by deacetylation of the extracted chitin from the ground shell at high pH and high temperature (117). Chitin based scaffold have been fabricated for tissue engineering to promote structure formation and cell proliferation (118). (119) (120). Chitin based scaffold has also been demonstrated to accelerate in wound healing processes (121).

Chitosan scaffolds have demonstrated excellent properties that are suitable for bone tissue engineering, which has been fabricated using chitosan alone (122-124) or with other natural polymers like silk (125, 126), starch (127, 128).

2.5.3.5 Gelatin

Gelatin is a denatured form of collagen and has excellent biocompatibility and biodegradability properties. Thus it is always in demand for tissue engineering (129). For many years, gelatin has been used as a carrier for drug delivery and dressing for wounds, but the new the growing interest is to fabricate electrospun scaffold by mixing other polymer such as PCL (130). Gelatin scaffolds have been shown to aid the cellular

functions of migration, proliferation, and penetration (131) and have been used for nerve (130), hepatic (132), and cartilage(133) regeneration.

2.5.3.6 Collagen

Collagen is probably one of most used natural polymer based biomaterial which is abundantly found in the human body. In many types of tissue various mechanical properties, such as strength, stiffness and toughness are attributed to the presence of collagen (47). Collagen being biocompatible, has been one of the favorable biomaterial when it comes to in-vivo implantation using the tissue engineering approach (134, 135). There are at least 27 types of collagen that have been discovered (136) and they are of different structures and properties and serve different functions. Among the different types of collagen, collagen type 1 is of particular interest in soft tissue regeneration as it is one of the major component of the extra cellular matrix and provides the structural integrity to tissue (137).

Among the synthetic and natural polymers that are both biocompatible and degradable that are available for scaffold fabrication, there are other considerations that should be taken into account. These include stability and degradation rate, ease of fabrication etc. In addition, another highly desirable property is the intrinsic bioactivity of the scaffold material. Among many of the natural polymers and especially those that are already part

of the body's extracellular matrix with collagen being a prime example, they are naturally the preferred choice for scaffold fabrication.

2.5.3.7 Collagen type I

Collagen molecules self-assemble into triple-helical structures that are packed together into the staggered patterns called fibril (138, 139). Type I collagen is composed to two $\alpha 1$ and one $\alpha 2$ left-handed coiled polypeptide chains with the characteristic "Gly-X-Y" amino acid sequence. In the entire sequence, glycine (Gly) is accounted for one third of all amino acid in collagen, and the sequence Gly-X-Y is then completed by the addition of X and Y where X and Y are in a random sequence of amino acids (140, 141). Proline (Pro) or hydroxyproline (Hyp) constitute about one-sixth of the total sequence (142). In addition, the sequence glycine-proline-hydroxyproline, occurs in more than 10% of the molecule. Thus, these sequence (as shown in figure 2) could be further explained by opting one of the following patterns as, Gly-Pro-X or Gly-X-Hyp, where X may be any of various other amino acid residues. Glycine is the only amino acid that contains hydrogen at both the non-backbone atoms to the α -carbon, this allows for tighter packing of the three peptide chains (143). These three polypeptide chains combine to create a single tropocollagen molecule, and has an approximate length of 300 nm long and 1.5 nm wide and each group have a gap of roughly 67nm (144).

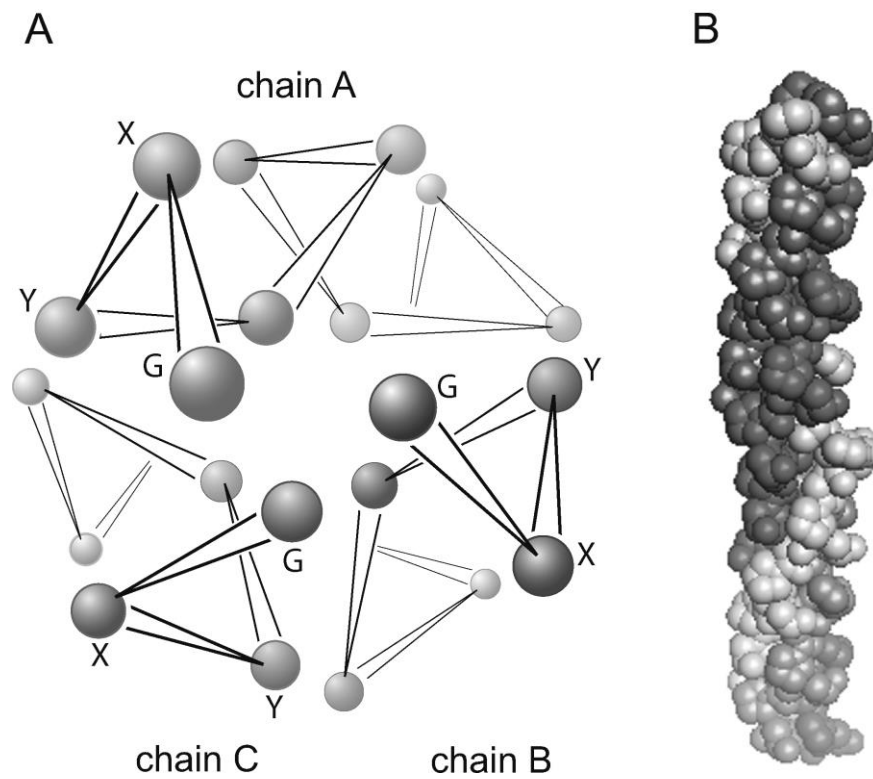


Figure 2 Collagen type 1 sequence could be further explained by opting one of the following patterns as, Gly-Pro-X or Gly-X-Hyp Adapted from (95)

2.6 Structure

One of the requirements for tissue engineering scaffold is interconnected porosity. This is required for several reasons. Porosity provides avenue for cell-cell communication and allow cells to migrate within the 3-dimensional structure of the scaffold. These pores would need to have dimensions comparable to cell sizes in the micrometer range. In

addition, the supply of nutrients including dissolved oxygen and the removal of metabolites including carbon dioxide also depend on it. Generally, there are two approaches towards the creation of porous structure in scaffolds. It can be in an integrated form like a sponge. The porous structure can also be formed using overlapping fibers. If nanofibers are used in scaffold fabrication, it has the advantage of maximizing cell-fiber surface interaction and porosity can also be controlled.

2.6.1 Choice of structure

Collagen is present in nanofiber form in the extracellular matrix. A scaffold using collagen type I as the biomaterial in the form of nanofiber would be more closely mimicking the natural extracellular matrix environment (89, 145) . It is the purpose of this thesis to explore the preparation of collagen nanofibers for tissue engineering applications.

2.7 Fibrous scaffold fabrication

There are a variety of methods to convert a polymer material into fibers. Some of the common and well-established methods include extrusion and spinning. Spinning is by far the most popular method (146, 147) . The spinning process can be further subdivided into melt spinning and solution spinning (81, 131). Solution spinning is more common as it has the advantage of forming smaller diameter fibers through solvent evaporation

during the spinning process. This approach also avoids the concern of polymer instability at elevated temperature like some of the proteins and can be applied to polymers without a well-defined melting point. Occasionally additional external forces are also added to augment the fiber spinning process. Examples of this approach are centrifugal spinning (148) and electrospinning (14). Among these techniques, electrospinning has emerged to be a favorite method of choice for making fibers with diameter in the nanometers to several micrometers range (149). This will be the methods used for the fabrication of collagen nanofibers in this study. The electrospinning process is reviewed in further details below.

2.8 Electrospinning

In the production of fibers from biomaterials for tissue engineering scaffold fabrication, electrospinning has emerged to be one of the most popular method of choice. This method is versatile and simple to setup and control and is cost-effective (150). In this technique, an electric field is used to draw fibers from a polymer solution in the fiber spinning process (151). More than 200 polymers have been used for electrospinning (152). Examples of biopolymers relevant to scaffold fabrication include silk fibroin (153), collagen (11) and chitosan (154).

2.8.1 History

The electrospinning technique has been known for over 100 years. It was first observed by Rayleigh in 1897 (155). In his early studies, he used a high voltage source to inject charge of a certain polarity into a polymer solution, which is then accelerated toward a collector of opposite polarity. This technique was later studied in more detail by Zeleny in 1914 (156).

The use of electrospinning to make polymer fibers was first patented by Formhals in 1934 (157, 158). Detailed experimental and theoretical studies was conducted by Tylor in 1979 (159). Researchers started to be aware of the potential of electrospinning in the mid-1990s (160). In the last two decades, potential usefulness of electrospun nanofibrous scaffolds have been demonstrated in a variety of in biomedical applications including wound dressing (161), artificial blood vessels (162), protective clothing material (163), drug release membrane (164). This motivates further research activities in this area of fiber production technology.

2.8.2 Experimental setup and the electrospinning process

A standard electrospinning setup consists of four basic components (as shown in Figure 3). A syringe pump, with a metal needle tip, a high voltage power supply and a grounded collector. The polymer is either melted or dissolved in a solvent, and then fed into the syringe.

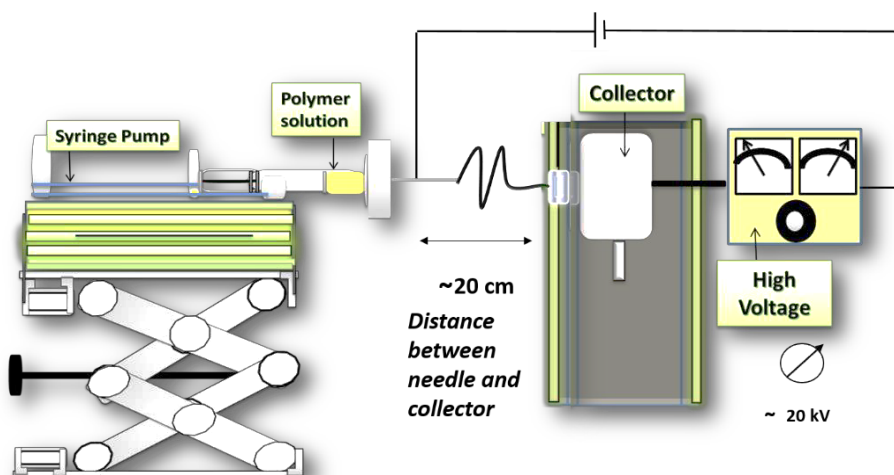


Figure 3 A standard electrospinning set consist of a syringe pump, with a metal needle tip, a high voltage power supply and a grounded collector.

In the electrospinning process, a polymer solution is loaded into the syringe of a syringe pump which has a metal syringe needle tip (82). The flow rate of solution is maintained by the syringe pump. An electric field is generated via a high voltage power supply to create an electrostatic force between the needle and the collector. This electrostatic force induces charge instability at the surface of the droplet, which is directly opposite to its surface tension (165). Eventually it overcomes the surface tension and a polymer solution jet is ejected with whipping motion from the needle tip. During the ejection process, the hemispherical surface of the fluid at the tip of the needle that elongates to form a conical shape known as the Taylor cone (166). Furthermore, the jet travels in the electric field and undergoes chaotic bending called whipping (167) before arriving at the collector electrode. Within the space between the needle tip and the collector, the solvent rapidly evaporates thus leading to the deposition of polymer fibers onto the collector electrode.

The arrangement of the electrospinning set up could be either horizontal or vertical as shown in Figure 4 (4A and 4B). These two-different types of electrospinning set-up have been studied to optimize fiber morphology (168). Gravitational force can play a role versus the electrostatic force, thus differentiating their effect on the fiber morphology. In the vertical setup, the gravitational force and the electrostatic force are in line and are acting in the same direction (Figure 4A) while in the horizontal set-up, the electrostatic force and gravitational force are perpendicular direction to each other (Figure 4B).

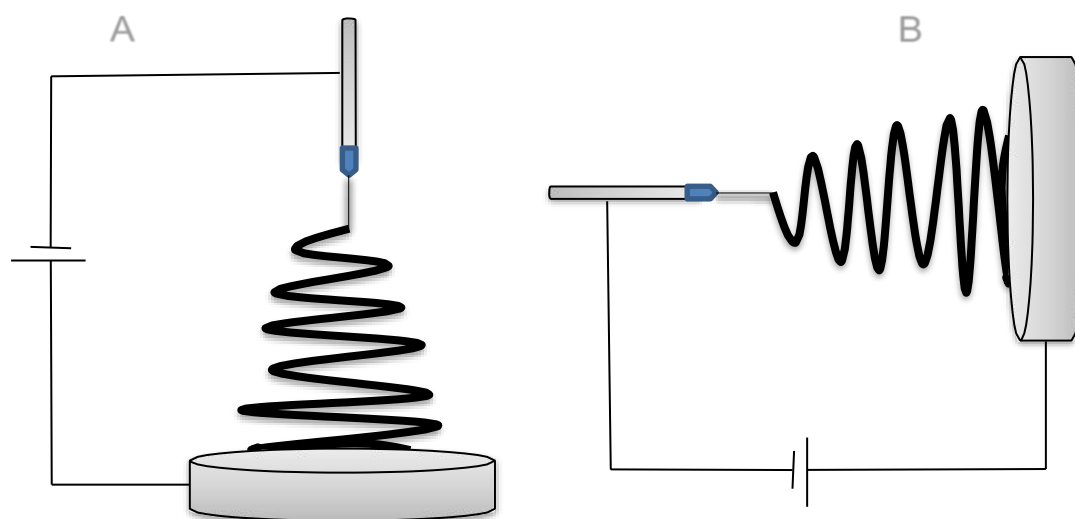


Figure 4 A Vertical set-ups for electrospinning B Horizontal set-ups for electrospinning

The difference in the horizontal versus the vertical electrospinning setup and the effect of gravitational forces on the process have been investigated. It has been demonstrated that gravity plays a role in influencing the shape of the Taylor cone although the effect of the gravitational force is relatively small compared to the electrostatic force being exerted on the polymer solution. This effect results in a variation in fiber diameter (12). In another study, the authors reported that for solid fibers the vertical set up produced smaller and finer fibers as the gravitational and electrostatic forces acted in the same direction (169). Fiber morphology of solid fiber does depends on the electrospinning setup arrangement. Fiber morphology was also found to be the finest with the vertical set up. In the horizontal setup, the average fiber diameter was larger although the fiber size was more uniform with a narrower fiber diameter distribution (170).

The collector used in electrospinning setup is made of a conductive material. In the fiber fabrication process, the conductive collector electrode removes any accumulated charge on the fibers (14). Also, due to this reduction of the repulsive charges it ends up with a compact network of fibers. On the other hand, a nonconductive collector leads to a more loosely packed network of fibers (171).

The electrospinning process normally would result in fibers deposited onto the collector electrode in random fashion. However, in many applications such as tissue engineering, it is desirable to have fibers produced with controlled orientations. The ability to produce oriented fibers has been quite extensively investigated. The main approach has been focusing on the collector electrode design. Some of these designs are shown in Figure 5. The most basic method for fiber alignment is the use of a collector electrode mounted

onto the surface of a rotating drum as illustrated in Figure 5A. This rotating drum is driven by a motor at a controlled speed. During the fiber production, fiber is deposited onto the rotating collector. Degree of alignment is varied by the speed of the drum and the rotation speed is adjusted for maximum fiber alignment (172). An alternative method is to use a knife-edge disk as the collector, as illustrated in Figure 5B. The rotation of the disk coupled with the electrostatic focuses of the electric field, allowing for fiber alignment (173). Parallel plate electrodes are also used as an alternative method for fiber alignment. In such set up two conductive plates are separated by a non-conductive gap and the charged jet to be simultaneously pulled in two directions (174). This causes aligned fibers to be deposited in the space between the plates as illustrated in Figure 5C.

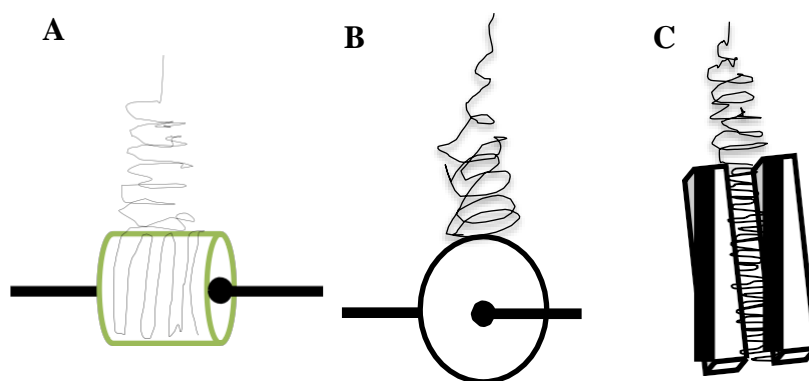


Figure 5 Types of collectors used to align electrospun fibers:
[A] Rotating mandrel [B] Rotating disk and [C] ‘Two-electrodes’ setup

2.8.3 Electrospinning parameters

There are numerous parameters that can influence the outcome of the electrospinning process. These parameters can be broadly classified into three categories. These are the polymer solution parameters, the process parameters and the environmental parameters as shown in Figure 6 (63).

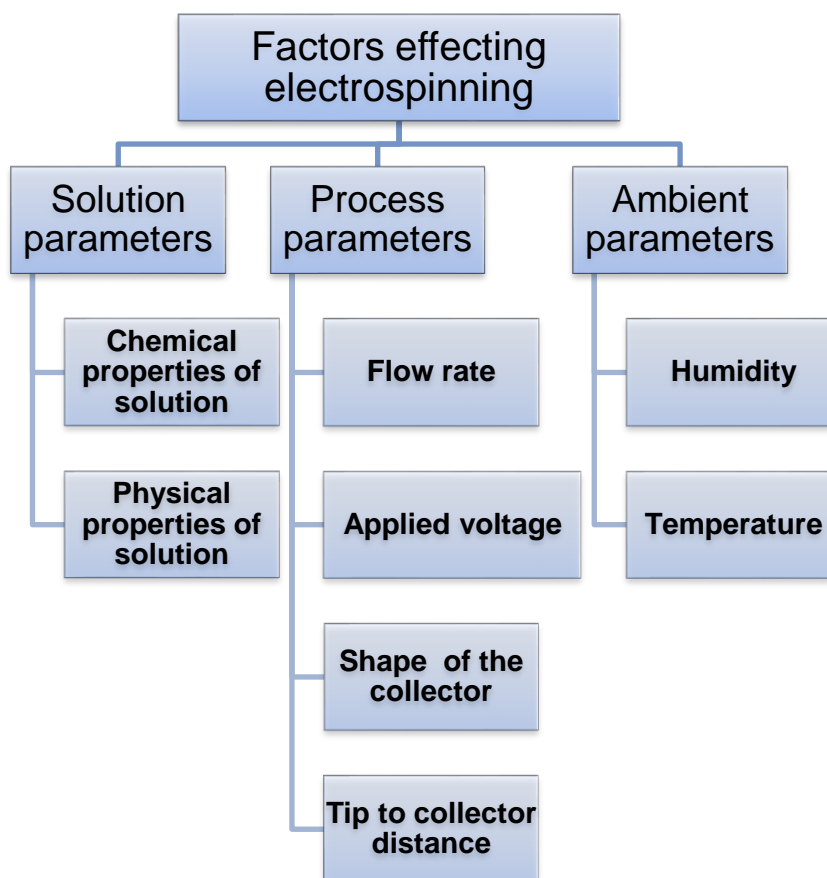


Figure 6 Factors effecting electrospinning

Polymer solution parameters are related to the physical and chemical properties of the polymer and the solvents used whereas the process parameters defines the actual electrospinning conditions used. The importance of the environmental parameters principally referring to the temperature and humidity of the experimental environment was not recognized and investigated until more recently.

Varying of some of these parameters even by small amounts can have a large effect on the quality of resulting fibers. However, it is often difficult to isolate and study the effects of these parameters as many of them are intimately interrelated. For example, modifying the distance between the tip of the needle and collector plate can change the relative electric field strength (175) and a change in polymer solution concentration can alter the solution viscosity (176) .

In general, once the quality goals of the product fiber has been set, the fiber spinning parameters can be adjusted by tuning any of these three groups of parameters. The process is re-iterative and very often, it can be quite challenging to optimize these conditions.

2.8.3.1 Polymer solution parameters

2.8.3.1.1 Polymer solution viscosity, concentration and molecular weight

The physical and chemical properties of a polymer and of the solvent used has a direct effect on whether the polymer can be electrospun into fibers to fabricate scaffolds. Solution viscosity, concentration and the polymer molecular weight has a significant effect on the polymer solution parameters for electrospinning (177). These parameters are interrelated to each other, as polymer concentration and molecular weight are the two important parameters that effect the viscosity of the polymer solution.

Polymer solution viscosity has a strong influence on the success of the electrospinning process. Too low a viscosity would lead to a failure of fiber formation while a very high viscosity may not allow a polymer solution jet to be formed. The viscosity of a polymer solution is a function of the polymer molecular weight and molecular geometry as well as the polymer solution concentration.

Molecular weight and molecular geometry has a direct effect on polymer solution viscosity (87). For a polymer with low molecular weight and at a given solution concentration, the viscosity of the solution would be lower than that of a comparable solution with the same polymer with a higher molecular weight. As a result, the lower molecular weight solution may not be able to allow fiber formation. Instead, the electrospinning process would more likely inclines to fabricate beads. But, at higher molecular weight, the fibers fabricated tend to have a larger average diameter although it does help in the reduction of bead formation (178). High molecular weight polymers are often preferred for use in electrospinning as they can provide the desired viscosity for fiber formation as fiber diameter can be tuned by adjusting the polymer solution concentration (179).

Molecular geometry or architecture can also have an influence on polymer solution viscosity. There are significant differences in viscosity between linear versus branched polymer molecules (150).

In a study of poly(L-lactide) (PLLA), an increase in polymer concentration was found to be accompanied by an increase in fiber diameter and decrease in bead formation (180). In this study, the fiber diameter was found to increase with increasing polymer solution concentration, from 150-500 nm for a 2% of PLLA to 800–3000 nm for a 5% of PLLA solution (181). At low polymer concentrations, the fibers did not dry before reaching the collector and therefore contained a higher percentage of beads. The results was attributed to the inadequacy in the amount of polymer entanglements available (182) .

2.8.3.1.2 Surface Tension

Surface tension of the polymer solution is an important parameter in stabilizing the polymer solution jet in the electrospinning process for fiber fabrication (150). In the electrospinning process the jet can be formed only if the electrostatic force overcomes the solution surface tension. Solution with higher surface tension would lead to the breakup of the jet leading to polymer bead formation (17). It is therefore important to minimize the polymer solution surface tension. One possible approach is by choosing solvents that result in lower solution surface tension.

2.8.3.1.3 Electrical Conductivity

Since the electrospinning process depends on the completion of the electrical circuit between the needle where the polymer solution reside and the collector electrode where the polymer fibers are deposited. Conductivity of the polymer solution is an important parameter that determines its success. Conductivity of a polymer solution depends on the type of polymer and the solvent used. Since most polymers are either poorly or non-electrically conductive, an increase in solution conductivity can be achieved by the addition of small amounts of salt or polyelectrolytes (87). Solution electrical conductivity also has an impact on the fiber diameter, as the conductivity of the solution increases, jet stretching will increase, resulting in smaller fiber diameters (183). However, another study have shown that increasing the salt concentration resulted in an increase in fiber diameters. This was attributed to a delay in the whipping instability due to increased polymer solution conductivity (167).

2.8.3.2 Process parameters

The process variables include the electric potential at needle tip, the distance between needle tip and collecting electrode, the polymer solution flow rate, the needle tip design and the collector geometry.

2.8.3.2.1 Needle of Tip to Collector distance

The distance between the needle tip to the collector determines the flight time of the polymer solution jet leading to the formation of solidified fiber at the collector. Several studies show that a decrease in this distance, regardless of the concentration of the polymer solution, results in the formation of wet fibers and beaded structures (184). On other hand, increasing this distance decreases the electric field gradient (12), which also results in bead formation. Some groups observed bead formation at shorter distances, which was eliminated when distance was increased (185). Thus, a balance between tip to collector distance or flight time and solution parameters is necessary for successful fiber formation and for desirable fiber diameter and morphology to be realized.

2.8.3.2.2 Applied Voltage

Applied voltage has been found to be one of the most crucial experimental parameters that affects the electrospinning results (177). However, some contradicting effects of voltage on fiber morphology and diameters have been reported. Fine fiber morphology of polyethylene oxide nanofibers were fabricated using at relatively low voltage of 5.5 kV, whereas at higher potentials these fibers had a high density of beads (186). One of studies also found that, polystyrene (PS) dissolved in the mixture of tetrahydrofuran (THF) and *N,N*-dimethyl formamide (DMF) improving the morphology of the fibers and reduced beading by increasing voltage (187). These contradicting views are due to the different solvents systems and polymers being used. Effect of voltage is a depending factor or coupled with other parameters of solution parameters including polymer

properties, solvent properties, surface tension of polymer solution and solution conductivity.

2.8.3.2.3 Flow Rate

Polymer solution flow rate determines the amount of solution being exposed to the electric field at a given time. Studies has revealed that with the use of a solvent having a faster evaporation rate, a lower flow rate results in the finer fiber (188). Although, a clear relationship between the flow rate and fiber diameter was not found, its influence on fiber morphology is quite distinct. The dimension of the needle also has an influence on fiber sizes. Smaller needle orifices have been reported to contribute to smaller fiber diameter (189).

2.8.3.3 Environmental parameters

Variations in environmental conditions can have a significant effect on the electrospinning process. This effect in increasing pronounce as the dimension of the fiber decreases. The two most important factors defining the environment conditions are temperature and humidity. Depending on the specific polymer/solvent combination used, small variations in these parameters can result in a large effect on the resulting fiber morphology and diameter. Due to the relative ease in controlling the environmental humidity, most of the studies have been on its effect. Relative humidity plays a critical role with the electrospinning process, making it difficult to fabricate scaffolds under certain conditions. For example, at lower humidities the polymer solution may dry up so quickly, causing the needle to clog and impossible to fabricate fibers (190) whereas,

in high humidity the technique fails to fabricate any fibers and electrospinning leading to the formation of beads occurs instead (191) (192).

To optimize the morphology of electrospun fibers, polymer solution parameters and processing conditions have been extensively studied over the past decade. On the other hand, there have been relatively few reports on the effect of ambient parameters on fiber morphology. One study involved a systematic investigation of the effect of temperature on fiber diameter(193). In this study, of effect of temperature shows that fiber diameter of poly (vinylidene fluoride) decreased with increasing temperatures (194). This decrease in diameter is attributed to the decrease in viscosity of the polymer solution at increased temperatures. Lower viscosity allows the columbic forces to increase stretching giving finer fibers. In related studies of the effect of temperature on electrospun silk nanofibers, a change in morphology of nanofibers from circular to flat with increasing of ambient temperature from 25 °C to 75 °C (195) was observed. The properties of solvent can play a role in influencing the effect of relative humidity on electrospinning outcome. When water was used as a solvent of polymer solution. Evaporation of water in the polymer solution would increase with decreasing environmental humidity leading to a shorter time to solidification of the polymer solution fiber. This was the case when an aqueous solution of poly(ethylene glycol)(PEG) was used in the electrospinning process. (10, 15). On the other hand, when alcohol or other water miscible solvents that is capable of absorbing water is used, an increase in humidity will result in the polymer solution absorbing water leading to a longer drying time. This would result in a longer stretching time leading to smaller diameter fiber formation (196, 197). In related studies of the effect of humidity on

electrospinning, correlation between fiber diameter and solvent systems used have been observed. The diameter of polyamide 4.6, polyamide 6.9, polyethylene oxide and, poly(vinylpyrrolidone) decreases with increasing relative humidity (198, 199). But, the diameter of cellulose acetate, Polyetherimide (PEI) increases with increasing relative humidity (197, 200). Another study of the humidity effect on poly(acrylonitrile) fiber formation also shows that an increase in relative humidity resulted in an increase in fiber diameter. The author proposed that the presence of more water molecules between the needle and collector at a high relative humidity decreases the intensity of the electric field leading to an increase in fiber diameter (201). All these studies indicate, that humidity and temperature have important effects on both diameter and morphology of electrospun nanofibers. However there is no systematic understanding of the relationship between humidity and the polymer solution properties.

2.9 Stabilization of electrospun collagen fiber

Collagen fiber in its native state is stable in the aqueous environment. This is due to its unique three-dimension stereochemistry that allow specific hydrogen bonding to generate its nature structure. However, collagen nanofibers produced by processes such as electrospinning are not stable in water. In fact, they disintegrate readily upon exposure to water or any aqueous media due to the inability to regenerate the nature stereochemistry. This problem is not unique to the use of the electrospinning process. Nevertheless, in order to make use of these fibers in the fabrication of scaffold for tissue engineering, they need to be stabilized at least temporarily. Several approaches have been used in the

stabilization of regenerated protein materials. The commonest approach is to use a chemical approach making use of chemical crosslinking agents. To avoid the potential toxicity of the chemical crosslinkers, physical methods have also been explored (202-204).

2.9.1 Chemical methods

Various techniques have been developed to impart aqueous stability to protein based fibers. Chemical crosslinking is one of the common approach for stabilizing collagen fiber in an aqueous environment (205). Among the chemical crosslinking agents available, glutaraldehyde is one of the most commonly used. When compared with other know chemical crosslinking agents, glutaraldehyde gives the highest degree of crosslinking to the material (206, 207). At higher concentration glutaraldehyde forms, long polymeric chains, having potential to link residues in a protein that are spaced far apart and thereby enhance the extent of crosslink formation. Studies have shown that collagen samples crosslinked using glutaraldehyde vapor for 12 hours, had an 18% reduction in porosity compared to the uncrosslinked or as fabricated sample (208). One of the first study on electrospun collagen fibers used glutaraldehyde vapor as the crosslinking agent (209, 210). But, one of the drawbacks using glutaraldehyde as a chemical crosslinking agent is the introduction of cytotoxicity into the collagen scaffold and as the scaffold degrades, the glutaraldehyde released would result in significant cell death (21, 211).

Another commonly used method is via the carbodiimide approach. In this approach the crosslinking agent can be either cyanamide or 1-ethyl-3-(3-dimethyl aminopropyl) carbodiimide (EDC) (212, 213). EDC is the most commonly studied. It has been used to enhance the stability of collagen scaffolds in the presences of N-Hydroxysuccinimide (NHS) and the degree of crosslinking of the collagen material can be controlled by varying the EDC/NHS concentration (214). When EDC is used as crosslinking agent for collagen scaffolds, the effect of crosslinking lasted up to three months (215).

Genipin is a natural crosslinking agent, and it is derived from geniposide found in the fruits of *Gardenia jasminoides* (26). Genipin was originally used as a food dye before its crosslinking properties was discovered. Genipin has been found to be ~10,000 times less cytotoxic than glutaraldehyde.

Genipin crosslinked electrospun collagen scaffolds showed remarkable changes in morphologies and pore sizes and the swelling ratio of the scaffolds could be tailored by adjusting crosslinking condition (26, 216, 217).

2.9.2 Physical stabilization

Contrast to the use of chemical agents to create bonds to stabilize polymer structures, the same can be achieved by non-chemical means (218). For example, thermal annealing can be used to impart aqueous stability to electrospun poly(vinyl alcohol) fibers by increasing the crystallinity of the polymer matrix without imparting significant chemical structural changes (29). In addition, mechanical strength of the electrospun polysulfone fiber

membranes, poly(L-lactic acid) (219) and poly(ϵ -caprolactone) (220) fiber mats can be improved by thermal annealing (221). Since no new chemicals are introduced, physical crosslinking methods have the advantages of being non-toxic and simple to implement.

2.9.2.1 Ion implantation

Ion beam treatment is one of the unique physical processing techniques based on accelerating ions with the required energy and then bombarding them on the target. Ion implantation takes place within a vacuum chamber and it offers us the freedom to choose ion species energy, current and dose (218). This beam of high-speed ions is focused on penetrating the surface and, induce chemical changes (222). Ion implantation is well known for its controllability, reproducibility and is independent of many of the constraints associated with other processing methods (30). This method of energy transfer offers the opportunity to be investigated as a new and novel approach to crosslinking electrospun collagen fibers.

This unique approach modifies the surface without damaging the surface morphology of the polymer fiber with ion species of your own choice. Helium ions have been implanted onto bulk collagen thin sheets to enhance their stability (223).

For a tissue engineering scaffold, the ability to tailor its stiffness, while controlling the dose delivery, is one of the most interesting feature of ion implantation. Ion implantation on fibers were also established by successfully implanting oxygen ions into electrospun polyurethane (PU) fibers (27) . This has been successfully

implemented onto the non-woven electrospun poly(vinyl alcohol) (PVA) fiber mats by using nitrogen and helium ions (29, 30) . The successful use of the reactive nitrogen ion indicates that it is also possible to perform chemical modification on electrospun polymer fibers. This offers an opportunity to impart or enhance desirable properties into electrospun tissue engineering scaffold materials. For example, nitrogen ions can be implanted to enhance cell adhesion and proliferation on scaffolds (28-30) . It is the intention in this thesis to investigate the effect of ion implantation on the stability of electrospun nanofibers.

2.9.2.1.1 Simulation for ion implantation

Simulation provides a basis for the implantation of ions into the material of interest and estimates the depth of the ion implanted and kinetic energy transfer (224) .

Stopping and Range of Ions in Matter (SRIM), is a computer simulation software package and the screen shot of the software is shown in the Figure 7. SRIM is used to estimate the ion trajectory during implantation experiments. Calculation, for the estimation is organized by using Monte-Carlos (statistical) algorithms. During the calculation, it allows the ion to make the jumps between calculated collisions and then averaging the collision results over the intervening gap.



Figure 7 Screen shot of Stopping and Range of Ions in Matter (SRIM), is a computer simulation software package

Transport of Ion in Matter (TRIM), is a software that is included in the SRIM program package. The screen shot is shown in Figure 8 (224, 225). TRIM allows simulation of up to eight layers of different material compositions. TRIM, estimates both the final 3D distribution of the ions and also all kinetic phenomena associated with the ion's energy loss as target damage, sputtering, ionization, and phonon production. These simulations help to calculate the collision event associated with energetic ion and gives an informative plot of collision event.

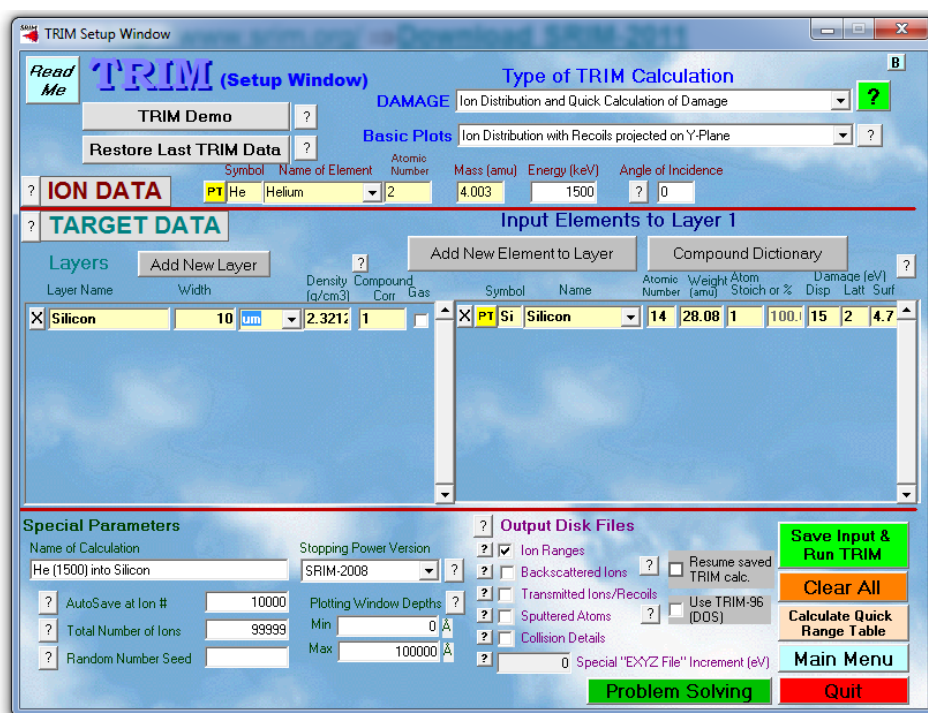


Figure 8 The screen shot of Transport of Ion in Matter (TRIM), is a software that is included in the SRIM program package.

2.9.2.2 Ion beam modification on polymer

There are two major interactions between the energetic ions and the material occurs during implantation. These are nuclear stopping and electronic stopping. When the energetic ions collide with the nuclei of the lattice atom, it is referred to as nuclear stopping and with this defect are created in the crystal structure. On the other hand, when the energetic ions collide with electrons of the lattice atoms, it is then termed as electronic stopping. At the end, the ion reaches the target through the implantation path. Due to these bombardments of the ions chemical modification are induced.

Polymer is a semi-crystalline material and ions can interact with both the crystalline and amorphous domains. Depending on the structure of a polymer chain, for some polymers, ion implantation can lead to a lowering of the molecular weight (226). On the other hand, for some other polymers, the ionization process could lead to the formation of free radicals that allow the chains to crosslink and thereby increase the molecular weight and stability (226). In an implantation process, both of these processes coexist, but usually one dominates over the other leading to either an increase or decrease in the polymer molecular weight (227). It is important to select the correct implantation parameters such as ion species, energy, beam current and dose to induce the desired chemical modifications (226). The ability to control these implantation parameters is very critical as excessive ion deposition, in the form of energy could result in permanent damage to the material (27, 28).

Usefulness of ion implantation to modify materials properties have been demonstrated. By introducing chemical modifications via boron ion implantation into polyimide and polyethersulfone matrices, the moisture uptake behavior of both polymer membranes was modified (228). The water contact angle of polyethylene was increased or decreased by the implantation of nitrogen (229) or oxygen ions respectively (230). Tribological properties of polyethylene were also modified via helium, argon (231) and nitrogen ion implantation (232).

2.9.2.3 Ion beam treatment for cell compatibility

The presence of nitrogen functionalities on a polymer surface has a strong influence on protein adsorption and cell adhesion (233). One of the studies improved the adhesion of endothelial cells on polytetrafluoroethylene films after neon ion implantation (234). On the other hand, fluorine ion implantation can be used to reduce cell attachment on poly(methyl methacrylate) to reduce the long-term failure rate for ophthalmic implants such as intraocular lens (235).

The induced ion has also been used to successfully modify the surface of natural polymers. It has been used to treat collagen films to control platelet adhesion and plasma protein adsorption (236).

It is the purpose of this thesis to study the preparation of collagen type I nanofibers by electrospinning. The electrospinning process will be optimized and the effect of humidity on fiber quality will be investigated. In addition, the method of ion implantation will be investigated as a method for crosslinking and stabilizing the electrospun collagen fibers. A chemically inert ion (helium) and a chemically reactive ion (nitrogen) will be studied to understand the chemical structural changes due to ion implantation and their correlation to the aqueous stability of the fibers. The resulting chemical and structural changes in the ion implanted collagen fibers will be examined. Stability of the ion implanted collagen fibers will be assessed in an aqueous environment using both water and cell culture media as the testing media.

Reference:

1. Wójtowicz J, Leszczyńska J, Walenko K, Lewandowska-Szumieł M. Tissue engineered products for pediatric patients. *Postępy Nauk Medycznych*. 2011.
2. Ikada Y. Challenges in tissue engineering. *Journal of the Royal Society Interface*. 2006;3(10):589-601.
3. Goldberg D, French B, Abt P, Gilroy R. Increasing the number of organ transplants in the United States by optimizing donor authorization rates. *American Journal of Transplantation*. 2015;15(8):2117-25.
4. Ramakrishna S, Ramalingam M, Kumar TS, Soboyejo WO. *Biomaterials: a nano approach*: CRC Press; 2016.
5. Dong C, Lv Y. Application of collagen scaffold in tissue engineering: recent advances and new perspectives. *Polymers*. 2016;8(2):42.
6. Perán M, García MA, Lopez-Ruiz E, Jiménez G, Marchal JA. How can nanotechnology help to repair the body? Advances in cardiac, skin, bone, cartilage and nerve tissue regeneration. *Materials*. 2013;6(4):1333-59.
7. Chan B, Leong K. Scaffolding in tissue engineering: general approaches and tissue-specific considerations. *European spine journal*. 2008;17(4):467-79.
8. O'Brien FJ. Biomaterials & scaffolds for tissue engineering. *Materials today*. 2011;14(3):88-95.
9. Cen L, Liu W, Cui L, Zhang W, Cao Y. Collagen tissue engineering: development of novel biomaterials and applications. *Pediatric research*. 2008;63(5):492-6.
10. Dvir T, Timko BP, Kohane DS, Langer R. Nanotechnological strategies for engineering complex tissues. *Nature nanotechnology*. 2011;6(1):13-22.
11. Khang G. *Handbook of Intelligent Scaffolds for Tissue Engineering and Regenerative Medicine*: CRC Press; 2017.
12. Bedian L, Rodríguez AMV, Vargas GH, Parra-Saldivar R, Iqbal HM. Bio-based materials with novel characteristics for tissue engineering applications—A review. *International Journal of Biological Macromolecules*. 2017.
13. Li WJ, Laurencin CT, Caterson EJ, Tuan RS, Ko FK. Electrospun nanofibrous structure: a novel scaffold for tissue engineering. *Journal of Biomedical Materials Research Part A*. 2002;60(4):613-21.

14. Dhandayuthapani B, Yoshida Y, Maekawa T, Kumar DS. Polymeric scaffolds in tissue engineering application: a review. *International Journal of Polymer Science*. 2011;2011.
15. Murphy CM, Haugh MG, O'Brien FJ. The effect of mean pore size on cell attachment, proliferation and migration in collagen–glycosaminoglycan scaffolds for bone tissue engineering. *Biomaterials*. 2010;31(3):461-6.
16. Karahan M, Nuran R. *Tissue Engineering and New Biomaterials*. Bio-orthopaedics: Springer; 2017. p. 65-70.
17. Mauck RL, Hung CT, Ateshian GA. Modeling of neutral solute transport in a dynamically loaded porous permeable gel: implications for articular cartilage biosynthesis and tissue engineering. *Journal of biomechanical engineering*. 2003;125(5):602-14.
18. Naahidi S, Jafari M, Logan M, Wang Y, Yuan Y, Bae H, et al. Biocompatibility of hydrogel-based scaffolds for tissue engineering applications. *Biotechnology Advances*. 2017.
19. Polak JM, Bishop AE. Stem cells and tissue engineering: past, present, and future. *Annals of the New York Academy of Sciences*. 2006;1068(1):352-66.
20. Humphrey JD, Dufresne ER, Schwartz MA. Mechanotransduction and extracellular matrix homeostasis. *Nature reviews Molecular cell biology*. 2014;15(12):802-12.
21. Rana D, Ratheesh G, Ramakrishna S, Ramalingam M. Nanofiber composites in cartilage tissue engineering. *Nanofiber Composites for Biomedical Applications*. 2017:325.
22. Zhou X, Qiu S, Xing W, Gangireddy CSR, Gui Z, Hu Y. Hierarchical Polyphosphazene@ Molybdenum Disulfide Hybrid Structure for Enhancing the Flame Retardancy and Mechanical Property of Epoxy Resins. *ACS Applied Materials & Interfaces*. 2017.
23. Cortese B, Gigli G, Riehle M. Mechanical gradient cues for guided cell motility and control of cell behavior on uniform substrates. *Advanced Functional Materials*. 2009;19(18):2961-8.
24. Zaari N, Rajagopalan P, Kim SK, Engler AJ, Wong JY. Photopolymerization in microfluidic gradient generators: microscale control of substrate compliance to manipulate cell response. *Advanced Materials*. 2004;16(23-24):2133-7.
25. Pek YS, Wan AC, Ying JY. The effect of matrix stiffness on mesenchymal stem cell differentiation in a 3D thixotropic gel. *Biomaterials*. 2010;31(3):385-91.

26. Levy-Mishali M, Zoldan J, Levenberg S. Effect of scaffold stiffness on myoblast differentiation. *Tissue Engineering Part A*. 2009;15(4):935-44.
27. Collins JM, Ayala P, Desai TA, Russell B. Three-Dimensional Culture with Stiff Microstructures Increases Proliferation and Slows Osteogenic Differentiation of Human Mesenchymal Stem Cells. *Small*. 2010;6(3):355-60.
28. Chen CS, Mrksich M, Huang S, Whitesides GM, Ingber DE. Geometric control of cell life and death. *Science*. 1997;276(5317):1425-8.
29. Mathieu PS, Lobo EG. Cytoskeletal and focal adhesion influences on mesenchymal stem cell shape, mechanical properties, and differentiation down osteogenic, adipogenic, and chondrogenic pathways. *Tissue Engineering Part B: Reviews*. 2012;18(6):436-44.
30. Choi YS, Vincent LG, Lee AR, Dobke MK, Engler AJ. Mechanical derivation of functional myotubes from adipose-derived stem cells. *Biomaterials*. 2012;33(8):2482-91.
31. Frantz C, Stewart KM, Weaver VM. The extracellular matrix at a glance. *J Cell Sci*. 2010;123(24):4195-200.
32. Tauseef M, Aqil M, Mehta D. Signaling Mechanisms Regulating Vascular Endothelial Barrier Function. *Emerging Applications, Perspectives, and Discoveries in Cardiovascular Research: IGI Global*; 2017. p. 17-42.
33. Peach MS, Ramos DM, James R, Morozowich NL, Mazzocca AD, Doty SB, et al. Engineered stem cell niche matrices for rotator cuff tendon regenerative engineering. *PloS one*. 2017;12(4):e0174789.
34. Li Y, Xiao Y, Liu C. The horizon of materiobiology: A perspective on material-guided cell behaviors and tissue engineering. *Chemical Reviews*. 2017;117(5):4376-421.
35. Resende RR, Fonseca EA, Tonelli FM, Sousa BR, Santos AK, Gomes KN, et al. Scale/topography of substrates surface resembling extracellular matrix for tissue engineering. *Journal of biomedical nanotechnology*. 2014;10(7):1157-93.
36. Guarino V, Causa F, Ambrosio L. Bioactive scaffolds for bone and ligament tissue. *Expert review of medical devices*. 2007;4(3):405-18.
37. Ramakrishna S. *An introduction to electrospinning and nanofibers*: World Scientific; 2005.
38. Knecht S, Erggelet C, Endres M, Sittlinger M, Kaps C, Stüssi E. Mechanical testing of fixation techniques for scaffold-based tissue-engineered grafts. *Journal of Biomedical Materials Research Part B: Applied Biomaterials*. 2007;83(1):50-7.
39. Pihlajamäki HK, Salminen ST, Tynninen O, Böstman OM, Laitinen O. Tissue restoration after implantation of polyglycolide, polydioxanone, polylevolactide, and

- metallic pins in cortical bone: an experimental study in rabbits. *Calcified tissue international*. 2010;87(1):90-8.
40. Erggelet C, Endres M, Neumann K, Morawietz L, Ringe J, Haberstroh K, et al. Formation of cartilage repair tissue in articular cartilage defects pretreated with microfracture and covered with cell-free polymer-based implants. *Journal of Orthopaedic Research*. 2009;27(10):1353-60.
 41. Ohara T, Itaya T, Usami K, Ando Y, Sakurai H, Honda MJ, et al. Evaluation of scaffold materials for tooth tissue engineering. *Journal of Biomedical Materials Research Part A*. 2010;94(3):800-5.
 42. Ulery BD, Nair LS, Laurencin CT. Biomedical applications of biodegradable polymers. *Journal of polymer science part B: polymer physics*. 2011;49(12):832-64.
 43. Hamburg MA, Collins FS. The path to personalized medicine. *N Engl J Med*. 2010;2010(363):301-4.
 44. Hegewald AA, Knecht S, Baumgartner D, Gerber H, Endres M, Kaps C, et al. Biomechanical testing of a polymer-based biomaterial for the restoration of spinal stability after nucleotomy. *Journal of orthopaedic surgery and research*. 2009;4(1):25.
 45. Niaounakis M. *Biopolymers: processing and products*: William Andrew; 2014.
 46. Gruber R, Weich H, Dullin C, Schliephake H. Ectopic bone formation after implantation of a slow release system of polylactid acid and rhBMP-2. *Clinical oral implants research*. 2009;20(1):24-30.
 47. Uto S, Nishizawa S, Takasawa Y, Asawa Y, Fujihara Y, Takato T, et al. Bone and cartilage repair by transplantation of induced pluripotent stem cells in murine joint defect model. *Biomedical Research*. 2013;34(6):281-8.
 48. Inui A, Kokubu T, Makino T, Nagura I, Toyokawa N, Sakata R, et al. Potency of double-layered Poly L-lactic Acid scaffold in tissue engineering of tendon tissue. *International orthopaedics*. 2010;34(8):1327-32.
 49. Xie C, Ritchie RP, Huang H, Zhang J, Chen YE. Smooth Muscle Cell Differentiation In Vitro. *Arteriosclerosis, thrombosis, and vascular biology*. 2011;31(7):1485-94.
 50. François S, Sarra-Bournet C, Jaffre A, Chakfé N, Durand B, Laroche G. Characterization of an air-spun poly (L-lactic acid) nanofiber mesh. *Journal of Biomedical Materials Research Part B: Applied Biomaterials*. 2010;93(2):531-43.
 51. Betancourt T, Byrne JD, Sunaryo N, Crowder SW, Kadapakkam M, Patel S, et al. PEGylation strategies for active targeting of PLA/PLGA nanoparticles. *Journal of Biomedical Materials Research Part A*. 2009;91(1):263-76.

52. Gavenis K, Schneider U, Groll J, Schmidt-Rohlfing B. BMP-7-loaded PGLA microspheres as a new delivery system for the cultivation of human chondrocytes in a collagen type I gel: the common nude mouse model. *Int J Artif Organs*. 2010;33(1):45-53.
53. Liu Y, Schwendeman SP. Mapping microclimate pH distribution inside protein-encapsulated PLGA microspheres using confocal laser scanning microscopy. *Molecular pharmaceutics*. 2012;9(5):1342-50.
54. Valizadeh H, Mohammadi G, Ehyaei R, Milani M, Azhdarzadeh M, Zakeri-Milani P, et al. Antibacterial activity of clarithromycin loaded PLGA nanoparticles. *Die Pharmazie-An International Journal of Pharmaceutical Sciences*. 2012;67(1):63-8.
55. Sachlos E, Czernuszka J. Making tissue engineering scaffolds work. Review: the application of solid freeform fabrication technology to the production of tissue engineering scaffolds. *Eur Cell Mater*. 2003;5(29):39-40.
56. Hutmacher DW, Schantz T, Zein I, Ng KW, Teoh SH, Tan KC. Mechanical properties and cell cultural response of polycaprolactone scaffolds designed and fabricated via fused deposition modeling. *Journal of Biomedical Materials Research Part A*. 2001;55(2):203-16.
57. Woodruff MA, Hutmacher DW. The return of a forgotten polymer—polycaprolactone in the 21st century. *Progress in Polymer Science*. 2010;35(10):1217-56.
58. Yoshimoto H, Shin Y, Terai H, Vacanti J. A biodegradable nanofiber scaffold by electrospinning and its potential for bone tissue engineering. *Biomaterials*. 2003;24(12):2077-82.
59. Toh WS, Lee EH, Cao T. Potential of human embryonic stem cells in cartilage tissue engineering and regenerative medicine. *Stem Cell Reviews and Reports*. 2011;7(3):544-59.
60. Walpoth BH, Bowlin GL. The daunting quest for a small diameter vascular graft. *Expert review of medical devices*. 2005;2(6):647-51.
61. Cheung H-Y, Lau K-T, Lu T-P, Hui D. A critical review on polymer-based bio-engineered materials for scaffold development. *Composites Part B: Engineering*. 2007;38(3):291-300.
62. Bhardwaj N, Kundu SC. Electrospinning: a fascinating fiber fabrication technique. *Biotechnology Advances*. 2010;28(3):325-47.
63. Malafaya PB, Silva GA, Reis RL. Natural–origin polymers as carriers and scaffolds for biomolecules and cell delivery in tissue engineering applications. *Advanced drug delivery reviews*. 2007;59(4):207-33.

64. Barnes CP, Sell SA, Boland ED, Simpson DG, Bowlin GL. Nanofiber technology: designing the next generation of tissue engineering scaffolds. *Advanced drug delivery reviews*. 2007;59(14):1413-33.
65. Simpson DG, Bowlin GL. Tissue-engineering scaffolds: can we re-engineer mother nature? *Expert review of medical devices*. 2006;3(1):9-15.
66. Zhu J, Marchant RE. Design properties of hydrogel tissue-engineering scaffolds. *Expert review of medical devices*. 2011;8(5):607-26.
67. Sottile J, Hocking DC. Fibronectin polymerization regulates the composition and stability of extracellular matrix fibrils and cell-matrix adhesions. *Molecular biology of the cell*. 2002;13(10):3546-59.
68. Sell S, McClure MJ, Barnes CP, Knapp DC, Walpoth BH, Simpson DG, et al. Electrospun polydioxanone–elastin blends: potential for bioresorbable vascular grafts. *Biomedical Materials*. 2006;1(2):72.
69. Boland ED, Matthews JA, Pawlowski KJ, Simpson DG, Wnek GE, Bowlin GL. Electrospinning collagen and elastin: preliminary vascular tissue engineering. *Front Biosci*. 2004;9(1422):e32.
70. Daamen W, Nillesen S, Hafmans T, Veerkamp J, Van Luyn M, Van Kuppevelt T. Tissue response of defined collagen–elastin scaffolds in young and adult rats with special attention to calcification. *Biomaterials*. 2005;26(1):81-92.
71. Rabaud M, Lefebvre F, Ducassou D. In vitro association of type III collagen with elastin and with its solubilized peptides. *Biomaterials*. 1991;12(3):313-9.
72. Lim DW, Nettles DL, Setton LA, Chilkoti A. In situ cross-linking of elastin-like polypeptide block copolymers for tissue repair. *Biomacromolecules*. 2007;9(1):222-30.
73. Daamen WF, Nillesen ST, Wismans RG, Reinhardt DP, Hafmans T, Veerkamp JH, et al. A biomaterial composed of collagen and solubilized elastin enhances angiogenesis and elastic fiber formation without calcification. *Tissue Engineering Part A*. 2008;14(3):349-60.
74. Heydarkhan-Hagvall S, Schenke-Layland K, Dhanasopon AP, Rofail F, Smith H, Wu BM, et al. Three-dimensional electrospun ECM-based hybrid scaffolds for cardiovascular tissue engineering. *Biomaterials*. 2008;29(19):2907-14.
75. Simionescu DT, Lu Q, Song Y, Lee J, Rosenbalm TN, Kelley C, et al. Biocompatibility and remodeling potential of pure arterial elastin and collagen scaffolds. *Biomaterials*. 2006;27(5):702-13.
76. McManus MC, Boland ED, Koo HP, Barnes CP, Pawlowski KJ, Wnek GE, et al. Mechanical properties of electrospun fibrinogen structures. *Acta Biomaterialia*. 2006;2(1):19-28.

77. McManus MC, Boland ED, Simpson DG, Barnes CP, Bowlin GL. Electrospun fibrinogen: feasibility as a tissue engineering scaffold in a rat cell culture model. *Journal of Biomedical Materials Research Part A*. 2007;81(2):299-309.
78. Mosesson MW, Siebenlist KR, Meh DA. The structure and biological features of fibrinogen and fibrin. *Annals of the New York Academy of Sciences*. 2001;936(1):11-30.
79. Zhang Q, Yan S, Li M. Silk fibroin based porous materials. *Materials*. 2009;2(4):2276-95.
80. Wang M, Jin H-J, Kaplan DL, Rutledge GC. Mechanical properties of electrospun silk fibers. *Macromolecules*. 2004;37(18):6856-64.
81. Jeong L, Lee KY, Park WH, editors. Effect of solvent on the characteristics of electrospun regenerated silk fibroin nanofibers. *Key Engineering Materials*; 2007: Trans Tech Publ.
82. Zarkoob S. Structure and morphology of regenerated silk nano-fibers produced by electrospinning 1998.
83. Zarkoob S, Reneker DH, Ertley D, Eby R, Hudson SD. Synthetically spun silk nanofibers and a process for making the same. *Google Patents*; 2000.
84. Sukigara S, Gandhi M, Ayutsede J, Micklus M, Ko F. Regeneration of Bombyx mori silk by electrospinning—part 1: processing parameters and geometric properties. *Polymer*. 2003;44(19):5721-7.
85. Sukigara S, Gandhi M, Ayutsede J, Micklus M, Ko F. Regeneration of Bombyx mori silk by electrospinning. Part 2. Process optimization and empirical modeling using response surface methodology. *Polymer*. 2004;45(11):3701-8.
86. Jin H-J, Fridrikh SV, Rutledge GC, Kaplan DL. Electrospinning Bombyx mori silk with poly (ethylene oxide). *Biomacromolecules*. 2002;3(6):1233-9.
87. Jin H-J, Chen J, Karageorgiou V, Altman GH, Kaplan DL. Human bone marrow stromal cell responses on electrospun silk fibroin mats. *Biomaterials*. 2004;25(6):1039-47.
88. Liu H, Ge Z, Wang Y, Toh SL, Sutthikhum V, Goh JC. Modification of sericin-free silk fibers for ligament tissue engineering application. *Journal of Biomedical Materials Research Part B: Applied Biomaterials*. 2007;82(1):129-38.
89. Seo YK, Choi GM, Kwon SY, Lee HS, Park YS, Song KY, et al., editors. The biocompatibility of silk scaffold for tissue engineered ligaments. *Key Engineering Materials*; 2007: Trans Tech Publ.

90. Liu H, Fan H, Wang Y, Toh SL, Goh JC. The interaction between a combined knitted silk scaffold and microporous silk sponge with human mesenchymal stem cells for ligament tissue engineering. *Biomaterials*. 2008;29(6):662-74.
91. Dutta PK, Dutta J, Tripathi V. *Chitin and chitosan: Chemistry, properties and applications*. 2004.
92. No HK, Meyers SP. Preparation and characterization of chitin and chitosan—a review. *Journal of aquatic food product technology*. 1995;4(2):27-52.
93. Akman AC, Tıǧlı RS, Gümüşderelioǧlu M, Nohutcu RM. bFGF-loaded HA-chitosan: A promising scaffold for periodontal tissue engineering. *Journal of Biomedical Materials Research Part A*. 2010;92(3):953-62.
94. Mizuno K, Yamamura K, Yano K, Osada T, Saeki S, Takimoto N, et al. Effect of chitosan film containing basic fibroblast growth factor on wound healing in genetically diabetic mice. *Journal of Biomedical Materials Research Part A*. 2003;64(1):177-81.
95. Judith R, Nithya M, Rose C, Mandal A. Application of a PDGF-containing novel gel for cutaneous wound healing. *Life sciences*. 2010;87(1):1-8.
96. Jayakumar R, Prabakaran M, Kumar PS, Nair S, Tamura H. Biomaterials based on chitin and chitosan in wound dressing applications. *Biotechnology Advances*. 2011;29(3):322-37.
97. Malafaya P, Pedro A, Peterbauer A, Gabriel C, Redl H, Reis R. Chitosan particles agglomerated scaffolds for cartilage and osteochondral tissue engineering approaches with adipose tissue derived stem cells. *Journal of Materials Science: Materials in Medicine*. 2005;16(12):1077-85.
98. Heinemann C, Heinemann S, Bernhardt A, Worch H, Hanke T. Novel textile chitosan scaffolds promote spreading, proliferation, and differentiation of osteoblasts. *Biomacromolecules*. 2008;9(10):2913-20.
99. Geng X, Kwon O-H, Jang J. Electrospinning of chitosan dissolved in concentrated acetic acid solution. *Biomaterials*. 2005;26(27):5427-32.
100. Ríos CN, Skoracki RJ, Miller MJ, Satterfield WC, Mathur AB. In vivo bone formation in silk fibroin and chitosan blend scaffolds via ectopically grafted periosteum as a cell source: a pilot study. *Tissue Engineering Part A*. 2009;15(9):2717-25.
101. Gobin AS, Froude VE, Mathur AB. Structural and mechanical characteristics of silk fibroin and chitosan blend scaffolds for tissue regeneration. *Journal of Biomedical Materials Research Part A*. 2005;74(3):465-73.
102. Martins AM, Santos MI, Azevedo HS, Malafaya PB, Reis RL. Natural origin scaffolds with in situ pore forming capability for bone tissue engineering applications. *Acta Biomaterialia*. 2008;4(6):1637-45.

103. Nakamatsu J, Torres FG, Troncoso OP, Min-Lin Y, Boccaccini AR. Processing and characterization of porous structures from chitosan and starch for tissue engineering scaffolds. *Biomacromolecules*. 2006;7(12):3345-55.
104. Young S, Wong M, Tabata Y, Mikos AG. Gelatin as a delivery vehicle for the controlled release of bioactive molecules. *Journal of controlled release*. 2005;109(1):256-74.
105. Ghasemi-Mobarakeh L, Prabhakaran MP, Morshed M, Nasr-Esfahani M-H, Ramakrishna S. Electrospun poly (ϵ -caprolactone)/gelatin nanofibrous scaffolds for nerve tissue engineering. *Biomaterials*. 2008;29(34):4532-9.
106. Zhang Y, Ouyang H, Lim CT, Ramakrishna S, Huang ZM. Electrospinning of gelatin fibers and gelatin/PCL composite fibrous scaffolds. *Journal of Biomedical Materials Research Part B: Applied Biomaterials*. 2005;72(1):156-65.
107. Fan J, Shang Y, Yuan Y, Yang J. Preparation and characterization of chitosan/galactosylated hyaluronic acid scaffolds for primary hepatocytes culture. *Journal of Materials Science: Materials in Medicine*. 2010;21(1):319-27.
108. Tan H, Wu J, Lao L, Gao C. Gelatin/chitosan/hyaluronan scaffold integrated with PLGA microspheres for cartilage tissue engineering. *Acta Biomaterialia*. 2009;5(1):328-37.
109. Sell SA, McClure MJ, Garg K, Wolfe PS, Bowlin GL. Electrospinning of collagen/biopolymers for regenerative medicine and cardiovascular tissue engineering. *Advanced drug delivery reviews*. 2009;61(12):1007-19.
110. Boekhoven J, Stupp SI. 25th anniversary article: supramolecular materials for regenerative medicine. *Advanced Materials*. 2014;26(11):1642-59.
111. Birk DE, Bruckner P. Collagen suprastructures. *Collagen*. 2005:185-205.
112. Villarreal-Gómez LJ, Cornejo-Bravo JM, Vera-Graziano R, Grande D. Electrospinning as a powerful technique for biomedical applications: a critically selected survey. *Journal of Biomaterials Science, Polymer Edition*. 2016;27(2):157-76.
113. Rault I, Frei V, Herbage D, Abdul-Malak N, Huc A. Evaluation of different chemical methods for cross-linking collagen gel, films and sponges. *Journal of Materials Science: Materials in Medicine*. 1996;7(4):215-21.
114. Zhu B. *Electrospun Collagen/Silk Tissue Engineering Scaffolds: Fiber Fabrication, Post-Treatment Optimization, and Application in Neural Differentiation of Stem Cells*: Illinois Institute of Technology; 2017.
115. Okuyama K, Okuyama K, Arnott S, Takayanagi M, Kakudo M. Crystal and molecular structure of a collagen-like polypeptide (Pro-Pro-Gly)₁₀. *Journal of molecular biology*. 1981;152(2):427-43.

116. Deshmukh SN, Dive AM, Moharil R, Munde P. Enigmatic insight into collagen. *Journal of oral and maxillofacial pathology: JOMFP*. 2016;20(2):276.
117. Shoulders MD, Raines RT. Collagen structure and stability. *Annual review of biochemistry*. 2009;78:929-58.
118. Long K. Development of synthetic α -helix mimetics as potent anticancer agents: University of Leeds; 2013.
119. Buehler MJ. Nature designs tough collagen: explaining the nanostructure of collagen fibrils. *Proceedings of the National Academy of Sciences*. 2006;103(33):12285-90.
120. Kolacna L, Bakesova J, Varga F, Kostakova E, Planka L, Necas A, et al. Biochemical and biophysical aspects of collagen nanostructure in the extracellular matrix. *Physiological Research*. 2007;56:S51.
121. Luo C, Stoyanov SD, Stride E, Pelan E, Edirisinghe M. Electrospinning versus fibre production methods: from specifics to technological convergence. *Chemical Society Reviews*. 2012;41(13):4708-35.
122. Stuart BH. *Polymer analysis*: John Wiley & Sons; 2008.
123. Stojanovska E, Canbay E, Pampal ES, Calisir MD, Agha O, Polat Y, et al. A review on non-electro nanofibre spinning techniques. *RSC Advances*. 2016;6(87):83783-801.
124. Albuquerque M, Valera M, Nakashima M, Nör J, Bottino M. Tissue-engineering-based strategies for regenerative endodontics. *Journal of dental research*. 2014;93(12):1222-31.
125. Huang Z-M, Zhang Y-Z, Kotaki M, Ramakrishna S. A review on polymer nanofibers by electrospinning and their applications in nanocomposites. *Composites science and technology*. 2003;63(15):2223-53.
126. Hasan MM, Alam AM, Nayem KA. Application of Electrospinning techniques for the production of tissue Engineering Scaffolds: A review. *European Scientific Journal, ESJ*. 2014;10(15).
127. Zarkoob S, Eby R, Reneker DH, Hudson SD, Ertley D, Adams WW. Structure and morphology of electrospun silk nanofibers. *Polymer*. 2004;45(11):3973-7.
128. Kundu B, Rajkhowa R, Kundu SC, Wang X. Silk fibroin biomaterials for tissue regenerations. *Advanced drug delivery reviews*. 2013;65(4):457-70.
129. Matthews JA, Wnek GE, Simpson DG, Bowlin GL. Electrospinning of collagen nanofibers. *Biomacromolecules*. 2002;3(2):232-8.

130. Ohkawa K, Cha D, Kim H, Nishida A, Yamamoto H. Electrospinning of chitosan. *Macromolecular Rapid Communications*. 2004;25(18):1600-5.
131. Bhattarai P, Thapa K, Basnet R, Sharma S. Electrospinning: how to produce nanofibers using most inexpensive technique? An insight into the real challenges of electrospinning such nanofibers and its application areas. *International Journal of Biomedical and Advance Research*. 2014;5(9):401-5.
132. Teo WE, Ramakrishna S. A review on electrospinning design and nanofibre assemblies. *Nanotechnology*. 2006;17(14):R89.
133. Gibson P, Schreuder-Gibson H, Pentheny C. Electrospinning technology: direct application of tailorable ultrathin membranes. *Journal of Coated Fabrics*. 1998;28(1):63-72.
134. Kannan B, Cha H, Hosie IC. *Electrospinning—Commercial Applications, Challenges and Opportunities*. *Nano-size Polymers*: Springer; 2016. p. 309-42.
135. Yarin AL, Koombhongse S, Reneker DH. Taylor cone and jetting from liquid droplets in electrospinning of nanofibers. *Journal of Applied physics*. 2001;90(9):4836-46.
136. Lee HW, Karim MR, Park JH, Bae DG, Oh W, Cheong IW, et al. Electrospinning and characterisation of poly (vinyl alcohol) blend submicron fibres in aqueous solutions. *Polymers & Polymer Composites*. 2009;17(1):47.
137. Zarghami N, Sheervalilou R, Fattahi A, Mohajeri A, Dadashpour M, Pilehvar-Soltanahmadi Y. An Overview on Application of Natural Substances Incorporated with Electrospun Nanofibrous Scaffolds to Development of Innovative Wound Dressings. *Mini reviews in medicinal chemistry*. 2017.
138. Marcolin C, Draghi L, Tanzi M, Faré S. Electrospun silk fibroin–gelatin composite tubular matrices as scaffolds for small diameter blood vessel regeneration. *Journal of Materials Science: Materials in Medicine*. 2017;28(5):80.
139. Thenmozhi S, Dharmaraj N, Kadirvelu K, Kim HY. Electrospun nanofibers: New generation materials for advanced applications. *Materials Science and Engineering: B*. 2017;217:36-48.
140. Laha A, Sharma CS, Majumdar S. Sustained drug release from multi-layered sequentially crosslinked electrospun gelatin nanofiber mesh. *Materials Science and Engineering: C*. 2017;76:782-6.
141. Ji Y, Li B, Ge S, Sokolov JC, Rafailovich MH. Structure and nanomechanical characterization of electrospun PS/clay nanocomposite fibers. *Langmuir*. 2006;22(3):1321-8.

142. Megelski S, Stephens JS, Chase DB, Rabolt JF. Micro-and nanostructured surface morphology on electrospun polymer fibers. *Macromolecules*. 2002;35(22):8456-66.
143. Subbiah T, Bhat G, Tock R, Parameswaran S, Ramkumar S. Electrospinning of nanofibers. *Journal of Applied Polymer Science*. 2005;96(2):557-69.
144. Abd Razak SI, Wahab IF, Fadil F, Dahli FN, Md Khudzari AZ, Adeli H. A review of electrospun conductive polyaniline based nanofiber composites and blends: processing features, applications, and future directions. *Advances in Materials Science and Engineering*. 2015;2015.
145. Frenot A, Chronakis IS. Polymer nanofibers assembled by electrospinning. *Current opinion in colloid & interface science*. 2003;8(1):64-75.
146. Moghe A, Gupta B. Co-axial electrospinning for nanofiber structures: preparation and applications. *Polymer Reviews*. 2008;48(2):353-77.
147. Migliaresi C, Ruffo GA, Volpato FZ, Zeni D. Advanced electrospinning setups and special fibre and mesh morphologies. *Electrospinning for Advanced Biomedical Applications and Therapies*(eds: NM Neves). 2012:23-68.
148. Boubée de Gramont F. *Electrospinning of Conducting Polymer Fibers for Stretchable Electronics: École Polytechnique de Montréal*; 2017.
149. Huang YS, Kuo CC, Shu YC, Jang SC, Tsen WC, Chuang FS, et al. Highly Aligned and Single-Layered Hollow Fibrous Membranes Prepared from Polyurethane and Silica Blends Through a Two-Fluid Coaxial Electrospun Process. *Macromolecular Chemistry and Physics*. 2014;215(9):879-87.
150. Rutledge GC, Fridrikh SV. Formation of fibers by electrospinning. *Advanced drug delivery reviews*. 2007;59(14):1384-91.
151. Lukáš D, Sarkar A, Martinová L, Vodsed'álková K, Lubasova D, Chaloupek J, et al. Physical principles of electrospinning (electrospinning as a nano-scale technology of the twenty-first century). *Textile Progress*. 2009;41(2):59-140.
152. Shin Y, Hohman M, Brenner M, Rutledge G. Experimental characterization of electrospinning: the electrically forced jet and instabilities. *Polymer*. 2001;42(25):09955-67.
153. Deitzel JM, Kleinmeyer J, Harris D, Tan NB. The effect of processing variables on the morphology of electrospun nanofibers and textiles. *Polymer*. 2001;42(1):261-72.
154. Tan S, Inai R, Kotaki M, Ramakrishna S. Systematic parameter study for ultra-fine fiber fabrication via electrospinning process. *Polymer*. 2005;46(16):6128-34.
155. Nuraje N, Khan WS, Lei Y, Ceylan M, Asmatulu R. Superhydrophobic electrospun nanofibers. *Journal of Materials Chemistry A*. 2013;1(6):1929-46.

156. Greiner A, Wendorff JH. Electrospinning: a fascinating method for the preparation of ultrathin fibers. *Angewandte Chemie International Edition*. 2007;46(30):5670-703.
157. Gu S-Y, Wang Z-M, Ren J, Zhang C-Y. Electrospinning of gelatin and gelatin/poly (l-lactide) blend and its characteristics for wound dressing. *Materials Science and Engineering: C*. 2009;29(6):1822-8.
158. Piras A, Nikkola L, Chiellini F, Ashammakhi N, Chiellini E. Development of diclofenac sodium releasing bio-erodible polymeric nanomats. *Journal of nanoscience and nanotechnology*. 2006;6(9-1):3310-20.
159. Pillay V, Dott C, Choonara YE, Tyagi C, Tomar L, Kumar P, et al. A review of the effect of processing variables on the fabrication of electrospun nanofibers for drug delivery applications. *Journal of Nanomaterials*. 2013;2013.
160. Reneker DH, Yarin AL. Electrospinning jets and polymer nanofibers. *Polymer*. 2008;49(10):2387-425.
161. Mit-uppatham C, Nithitanakul M, Supaphol P. Ultrafine electrospun polyamide-6 fibers: effect of solution conditions on morphology and average fiber diameter. *Macromolecular Chemistry and Physics*. 2004;205(17):2327-38.
162. Chowdhury M, Stylios GK. Analysis of the effect of experimental parameters on the morphology of electrospun polyethylene oxide nanofibres and on their thermal properties. *Journal of the Textile Institute*. 2012;103(2):124-38.
163. Li Z, Wang C. Effects of working parameters on electrospinning. *One-Dimensional Nanostructures*: Springer; 2013. p. 15-28.
164. Rasel SM. An advanced electrospinning method of fabricating nanofibrous patterned architectures with controlled deposition and desired alignment: University of Ontario Institute of Technology (Canada); 2015.
165. Lee K, Kim H, Bang H, Jung Y, Lee S. The change of bead morphology formed on electrospun polystyrene fibers. *Polymer*. 2003;44(14):4029-34.
166. Greiner A, Wendorff J. Functional self-assembled nanofibers by electrospinning. *Self-Assembled Nanomaterials I*: Springer; 2008. p. 107-71.
167. Serra C, Berton N, Bouquey M, Prat L, Hadziioannou G. A predictive approach of the influence of the operating parameters on the size of polymer particles synthesized in a simplified microfluidic system. *Langmuir*. 2007;23(14):7745-50.
168. Zalani MM. Encapsulation of Therapeutic Protein Within Polymeric Nanofiber Using Co-axial Electrospinning: UMP; 2012.

169. Valizadeh A, Farkhani SM. Electrospinning and electrospun nanofibres. *IET nanobiotechnology*. 2013;8(2):83-92.
170. Ahmed FE, Lalia BS, Hashaikh R. A review on electrospinning for membrane fabrication: challenges and applications. *Desalination*. 2015;356:15-30.
171. Tripatanasuwan S, Zhong Z, Reneker DH. Effect of evaporation and solidification of the charged jet in electrospinning of poly (ethylene oxide) aqueous solution. *Polymer*. 2007;48(19):5742-6.
172. Yeow M, Liu Y, Li K. Morphological study of poly (vinylidene fluoride) asymmetric membranes: effects of the solvent, additive, and dope temperature. *Journal of Applied Polymer Science*. 2004;92(3):1782-9.
173. Amiralijan N, Nouri M, Kish MH. Effects of some electrospinning parameters on morphology of natural silk-based nanofibers. *Journal of Applied Polymer Science*. 2009;113(1):226-34.
174. Reneker DH, Yarin AL, Fong H, Koombhongse S. Bending instability of electrically charged liquid jets of polymer solutions in electrospinning. *Journal of Applied physics*. 2000;87(9):4531-47.
175. Thompson C, Chase GG, Yarin A, Reneker D. Effects of parameters on nanofiber diameter determined from electrospinning model. *Polymer*. 2007;48(23):6913-22.
176. Fashandi H, Karimi M. Pore formation in polystyrene fiber by superimposing temperature and relative humidity of electrospinning atmosphere. *Polymer*. 2012;53(25):5832-49.
177. De Vrieze S, Van Camp T, Nelvig A, Hagström B, Westbroek P, De Clerck K. The effect of temperature and humidity on electrospinning. *Journal of materials science*. 2009;44(5):1357.
178. De Schoenmaker B, Van der Schueren L, Ceylan Ö, De Clerck K. Electrospun polyamide 4.6 nanofibrous nonwovens: parameter study and characterization. *Journal of Nanomaterials*. 2012;2012:14.
179. Oğulata RT, İçoğlu Hİ. Interaction between effects of ambient parameters and those of other important parameters on electrospinning of PEI/NMP solution. *The Journal of The Textile Institute*. 2015;106(1):57-66.
180. Fashandi H, Karimi M. Comparative studies on the solvent quality and atmosphere humidity for electrospinning of nanoporous polyetherimide fibers. *Industrial & Engineering Chemistry Research*. 2013;53(1):235-45.
181. Huang L, Bui NN, Manickam SS, McCutcheon JR. Controlling electrospun nanofiber morphology and mechanical properties using humidity. *Journal of polymer science part B: polymer physics*. 2011;49(24):1734-44.

182. van Zuijlen PP, Ruurda JJ, van Veen HA, van Marle J, van Trier AJ, Groenevelt F, et al. Collagen morphology in human skin and scar tissue: no adaptations in response to mechanical loading at joints. *Burns*. 2003;29(5):423-31.
183. Birmingham JD, Vilim V, Kraus VB. Collagen biomarkers for arthritis applications. *Biomarker Insights*. 2006;1:61.
184. Gelse K, Pöschl E, Aigner T. Collagens—structure, function, and biosynthesis. *Advanced drug delivery reviews*. 2003;55(12):1531-46.
185. Reddy N, Reddy R, Jiang Q. Crosslinking biopolymers for biomedical applications. *Trends in biotechnology*. 2015;33(6):362-9.
186. Bowes J, Cater C. Crosslinking of collagen. *Journal of Chemical Technology and Biotechnology*. 1965;15(7):296-304.
187. Ma L, Gao C, Mao Z, Zhou J, Shen J. Enhanced biological stability of collagen porous scaffolds by using amino acids as novel cross-linking bridges. *Biomaterials*. 2004;25(15):2997-3004.
188. Torres-Giner S, Gimeno-Alcaniz JV, Ocio MJ, Lagaron JM. Comparative performance of electrospun collagen nanofibers cross-linked by means of different methods. *ACS Applied Materials & Interfaces*. 2008;1(1):218-23.
189. Wu L, Yuan X, Sheng J. Immobilization of cellulase in nanofibrous PVA membranes by electrospinning. *Journal of Membrane Science*. 2005;250(1):167-73.
190. Sisson K, Zhang C, Farach-Carson MC, Chase DB, Rabolt JF. Evaluation of cross-linking methods for electrospun gelatin on cell growth and viability. *Biomacromolecules*. 2009;10(7):1675-80.
191. Gough JE, Scotchford CA, Downes S. Cytotoxicity of glutaraldehyde crosslinked collagen/poly (vinyl alcohol) films is by the mechanism of apoptosis. *Journal of Biomedical Materials Research Part A*. 2002;61(1):121-30.
192. Hosseinkhani H, Inatsugu Y, Hiraoka Y, Inoue S, Tabata Y. Perfusion culture enhances osteogenic differentiation of rat mesenchymal stem cells in collagen sponge reinforced with poly (glycolic acid) fiber. *Tissue engineering*. 2005;11(9-10):1476-88.
193. Gratzner PF, Lee JM. Control of pH alters the type of cross-linking produced by 1-ethyl-3-(3-dimethylaminopropyl)-carbodiimide (EDC) treatment of acellular matrix vascular grafts. *Journal of Biomedical Materials Research Part A*. 2001;58(2):172-9.
194. Kazenwadel F, Wagner H, Rapp B, Franzreb M. Optimization of enzyme immobilization on magnetic microparticles using 1-ethyl-3-(3-dimethylaminopropyl) carbodiimide (EDC) as a crosslinking agent. *Analytical Methods*. 2015;7(24):10291-8.

195. Jafari-Sabet M, Nasiri H, Ataee R. The Effect of Cross-Linking Agents and Collagen Concentrations on Properties of Collagen Scaffolds. *Journal of Archives in Military Medicine*. 2016;4(4).
196. Singh P, Nagpal R, Singh UP, Manuja N. Effect of carbodiimide on the structural stability of resin/dentin interface. *Journal of conservative dentistry: JCD*. 2016;19(6):501.
197. Huang GP, Shanmugasundaram S, Masih P, Pandya D, Amara S, Collins G, et al. An investigation of common crosslinking agents on the stability of electrospun collagen scaffolds. *Journal of Biomedical Materials Research Part A*. 2015;103(2):762-71.
198. Mekhail M, Wong KKH, Padavan DT, Wu Y, O'Gorman DB, Wan W. Genipin-cross-linked electrospun collagen fibers. *Journal of Biomaterials Science, Polymer Edition*. 2011;22(17):2241-59.
199. Timnak A, Gharebaghi FY, Shariati RP, Bahrami S, Javadian S, Emami SH, et al. Fabrication of nano-structured electrospun collagen scaffold intended for nerve tissue engineering. *Journal of Materials Science: Materials in Medicine*. 2011;22(6):1555-67.
200. Utke I, Moshkalev S, Russell P. *Nanofabrication using focused ion and electron beams: principles and applications*: Oxford University Press; 2012.
201. Wong KKH, Hutter JL, Zinke-Allmang M, Wan W. Physical properties of ion beam treated electrospun poly (vinyl alcohol) nanofibers. *European Polymer Journal*. 2009;45(5):1349-58.
202. Huda MS, Drzal LT, Mohanty AK, Misra M. Effect of fiber surface-treatments on the properties of laminated biocomposites from poly (lactic acid)(PLA) and kenaf fibers. *Composites science and technology*. 2008;68(2):424-32.
203. Lee SJ, Oh SH, Liu J, Soker S, Atala A, Yoo JJ. The use of thermal treatments to enhance the mechanical properties of electrospun poly (ϵ -caprolactone) scaffolds. *Biomaterials*. 2008;29(10):1422-30.
204. Tan EP, Lim C. Effects of annealing on the structural and mechanical properties of electrospun polymeric nanofibres. *Nanotechnology*. 2006;17(10):2649.
205. Ballerini M, Milani M, Batani D, Squadrini F, editors. *Focused ion beam techniques for the analysis of biological samples: A revolution in ultramicroscopy?* Society of Photo-Optical Instrumentation Engineers (SPIE) Conference Series; 2001.
206. Wong KKH, Zinke-Allmang M, Wan W. N⁺ surface doping on nanoscale polymer fabrics via ion implantation. *Nuclear Instruments and Methods in Physics Research Section B: Beam Interactions with Materials and Atoms*. 2006;249(1):362-5.
207. Chu PK, Chen J, Wang L, Huang N. Plasma-surface modification of biomaterials. *Materials Science and Engineering: R: Reports*. 2002;36(5):143-206.

208. Wong K, Zinke-Allmang M, Wan W, Zhang J, Hu P. Low energy oxygen ion beam modification of the surface morphology and chemical structure of polyurethane fibers. *Nuclear Instruments and Methods in Physics Research Section B: Beam Interactions with Materials and Atoms*. 2006;243(1):63-74.
209. Sugita Y, Suzuki Y, Someya K, Ogawa A, Furuhashi H, Miyoshi S, et al. Experimental evaluation of a new antithrombogenic stent using ion beam surface modification. *Artificial organs*. 2009;33(6):456-63.
210. Ziegler JF, Biersack J, Littmark U. *The stopping and range of ions in matter*, Vol. 1. 1, Pergamon Press, New York. 1985.
211. Ziegler J, Biersack J, Littmark U. *the stopping Power and Ranges of Ions in Matter. The Stopping and Range of Ions in Solids*. 1985;1.
212. Dong H, Bell T. State-of-the-art overview: ion beam surface modification of polymers towards improving tribological properties. *Surface and Coatings Technology*. 1999;111(1):29-40.
213. Kadlubowski S, Grobelny J, Olejniczak W, Cichomski M, Ulanski P. Pulses of fast electrons as a tool to synthesize poly (acrylic acid) nanogels. Intramolecular cross-linking of linear polymer chains in additive-free aqueous solution. *Macromolecules*. 2003;36(7):2484-92.
214. Guenther M, Sahre K, Suchanek G, Gerlach G, Eichhorn K-J. Influence of ion-beam induced chemical and structural modification in polymers on moisture uptake. *Surface and Coatings Technology*. 2001;142:482-8.
215. Barankin MD. *Thin film coatings with an atmospheric-pressure plasma*: University of California, Los Angeles; 2010.
216. Sprang N, Theirich D, Engemann J. Plasma and ion beam surface treatment of polyethylene. *Surface and Coatings Technology*. 1995;74:689-95.
217. Hareesh K, Sen P, Bhat R, Bhargavi R, Nair GG, Sanjeev G. Proton and alpha particle induced changes in thermal and mechanical properties of Lexan polycarbonate. *Vacuum*. 2013;91:1-6.
218. Chen J, Lau S, Sun Z, Tay B, Yu G, Zhu F, et al. Structural and mechanical properties of nitrogen ion implanted ultra high molecular weight polyethylene. *Surface and Coatings Technology*. 2001;138(1):33-8.
219. Mwale F, Petit A, Wang HT, Epure LM, Girard-Lauriault P-L, Ouellet JA, et al. The potential of N-rich plasma-polymerized ethylene (PPE: N) films for regulating the phenotype of the nucleus pulposus. *The open orthopaedics journal*. 2008;2:137.

220. Kusakabe M, Suzuki Y, Nakao A, Kaibara M, Iwaki M, Scholl M. Control of endothelial cell adhesion to polymer surface by ion implantation. *Polymers for Advanced Technologies*. 2001;12(8):453-60.
221. Li D, Cui F, Gu H. F⁺ ion implantation induced cell attachment on intraocular lens. *Biomaterials*. 1999;20(20):1889-96.
222. Kurotobi K, Suzuki Y, Nakajima H, Suzuki H, Iwaki M. Platelet adhesion and plasma protein adsorption control of collagen surfaces by He⁺ ion implantation. *Nuclear Instruments and Methods in Physics Research Section B: Beam Interactions with Materials and Atoms*. 2003;206:532-7.

Chapter 3

3 Materials and Methods

3.1 Materials

- ❖ The following were purchased from Sigma Aldrich, Oakville, ON, Canada:
 - 1, 1, 1,3,3,3 hexafluoroisopropanol ($\geq 99\%$)
 - Stannous Chloride (anhydrous, 99.99%)
 - Sodium acetate trihydrate ($\geq 99\%$)
 - Ethylene glycol (spectrophotometric grade, $\geq 99\%$)
- ❖ Ninhydrin (99 %) was purchased from VWR International, ON, Canada
- ❖ Dulbecco's modified essential medium (DMEM) was purchased from Life Technologies, Mustang Market, ON, Canada
- ❖ Glacial acetic acid was purchased from Caledon Labs, Georgetown, ON, Canada

3.2 Method

3.2.1 Isolation and purification of type I collagen from rat tails

Collagen type I derived from rat tail was used in collagen fiber preparation. The crude collagen isolated from rat tails was purified using an established procedure (237, 238). Briefly crude collagen was soaked in 70% aqueous ethanol for 30

minutes and then air dried. It was then sterilized using UV lamp overnight. The sterile crude collagen was purified by digesting in a 0.0175M acetic acid solution at 4°C for 7 days. The resulting solution was centrifuged at 11,000 rpm for 2 hours and the supernatant containing the purified collagen was collected. It was lyophilized to give the purified collagen type I in powder form.

3.2.2 Electrospinning

For electrospinning experiments, purified collagen type I was used to prepare the electrospinning solutions. Lyophilized rat tail collagen type I was dissolved in hexafluoroisopropanol (HFIP). Solutions with collagen concentrations of 5 and 5.5 wt% were prepared. Collagen fibers were produced in a custom built environmental control chamber at controlled temperature of 21 ± 2 °C. The relative humidity was controlled over the range of $10 - 70 \pm 5$ %. A voltage of 20 kV, (Glassman High Voltage Inc.) and a distance between the syringe needle (22-gauge) and the collector electrode of 20 cm were used. Collagen solution flowrate was controlled by a single syringe pump (KD Scientific Inc.) at 0.15 mL/hr. Electrospun fibers were collected on a custom designed stationary aluminum collector as shown in Figure 1 for further characterization.



Figure 9 : The electrospinning setup with a collector

3.2.3 Ion implantation

There are two major interactions between the energetic ions and the material occurs during implantation and they are Nuclear stopping and Electronic stopping (239). When defects are created in the crystal structure due to the collision of ion with the nuclei of the lattice atom, such defects are referred as Nuclear stopping. On the other hand, when the collision is with electrons of the lattice atoms it is then referred as electronic stopping in such stopping defects are extraneous.

At the end the ion reaches the implantation path and are stopped, which induces the chemical modification and this doping site depends on the reactivity of the ion (240).

In this study, Nitrogen (N^+) and Helium (He^+) ions are used for crosslinking. And, these the ion beams are generated using 1.7 MV Tandem accelerator (from The

University of Western Ontario). There are two ion sources (as shown in the figure 2 below), duoplasmatron for He^- from Helium gas and sputter sources for N^- from graphite–boron nitride, shown at the right are capable of generating a wide range of non-radioactive elements for the beams.

The tandem accelerator accelerates the ions in two stages. First, the negative ions produced from the sources are attracted by the high positive voltage at the terminal halfway down the accelerator tank. In the terminal, they pass a short section called the stripping canal; the negative ions lose two or more electrons in collisions with a stripping gas (N_2). Then at the second stage, the now positive ions are accelerated away from positive terminal voltage. This tandem effect is very effective to generate high-energy ion beams with energies up to a few MeV.

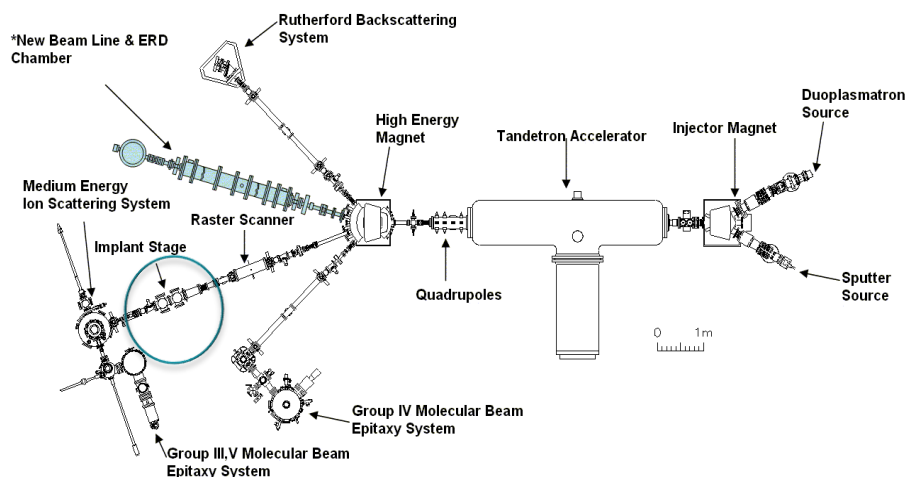


Figure 10 Image: Courtesy of Tandemtron Lab at University of Western Ontario. Nitrogen ion (N^+) and helium ion (He^+) beams were generated using the General Ionex 1.7 MV tandemtron accelerator at The University of Western Ontario.

The beam currents were kept below 200 nA. Ion beam treatment was performed with the sample placed vertically at room temperature in ultra-high vacuum (10^{-8} torr). An ultra-high vacuum beam line is necessary to keep the beam line free of residual gas. This prevents beam intensity reducing collisions between the ions and the molecules, or the formation of a contamination layer on the sample during the implantation.

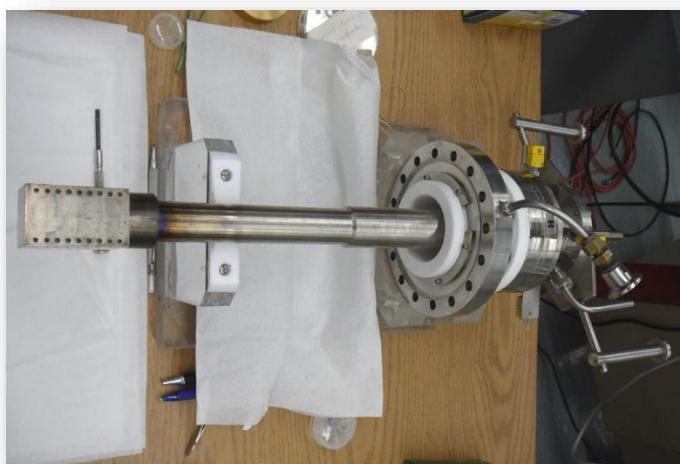


Figure 11 Implantation stage Image: Courtesy of Tandetron Lab at University of Western Ontario

In our work, Nitrogen (N^+) and Helium (He^+) ion beams are generated and implanted on the fabricated fibers on silicon wafers. Energies of N^+ and He^+ beam was 1.7 MeV and 520 keV, respectively.

Nano fibers, were fabricated on the silicon wafer and each of the sample size were ~ 1.9 cm. These samples were mounted on the sample holder with 1.0 μ m thick tantalum (Ta)

foil (Ta, 99.9% purity, Goodfellow Cambridge Ltd.) The thickness of the Ta foil was determined by the simulation software package SRIM-2008(239) (241) (242) that provides, theoretical estimation of the energies in our case. The projected estimation from the software, gave us the doping depth profiles and the total deposited energy distribution of the two-ion species in the collagen fibers after transmission through the Ta foil. More so, the simulation takes into account of each ion beam straggling in the foil, which is a process that magnifies the energy distribution of an ion beam when single ions interact randomly.

Ta foil, has two advantages in this work. First, it reduces the energy that reaches the collagen fibers, preventing it from the burns due to overheating. Second, the advantage of using ion beam with a broad energy spectrum, as opposed to a monochromatic energy, is that the implanted ions have a more uniform distribution of the treated materials. If using a mono-energy ion beam, the depth profile of the implanted ions will have a normal distribution with the maximum ion concentration located inside the treated material and minimal ions up on the surface or near surface region. Also, by doing so the area at the maximum normal distribution will burn and damage the amine/amide functional groups on the collagen sample surface and, which would lead to no crosslinking process or ion beam treatment of the given sample. In other words, the selective use of a broadband energy ion beam may be advantageous for controlling the depth distribution of ions within the collagen nanofibers.

The stimulation results, using a 1.0 μm thick Ta foil reduces the initial ion energies of 1.7 MeV for N^+ and 520 keV for He^+ to energy distributions ranging from 0 to 300 keV for N^+ and 0 to 100 keV for He^+ . Table 3.2, gives the specification of two different ion

species used to crosslink the collagen fibers with two different energies, and three different doses.

Table 2 The specification of two different ion species used to crosslink the collagen fibers with two different energies, and three different doses.

	Nitrogen (N ⁺)	Helium (He ⁺)
Energy:	0 to 300 keV	0 to 100 keV
Dose (ions/cm²):	4 x 10¹⁵	
Dose (ions/cm²):	8 x 10¹⁵	
Dose (ions/cm²):	1.2 x 10¹⁶	

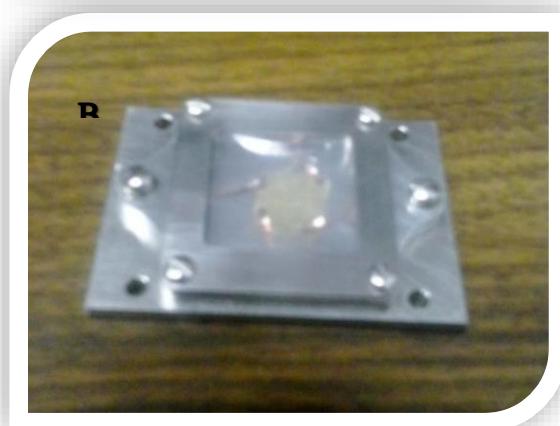
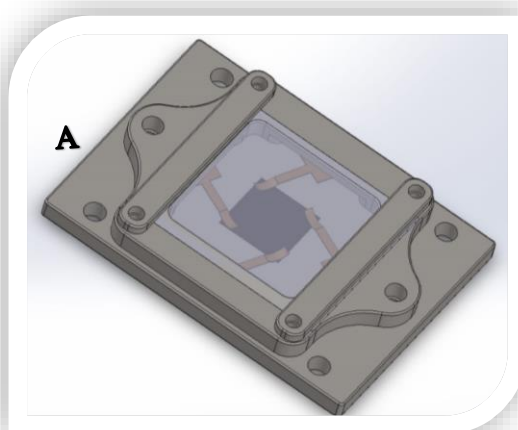
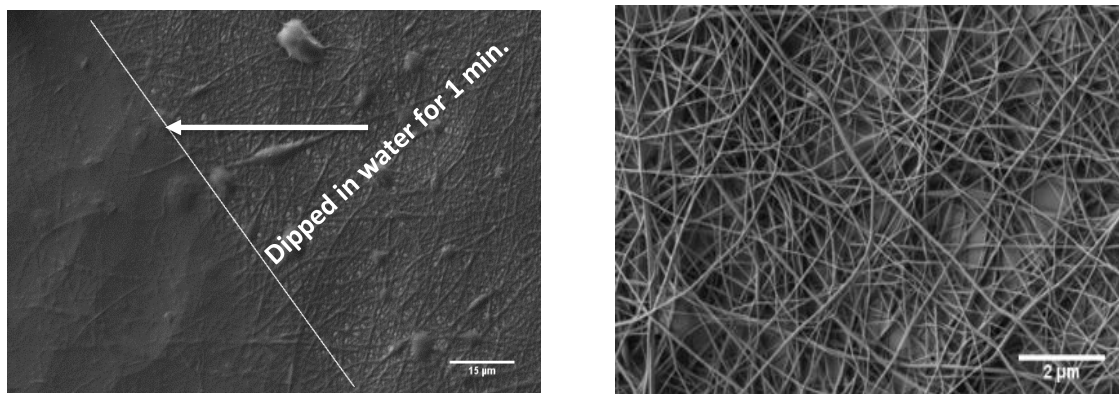


Figure 12 A: Design of sample holder B: Sample holder

3.3 Characterization

3.3.1 Fiber stability

Fabricated electrospun collagen fiber was stabilized using ion beam implantation. This implantation was varied using two different species and three different doses of each. The fabricated collagen fibers were highly hydrophilic in nature and spontaneously dissolved upon contact with water. The as-spun collagen fibers are not stable in aqueous environment.



A: As - spun in water for 1min

B: Electrospun scaffolds

Figure 13 : A: As-spun in water for 1min B: Electrospun scaffolds The line indicates the water surface. The left part of the sample was immersed in water.

Figure 13, above shows an as-spun scaffold after soaked in water for 1 minute. The fibers immersed in water completely lost their fiber morphology and gelled. Due to the hydrophilicity of the as-spun collagen fibers, even the fibers above the water surface attracted water and readily absorbed water and swelling and deformation are observed in the test sample. In order to stabilize the collagen fibrous scaffolds in aqueous environment, the scaffolds were treated with energetic helium and nitrogen ion beam at the Tandetron lab at UWO.

A systematic study was carried out to determine the collagen fiber stability on each crosslinked ion. Two different ion species treatment was carried out, to study the comparative effect of each ion. Each of these ion species, were varied with three different ion doses. After crosslinking, each sample was exposed to water and cell culture media (DMEM) for 7 days respectively. Each of the sample, were imaged using SEM to study the morphology changes, after seven days' implantation (for each of the conditions).

3.3.2 Scanning electron microscopy (SEM)

Each of the experiments were done on a different day and/or different months to see the consistency and reproducibility of the work. Collagen fiber size and morphology were determined using a high-resolution scanning electron microscope by using a Leo

1540XB (LEO Electron Microscopy Ltd). The fibers were not sputter coated and an accelerating voltage of 1 kV to 3 kV was used.

3.3.3 Fiber diameters

A Java based image processing program, Image J (National Institutes of Health) was used to measure the fiber diameter and understand the morphology of the images.

Four SEM images were acquired for each crosslinked collagen nanofibers and, twenty-five fibers were randomly picked from each image and measured. Thus, the total fiber diameters measured were 100 for each image (sample). Each condition was repeated six times to get, approximately 600 + fibers were measured for each of the conditions.

3.3.4 Fiber stability in aqueous media

The average as-spun fiber was then calculated as $D_{\text{as-spun}}$. Fiber diameter of crosslinked (ion implanted) sample for 100 fibers was measured for n-6, for both the ion species for implantation (He^+ and N^+) and, for three different ion doses. Average of ion implanted crosslinked collagen fibers, for each condition was measured as $D_{\text{crosslinked}}$.

The change in fiber diameter was determined using the following equation:

$$\% \text{ Change in diameter after ion implantation} = 100 \% \times \frac{(D_{\text{crosslinked}} - D_{\text{as-spun}})}{D_{\text{as-spun}}}$$

Each of the ion implanted, crosslinked collagen nanofiber (samples) were tested for seven days for aqueous stability using swelling effect as a factor after soaking the sample in water (H₂O) and cell culture (DMEM) for seven (7) days.

Each (ion implanted) crosslinked sample (for both the ion species for implantation (He⁺ and N⁺) and, for three different ion dose), were cut in half and one half was placed in distilled water, while the other half was placed in cell culture media (DMEM) for the seven days. These treated samples were rinsed with water to remove any salt deposition on fiber over time and, then imaged using SEM. Average fiber diameter, as **D_{final}** was calculated for both, water and cell culture media (DMEM).

The percentage of swelling, was then calculated, by using the formula below.

$$\begin{aligned} \% \text{ Change in diameter after exposure to aqueous solutions} \\ = 100 \% \times \frac{(D_{\text{final}} - D_{\text{crosslinked}})}{D_{\text{crosslinked}}} \end{aligned}$$

3.3.5 X-ray photoelectron Spectroscopy (XPS)

X-ray photoelectron spectroscopy (XPS) is a highly sensitive surface analysis technique, and its analysis depth is 1 nm to 10 nm from the surface. XPS technique is used to

determine the elemental composition of chemical in electronic state of the elements that exist at a sample surface. XPS uses low energy X-ray photons to penetrate through the surface and excite the core electron of each individual atom in the sample. The kinetic energy of an electron that escaped from the surface is equal to the difference between the incident photons energy ($h\nu$) and the binding energy of the electron in the atom, it also includes a correction for the work function of the electron(243).

XPS technique was, conducted twice on collagen nanofibers sample, right after the fibers were fabricated and these results mimicked, as control to the experiment. The second scan was done on ion implanted, crosslinked collagen nanofibers to study the chemical composition after ion implantation. Two different resolutions of spectra are generated to analysis these results. First, a full survey spectrum scans and reveals the elemental composition of the surface. And, the second is the high-resolution spectrum performed to collect in depth study of chemical bonding characterization on the sample.

The number of electron is independent on the chemical state, each electron detected at a kinetic energy represents one specific element present at the sample surface. Every orbiting electron in an atom is sensitive to the chemical environment of the atom and more so, the binding energy shift is dependent on the chemical state and the molecular structure.

The XPS system from Kratos Axis Ultra with a 210 W Al-K α monochromatic source was used to analyze chemical modifications resulting from the ion implanted collagen nanofibers. For this study, the full scan pass energy of the survey scan was 160 eV and the high-resolution scan was 20 eV. The program CasaXPS (Casa Software Ltd.) was

used to construct and curve-fit multiple peaks for the data envelop that appeared in the core-level energy spectra based on the built-in Marquardt-Levenberg (244) optimization algorithm.

3.4 Fiber degradation of crosslinked collagen nanofibers

Ninhydrin assay was conducted on each condition after ion implantation. The main objective was to quantify the amount of free primary amine group right after implantation. Although, this assay does not provide any information on the density or nature of crosslinking. But, estimating the free amine group in the given sample right after crosslinking, it will give the rate of the degradation of these ions implanted fiber with respect to the dose delivered. And this, quantification of the free amine group will also provide us with a good indication of the degree of crosslinking of electrospun collagen nanofibers.

Each of my samples for ninhydrin assay, were fabricated by electrospun technique on 1cm by 1cm silicon wafer with same time interval of fifteen (15) minutes. These samples were then ion implanted with respective dose, energy and species. Control (n=3) to this experiment were the as spun electrospun collagen nanofibers.

A ninhydrin solution was prepared according to Starcher et al.(245), however the quantities were different. A 4 N sodium acetate buffer was prepared by dissolving 544 g of sodium acetate trihydrate in 100 ml of glacial acetic acid and 400 ml of distilled water. The solution was left to mix overnight and the final pH was measured to be 5.5. A stannous chloride solution was prepared by adding 100 mg of SnCl₂ to 1 ml of ethylene

glycol. The ninhydrin solution was prepared by dissolving 800 mg of ninhydrin in a mixture of 30 ml of ethylene glycol and 10 ml of the 4 N acetate buffer. 1 ml of the stannous chloride suspension was added and the solution was stirred for one hour. A linear calibration curve was created using different glycine concentrations.

Crosslinked samples were then placed in vials containing 2 ml of distilled water mixed with 1 ml of the ninhydrin solution. The vials were placed in an 80 °C water bath for 15 minutes and then left to cool down. A Beckman DU spectrophotometer was used to measure the optical absorbance at 570 nm, which is the typical absorbance for the purple complex that is formed upon the reaction of ninhydrin with amino acids. After measuring the absorbance, the calibration curve (Refer to Appendix) was used to determine the concentration of free amino acids in solution. Followed by calculating the degree of crosslinking. We used following formula to calculate the degree of crosslinking at different dose and energies.

The degree of crosslinking was determined by the following equation:

$$\text{Degree of crosslinking \%} = \frac{[AC \text{ non - crosslinked} - AC \text{ crosslinked}] * 100}{AC \text{ non - crosslinked}}$$

Where AC is the Amine concentration at different dose.

3.5 Statistical Analysis

All statistics were performed using OriginPro8 (OriginLab corporation).

Propagation of error, over lapping law were done on the data using Microsoft Excel (Microsoft Corp).

Reference:

1. Robinson JJ. Comparative biochemical analysis of sea urchin peristome and rat tail tendon collagen. *Comparative Biochemistry and Physiology Part B: Biochemistry and Molecular Biology*. 1997;117(2):307-13.
2. Silver F, Trelstad R. Type I collagen in solution. Structure and properties of fibril fragments. *Journal of Biological Chemistry*. 1980;255(19):9427-33.
3. Ziegler JF, Biersack JP. *The stopping and range of ions in matter*: Springer; 1985.
4. Ziegler J, Manoyan J. The stopping of ions in compounds. *Nuclear Instruments and Methods in Physics Research Section B: Beam Interactions with Materials and Atoms*. 1988;35(3):215-28.
5. Ziegler JF, Biersack JP. *SRIM-2008, Stopping Power and Range of Ions in Matter*. 2008.
6. Ziegler J. „James Ziegler-SRIM & TRIM,“. 2013.
7. Watts JF, Wolstenholme J. *An introduction to surface analysis by XPS and AES. An Introduction to Surface Analysis by XPS and AES*, by John F Watts, John Wolstenholme, pp 224 ISBN 0-470-84713-1 Wiley-VCH, May 2003. 2003:224.
8. Press WH. *Numerical Recipes with Source Code CD-ROM 3rd Edition: The Art of Scientific Computing*: Cambridge University Press; 2007.
9. Starcher B. A ninhydrin-based assay to quantitate the total protein content of tissue samples. *Analytical biochemistry*. 2001;292(1):125-9.

Chapter 4

4 Effect of humidity on electrospun polymer fibers

4.1 Introduction

Polymers in the form of submicron fiber find a broad range of applications in areas ranging from non-woven filter medium to scaffold for tissue engineering (163, 246-249). They also find a wide range of application in the formation of polymer composites (165, 250-258). Diameter, fiber surface morphology and quality are important parameters that often determine their suitability for specific applications.

Electrospinning is a popular method used to produce submicron polymer fibers. Most of the fiber preparation process parameters have been extensively studied for the control of fiber size and morphology(12, 14-18, 259-266) . However, there remain a group of parameters that little attention has been paid to until recently. This are the environmental parameters of the electrospinning process [17, 18, 22]. The environmental parameters include temperature and humidity of the fiber formation environment. Between these two parameters, it is probably easier to control the environmental humidity than its temperature. Moreover, some polymers, especially the biopolymers, have limited thermal

stability. As a result, most of the studies reported on environmental control to date have been on the humidity effect on the electrospinning process [30 – 36].

The impact of humidity on electrospinning towards fiber formation using polymer solutions has been assessed mostly in terms of its effect on fiber diameter. The effect of humidity on polyethylene oxide (PEO) fiber formation by electrospinning with water as the solvent was reported by Tripatanasuwan et al.(193). An inverse relationship between humidity and fiber diameter was reported. That is, as humidity increases, fiber diameter decreases. In another study on poly(acrylonitrile) (PAN) and polysulfone (PSF) fibers using dimethyl formamide (DMF) as solvent, the opposite trend on diameter dependence on humidity was observed (201). A study by Hardick et al.(267) on the temperature and humidity effect on electrospinning found that for cellulose acetate with a degree of acetylation of 40 % in a solvent system consisting of 40/40/20 of acetone/DMF/ethanol was used, the fiber diameter increases with increasing humidity at 25 °C. More recent studies include polyamides in a mixed formic acid/acetic acid solvent system which demonstrated the inverse effect of humidity on fiber diameter (268); polyetherimide with either N-methyl-pyrrolidone (NMP) (269) or with NMP, DMF and dimethyl acetamide (DMAc) as solvents (200) demonstrated a positive correlation of humidity with fiber diameter. A study on the humidity and solution viscosity effect on the electrospinning of polycaprolactone (PCL) in chloroform/DMF 80/20, poly(ethylene glycol) (PEG) in chloroform and poly(carbonate urethane) (PCU) in DMAc further highlights the importance the environmental parameters on fiber formation and fiber structure and morphology (270). For PCL and PCU, continuous fibers were formed at ~50-60 %

humidity. For PEG, continuous fibers were not formed over the humidity range (5-75 %) investigated. These studies established the causation between humidity of the electrospinning environment and product fiber diameter when polymer solutions were used in the process. However, the rationale behind the seemingly conflicting trends of the humidity effect on fiber diameter and morphology is still not well understood.

Recognizing the importance of the role of submicron fibrous scaffold in tissue engineering, we have carried out a study of the humidity effect on collagen type 1 and PCL fiber formed by electrospinning using the water miscible solvents of hexafluoroisopropanol (HFIP) and trifluoroethanol (TFE) respectively. Collagen is the major protein in nanofiber form in the extracellular matrix of mammals. It is a natural choice as a scaffold material although the electrospun fibers have to be further stabilized (25, 26, 271-274) . PCL is a synthetic biocompatible polyester which, in various microporous forms, have been investigated extensively as tissue engineering scaffold (275-282) The ability of use the humidity to control and tune fiber size and morphology will be investigated. Based on our results, and additional data in the literature, we will also demonstrate a basis to better understand the mechanism controlling the trends of fiber diameter dependency on humidity derived from polymer solutions using the electrospinning process.

4.2 Experimental

Collagen type I derived from rat tail was used in collagen fiber preparation. The crude collagen isolated from rat tails was purified using an established procedure (237, 238). Briefly crude collagen was soaked in 70% aqueous ethanol for 30 minutes and then air dried. It was then sterilized using UV lamp overnight. The sterile crude collagen was purified by digesting in a 0.0175M acetic acid solution at 4°C for 7 days. The resulting solution was centrifuged at 11,000 rpm for 2 hours and the supernatant containing the purified collagen was collected. It was lyophilized to give the purified collagen type I in powder form.

For electrospinning experiments, purified collagen type I was used to prepare the electrospinning solutions. Lyophilized rat tail collagen type I was dissolved in hexafluoroisopropanol (HFIP). Solutions with collagen concentrations of 5 and 5.5 wt% were prepared. Collagen fibers were produced in a custom built environmental control chamber at controlled temperature of 21 ± 2 °C. The relative humidity was controlled over the range of $10 - 70 \pm 5$ %. A voltage of 20 kV, (Glassman High Voltage Inc.) and a distance between the syringe needle (22-gauge) and the collector electrode of 20 cm were used. Collagen solution flowrate was controlled by a single syringe pump (KD Scientific Inc.) at 0.15 mL/hr. Electrospun fibers were collected on the collector electrode for further characterization.

For electrospinning of PCL fibers, a solution of 12 wt% PCL was prepared by dissolving PCL ($M_n = 80$ kDa, Sigma Aldrich) in trifluoroethanol (TFE) (Sigma Aldrich) at room temperature.

Electrospun PCL fibers were produced using the electrospinning technique in an environmental controlled chamber similar to the one used for the preparation of collagen type I fibers. A potential difference was applied between the collector electrode and a metal syringe containing the PCL solution. The collector electrode was placed 20 cm away from the tip of the needle at a potential of 20 kV by connecting to a high-voltage power supply (Glassman High Voltage, Inc.). A syringe pump (Model 33, Harvard Apparatus) was used to extrude the PCL solution at a flow rate of 0.15 mL/hr. PCL fibers were electrospun at room temperature in a controlled humidity environment with the relative humidity ranged from 20 to 55%. The temperature and relative humidity were recorded at the beginning and the end of each run using a humidity and temperature monitor (OMEGA Engineering Inc.) to ensure the temperature and humidity level were maintained at 21 ± 2 °C and within $\pm 5\%$ relative humidity respectively. All fibers were collected for further characterization.

Humidity control was achieved using a custom built split flow chamber. A dry nitrogen stream was split into two. One stream flowed through a water bath where it was saturated with water vapour and the other stream remained dry. Relative humidity was controlled by controlling the ratio of the blending of these two streams. A humidity control within the range of $10 - 70 \pm 5$ % RH at a temperature of 21 ± 2 °C can be achieved.

Electrospun PCL and collagen fiber size and morphology were determined using a high resolution scanning electron microscope (LEO 1540XB). The fibers were not sputter coated and an accelerating voltage of 1 kV was used. For fiber diameter determination, the ImageJ software (NIH, Bethesda, MD, USA) was used. For each RH used, four SEM images were acquired at different locations for each sample. For each image, 30 fiber diameters were measured at randomly selected locations. Thus, a total of 120 measurements were made for each sample.

To examine the detailed fiber surface morphology, high resolution SEM images were acquired. These images have resolution of ~ 20 nm to ensure that any detailed morphological feature can be visualized.

4.3 Results and Discussion

It has been shown in the literature that good quality collagen fibers can be produced via the electrospinning process by using an appropriate choice of process parameters, solvent used and solution concentration (11, 216). In the present study, we have determined that using a collagen solution at a concentration of 5 – 5.5 wt % and HFIP as solvent, an extrusion tip to collector distance of 20 cm and a voltage of 20 kV allowed for the production of good quality fibers.

At constant humidity, fiber diameter can be controlled by varying the collagen solution concentration. Thus, at a collagen concentration of 5 wt %, nanometer diameter fibers were produced. An increase of the collagen solution concentration from 5 to 5.5 wt % resulted in fibers with diameters in the micrometer range. In both cases, the effect of environmental humidity was systematically investigated and the results are shown in Figure 1A and Figure 1B.

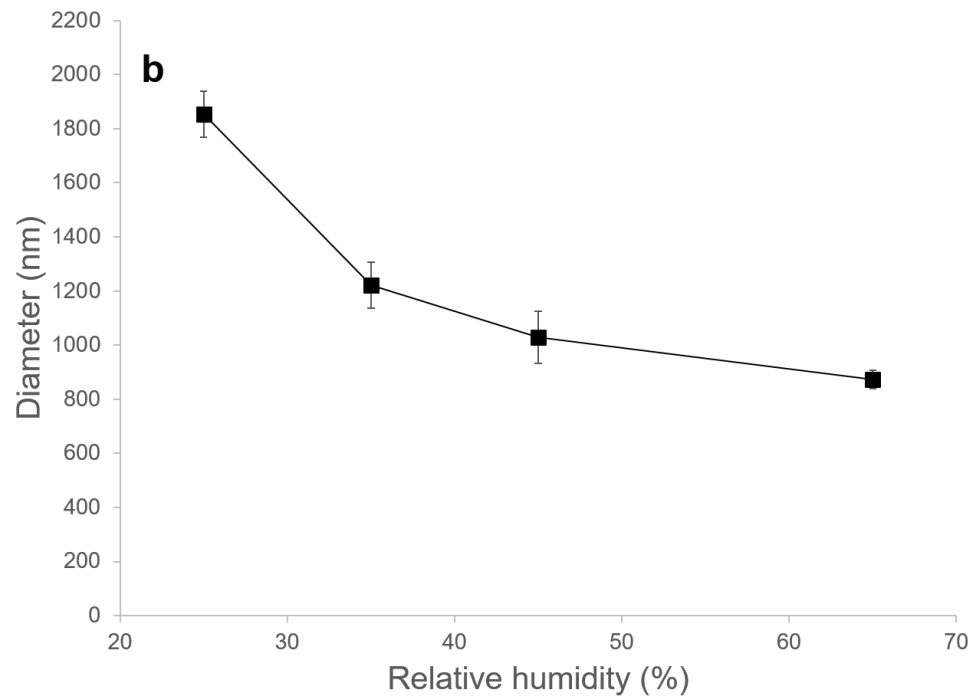
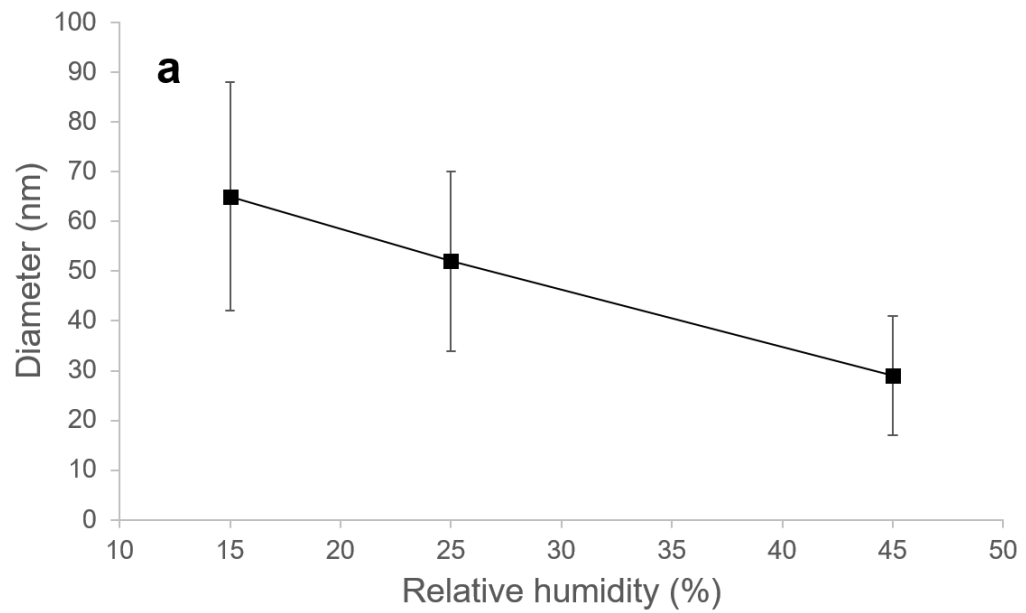


Figure 14 Effect of humidity on average fiber diameter of electrospun collagen fibers using collagen in HFIP solutions (a) collagen concentration at 5 wt%; (b) collagen concentration at 5.5 wt%

There were several reports in the literature on collagen fiber preparation using electrospinning (26, 283-285) . In these studies, humidity of the electrospinning environment was not controlled. As a result, its effect on the resultant fiber diameters had not been reported. As shown in Figures 1A and 1B, based on our current results, a significant and systematic dependence of fiber diameter on the ambient humidity of the electrospinning environment was observed. These results illustrate the importance of taking the environmental parameters such as humidity into consideration to ensure experimental reproducibility. Moreover, humidity as an electrospinning parameter also provides an opportunity to fine tune the fiber diameter range which may be important for a given application.

In tissue engineering, one of the approaches to construct a porous scaffold is by way of assembling submicron fibers. Collagen fiber, in submicron dimensions, is a component of the extracellular matrix. The use of collagen fiber based scaffold is therefore an attractive alternative in tissue engineering. Results in Figures 1A and 1B show that by controlling the humidity of the electrospinning process, fibers in the range of less than 50 nm to about 1000 nm can be produced. This range of size control via humidity control would allow for tuning the collagen fiber diameter for an intended application. For example, a recent report of the structure of the tympanic membrane that consists of two layers of collagen fibers with local orthogonal organization, the collagen fibers have diameters in a

narrow range centered around 30 nm (286). For tympanic membrane repair, the humidity parameter can be used advantageously to tune

fibers diameter to within the appropriate range similar to that of the natural tissue for use as scaffold which can also be implanted directly.

In addition to fiber diameter, effect of humidity on the quality of collagen fibers were also assessed in terms of their fiber morphology and fusion of overlapping fibers. High resolution SEM images of collagen fibers prepared at 5 wt % solutions are shown in Figure 2. It can be seen that at a resolution of up to ~20 nm, the fibers surface is smooth and free of pores and other imperfections. This indicates that no premature phase separation of the components in the polymer solution took place in the electrospinning process. Moreover, the fibers are free standing without fusion of overlapping fibers. This is an indication that sufficient time had been given to allow the solvent to evaporate in the solution jet as the fiber arrives at the collector electrode surface.

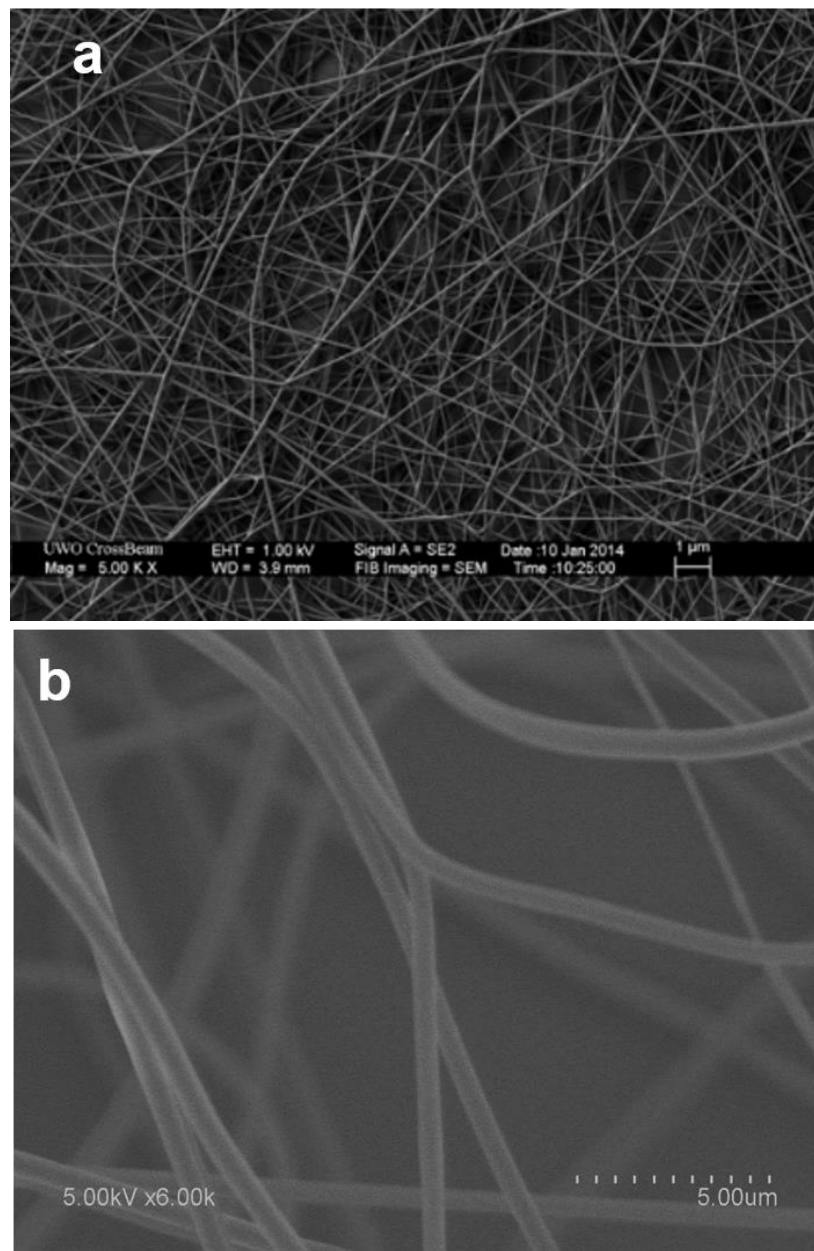


Figure 15 SEM images of electrospun collagen fibers at a humidity of $45 \pm 5\%$ (a) collagen concentration of 5 wt%; (b) collagen concentration of 5.5 wt%

Contrast to the collagen fibers and as shown in Figure 3, the PCL fibers we prepared from a solution with TFE as solvent, no clear fiber diameter dependency on humidity was observed. High resolution SEM images shown in Figure 4 demonstrate that, similar to the collagen fibers shown in Figure 3, these fibers are free standing and have smooth surfaces and are free of pores and other defects.

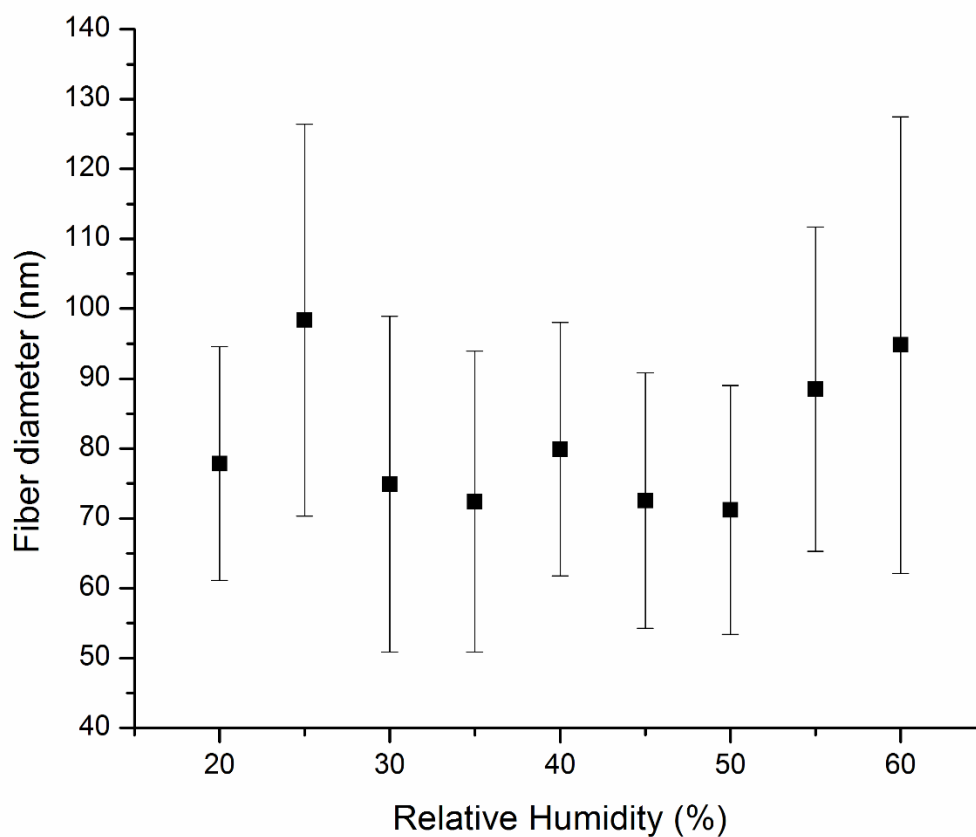


Figure 16 Effect of humidity on average fiber diameter of electrospun polycaprolactone (PCL) fibers using a 12 wt% PCL in trifluoroethanol solution

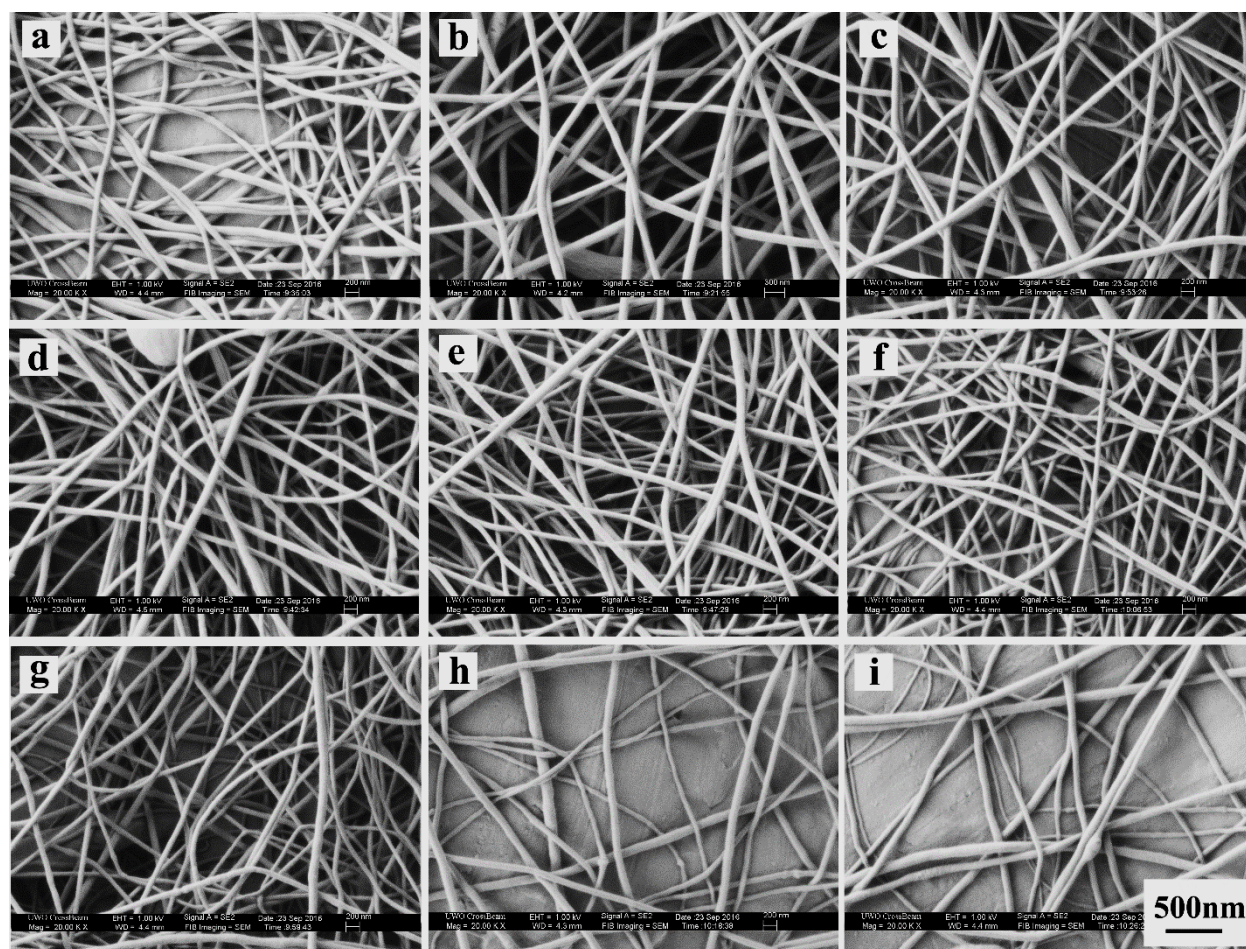


Figure 17 SEM micrographs of electrospun PCL nanofibers prepared using a 12 wt% PCL in trifluoroethanol solution at different relative humidity levels (a) 20%; (b) 25%; (c) 30%; (d) 35%; (e) 40%; (f) 45%; (g) 50%; (h) 55%; (i) 60%. The scale bar (500 nm) at the 1

Since PCL is a biocompatible and degradable polyester that has been studied extensively for tissue engineering applications, it is important to be able to process it into fibers for the fabrication of scaffolds (277-279, 287, 288). Our method is capable of delivering fairly good quality submicron diameter fibers with average fiber diameter of 79 ± 23 nm that are free standing and are defect free. Moreover, increasing humidity has very little

effect on the resulting fiber diameter indicating any ingress of water into the polymer solution jet does not affect the solidification process.

Although there were numerous studies in the electrospinning of PCL fibers (177, 277-282, 287-291) the effect of humidity on the resulting fiber diameter remain sparsely studied. Our current results can be contrasted with recent results reported in the literature(270). This study used a solvent system of chloroform/DMF 80/20. Within a narrow humidity range of ~50 – 75 %, continuous fibers were formed. Outside this range, broken fibers were produced. Moreover, these fibers were with relatively rough surfaces and were porous. The difference between our results versus the literature may be attributed to the properties of the solvents chosen. Our PCL solution was prepared using trifluoroethanol (TFE) as the solvent while the previous report used a mixture of chloroform/DMF 80/20. While TFE is miscible with water, chloroform, the major component in the chloroform/DMF 80/20 solvent system is not. In fact, we determined that water is not miscible with the chloroform/DMF 80/20 solvent system. In this case, any water ingress into the polymer solution from the environment can trigger phase separation leading to the formation of micro droplets in the polymer solution, which could lead to the formation of pores and other imperfections in the fiber and rough surfaces as have been reported (270).

Our results on collagen and PCL fibers, together with additional data of the humidity effect on the electrospun fiber diameter in the literature, are collected and presented in

Figure 5. These results demonstrate the importance of the control of humidity of the electrospinning environment for consistent results. Moreover, this effect can be advantageously used to produce fibers of the desired diameters. The correlation between fiber diameter and humidity seems to be rather random. This should not be a surprise considering the properties of the polymers used range from the very hydrophilic (e.g. PEG) to the very hydrophobic and polar (e.g. PAN) and those with properties somewhere in between. In addition, the solvent used have properties that range from protic (e.g. water) to polar aprotic (e.g. DMF) with water miscibility properties varying from miscible (e.g. HFIP) to immiscible (e.g. chloroform). However, on closer inspection of the data in Figure 5, it can be seen that the results can be broadly classified into three groups. There is a group of polymer fibers that were derived from polymer solutions with water insoluble polymer and water miscible solvent that exhibit positive correlation between humidity and fiber diameter (Group 1). Fibers derived from polyacrylonitrile (PAN), polysulfone (PS), polyetherimide (PEI) and cellulose acetate (CA) belong to this group. Fibers derived from polymer solutions consisting of water soluble/swellable polymers in water miscible solvents would produce polymer fibers that show the reverse trend (Group 2). That is, their fiber diameters decreases with increasing environmental humidity. Poly(ethylene oxide) (PEO), collagen and polyamides 4.6 and 6.9 (PA) fibers falls within this group. There is also the case that the polymer fibers that exhibits little humidity effect on their fiber diameters (Group 3). The PCL fibers we prepared using the water miscible TFE as solvent falls into this group.

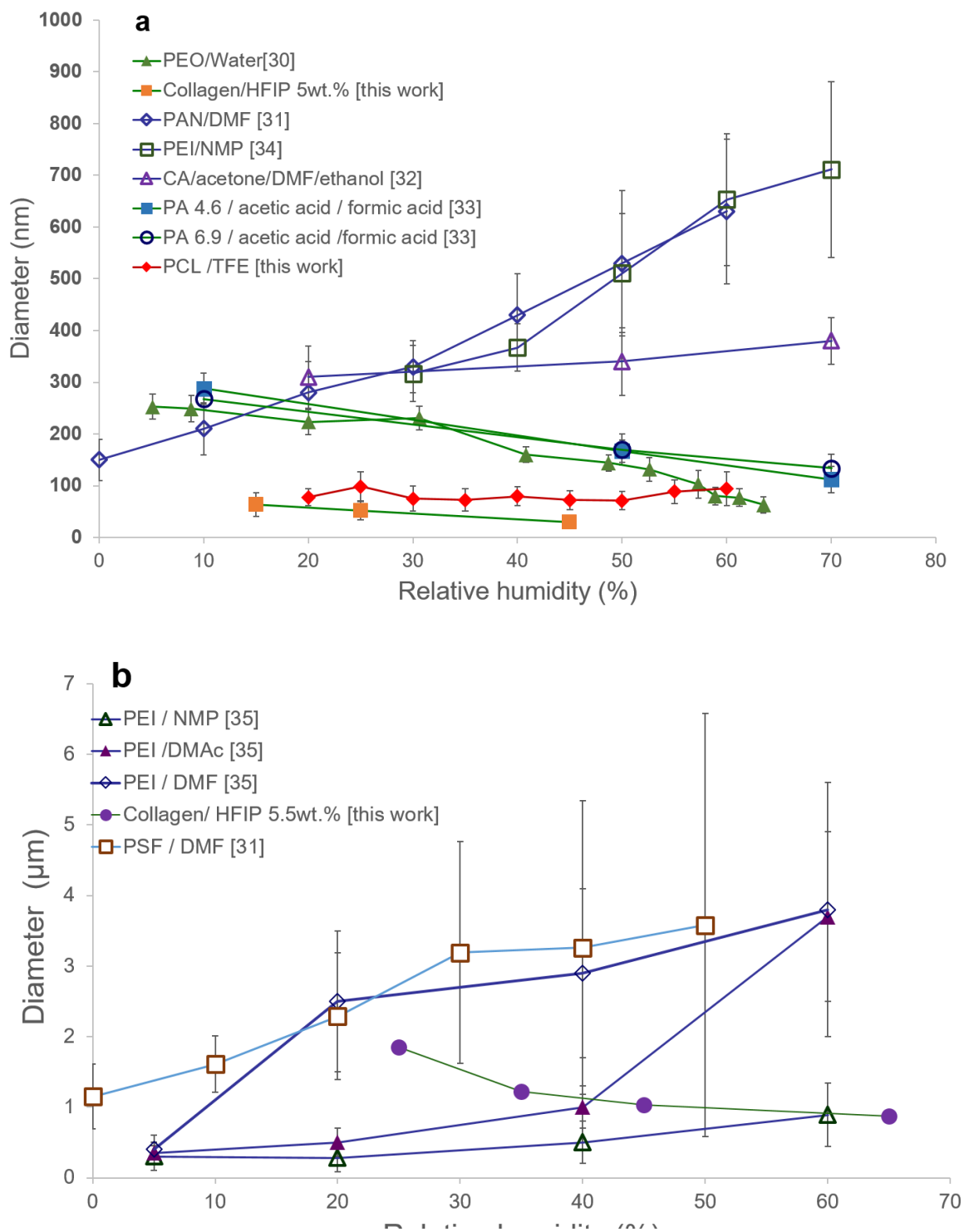


Figure 18 A summary plot of the effect of humidity on average fiber diameter of electrospun polymer fibers produced using polymer solutions (a) data for fibers with maximum diameters up to 1 μm (b) data for fibers with maximum diameters above 1 μm .

An understanding of the fiber diameter – humidity correlations of fibers produced by the electrospinning process would aid in the design of the polymer solution based electrospinning process and the prediction of the quality of the resulting fibers.

The electrospinning process using a polymer solution leading to solid polymer fiber formation and deposition at the collector electrode is fairly well understood and documented (14-17, 260, 261, 265).

If electrospinning is carried out in the absence of humidity or under the assumption that the effect of humidity can be ignored, for optimum fiber formation, the process would start with the polymer solution being extruded out of the nozzle, follow by the polymer solution jet being stretched by the electric field gradient as it travels towards the collector electrode. During this time, solvent evaporates and the polymer fiber solidifies. Ideally, solidification should take place as the solution jet arrives at the collector electrode to allow for maximum stretching for the formation of minimum diameter solid fiber. In reality, the timing for solvent evaporation/polymer solidification and arrival of the fiber at the collector electrode is seldom perfect. Two possible outcomes can be envisioned. The mismatch could lead to early solidification of the polymer solution jet. That is, solid fiber is formed well before reaching the collector electrode without making full use of the stretching effect of the electric field gradient. In this case, fiber size will be larger than

optimum. If this mismatch leads to late solidification of the polymer solution jet, solid fiber would not be formed upon reaching the collector electrode. This could lead to a failure of fiber formation, distorted fiber morphology and fusion of overlapping fibers.

As the results in Figure 5 show, humidity does have a significant and systematic effect on the outcome of the electrospinning process using polymer solutions. To understand his effect, we have to take into account the properties of the polymer as well as the solvent and their interaction with water in the form of humidity. For the purpose of our discussion, the polymers used can be broadly classified as either water insoluble or water soluble/swellable. Solvents used are either water miscible or immiscible. There could also be cases where solubility can be attributed to specific chemical interactions/reactions.

For a polymer solution consisting of water insoluble polymer dissolved in a water miscible solvent/solvent system, the presence of humidity in the electrospinning environment will decrease polymer solubility but the solution would remain in a single phase and is homogeneous. The insolubility of the polymer in water would result in solid fiber formation taking place earlier than in the absence of humidity. Time to solid fiber formation will decrease as humidity increases. As a result, increases in humidity will lead to an increase in fiber diameter thus explaining the polymer/solvent systems that give results falling within Group 1. However, increasing humidity will not have significant effect on the morphology and structure of the fibers. As shown in Figure 5, experimental

systems that fall into Group 1 behavior include PAN/DMF; PSF/DMF; PEI/NMP; PEI/DMF; PEI/DMAc; PEI/NMP and cellulose acetate/acetone:DMF:ethanol 40:40:20 [31, 34, 35].

In the case when a water insoluble polymer is dissolved in a water immiscible solvent/solvent system for electrospinning, increase in humidity will decrease polymer solubility and creation of a new phase of micro/nano-water droplets. Since the polymer is insoluble in water, solid fiber formation will take place earlier than in the absence of humidity. The end result would be an increase in fiber diameter with increasing humidity. With water in the form of dispersed micro/nano-droplets, the most likely results are formation of non-continuous or broken fibers and failure of fiber formation. There will also be significant effect on fiber morphology and structure, and could lead to rough surfaces and porosity. Result in the literature that falls into this category is PCL/chloroform:DMF 80:20 (270).

When the electrospinning solution is made up of water soluble/swellable polymer with solvent that is either water or water miscible, the presence of humidity will decrease polymer solution concentration. With the reduction of polymer solution concentration, solid fiber formation will be delayed than in the absence of humidity. This would allow the polymer solution jet to take full advantage of the stretching effect due to the electric field leading to smaller fiber diameter. As humidity increases, the fiber diameter will decrease progressively giving rise to behavior that falls within Group 2. The progressive dilution of the polymer solution may also lead to failure of fiber formation; distorted fiber

morphology and fusion of overlapping fibers. However, this will not have significant effect on the surface morphology and structure of the fibers. As shown in Figure 5, experimental systems that belong to Group 2 include PEO/water and collagen/HFIP.

Irrespective of whether the polymer/solvent systems behavior fall within Group 1 or Group 2, their sensitivity to humidity are not necessarily the same. This difference in sensitivity can be taken as an indication that the tolerance of the polymer solution to humidity which can be expressed from the polymer – water – solvent phase diagram (200). There exists the possibility that within the humidity range being considered, the effect on diameter is very small or minimal. This is the case for the PCL/TFE system reported in this study and falls within Group 3 of our classification.

When a water immiscible solvent is used to prepare a water soluble/swellable polymer solution, water ingression due to non-zero humidity will create a new phase of micro/nano-water droplets in the polymer solution jet with polymer distributed between the two immiscible phases. Depending on the relative solubility of the polymer in the two phases, fiber formation and humidity effect on fiber diameter would be difficult to predict and would likely result in the formation of broken fibers or failure to form fiber. If fibers can be formed, the presence of two phases in the polymer solution jet will have a significant effect on fiber morphology and structure and could lead to rough surfaces and porosity. Behavior of the PEG/chloroform system is consistent with the description of a water soluble polymer/water immiscible solvent system (270).

When a water insoluble polymer is dissolved in a solvent system via specific polymer/solvent interaction which is miscible with water to form the polymer solution for electrospinning, consideration has to be given to the specific interaction effect. One such system is the polyamides dissolved in a solvent system consisting of a mixture of formic acid and acetic acid. In this solvent system, formic acid is the solvent and acetic acid is a non-solvent. Dissolution of polyamides in formic acid involves the protonation of the amide groups in the polymer to form a polyelectrolyte (198, 292-294) . In this case, humidity ingression into the polymer solution jet results in a dilution of the polymer concentration but will allow a single homogeneous phase to be maintained. The net result would be a decrease in fiber diameter with increasing humidity (Group 2 behavior) as reported (268) and shown in Figure 5.

4.4 Conclusions

The preparation of collagen type 1 and PCL fiber by electrospinning and the effect of humidity on fiber diameter and morphology have been investigated. While collagen type 1 fiber diameter showed an inverse dependence on humidity, PCL fiber size is relatively independent of humidity. These results were explained in terms of the solubility of the polymer in water and the water miscibility properties of the solvents used.

Depending on the polymer solubility in water and the solvent miscibility with water, fiber diameter dependence on humidity can be classified into 3 groups. Group 1 consists of

polymer solutions that give fibers with fiber diameter increasing with increasing humidity; Group 2 with fiber diameter decreasing with increasing humidity and Group 3 with fiber diameter showing little or no dependence on humidity. This classification leads to a more rational understanding of the past and current results. It would also be useful in the planning of electrospinning experiments in terms of choice of solvent system for a polymer of interest.

Reference:

1. Place ES, Evans ND, Stevens MM. Complexity in biomaterials for tissue engineering. *Nature materials*. 2009;8(6):457-70.
2. Thenmozhi S, Dharmaraj N, Kadirvelu K, Kim HY. Electrospun nanofibers: New generation materials for advanced applications. *Materials Science and Engineering: B*. 2017;217:36-48.
3. Pham QP, Sharma U, Mikos AG. Electrospinning of polymeric nanofibers for tissue engineering applications: A review. *Tissue Engineering*. 2006 May;12(5):1197-211.
4. Place ES, George JH, Williams CK, Stevens MM. Synthetic polymer scaffolds for tissue engineering. *Chemical Society Reviews*. 2009;38(4):1139-51.
5. Kretlow JD, Mikos AG. Mineralization of synthetic polymer scaffolds for bone tissue engineering. *Tissue Engineering*. 2007;13(5):927-38.
6. Zhu Y, Yang B, Chen S, Du J. Polymer vesicles: Mechanism, preparation, application, and responsive behavior. *Progress in polymer science*. 2017;64:1-22.
7. Khan N. Applications of electrospun nanofibers in the biomedical field. *Studies by Undergraduate Researchers at Guelph*. 2012;5(2):63-73.
8. Sell SA, Wolfe PS, Garg K, McCool JM, Rodriguez IA, Bowlin GL. The use of natural polymers in tissue engineering: a focus on electrospun extracellular matrix analogues. *Polymers*. 2010;2(4):522-53.
9. Han D, Steckl AJ. Superhydrophobic and oleophobic fibers by coaxial electrospinning. *Langmuir*. 2009;25(16):9454-62.
10. Zhang H, Zhao C, Zhao Y, Tang G, Yuan X. Electrospinning of ultrafine core/shell fibers for biomedical applications. *Science China Chemistry*. 2010;53(6):1246-54.
11. Chen Q, Ahmed I, Knowles J, Nazhat S, Boccaccini A, Rezwani K. Collagen release kinetics of surface functionalized 45S5 Bioglass®-based porous scaffolds. *Journal of Biomedical Materials Research Part A*. 2008;86(4):987-95.
12. Ji Y, Li B, Ge S, Sokolov JC, Rafailovich MH. Structure and nanomechanical characterization of electrospun PS/clay nanocomposite fibers. *Langmuir*. 2006;22(3):1321-8.

13. Ignatova M, Manolova N, Rashkov I. Electrospun Antibacterial Chitosan-Based Fibers. *Macromolecular Bioscience*. 2013;13(7):860-72.
14. Salalha W, Dror Y, Khalfin RL, Cohen Y, Yarin AL, Zussman E. Single-walled carbon nanotubes embedded in oriented polymeric nanofibers by electrospinning. *Langmuir*. 2004;20(22):9852-5.
15. Li Y, Chen F, Nie J, Yang D. Electrospun poly (lactic acid)/chitosan core-shell structure nanofibers from homogeneous solution. *Carbohydrate polymers*. 2012;90(4):1445-51.
16. Mujica-Garcia A, Sonseca A, Arrieta MP, Yusef M, López D, Gimenez E, et al. Electrospun Fibers Based on Biopolymers. *Advanced Surface Engineering Materials*. 2016:385-438.
17. Saehana S, Iskandar F, Abdullah M. Optimization of electrospinning parameter by employing genetic algorithm in order to produce desired nanofiber diameter. *World Academy of Science, Engineering and Technology, International Journal of Chemical, Molecular, Nuclear, Materials and Metallurgical Engineering*. 2013;7(1):86-91.
18. Bhardwaj N, Kundu SC. Electrospinning: A fascinating fiber fabrication technique. *Biotechnology Advances*. 2010 May-Jun;28(3):325-47.
19. Thompson C, Chase GG, Yarin A, Reneker D. Effects of parameters on nanofiber diameter determined from electrospinning model. *Polymer*. 2007;48(23):6913-22.
20. Subbotin A, Stepanyan R, Chiche A, Slot J, Ten Brinke G. Dynamics of an electrically charged polymer jet. *Physics of fluids*. 2013;25(10):103101.
21. Arinstein A, Zussman E. Electrospun polymer nanofibers: mechanical and thermodynamic perspectives. *Journal of polymer science part B: Polymer physics*. 2011;49(10):691-707.
22. Thompson CJ, Chase GG, Yarin AL, Reneker DH. Effects of parameters on nanofiber diameter determined from electrospinning model. *Polymer*. 2007;48(23):6913-22.
23. Lannutti J, Reneker D, Ma T, Tomasko D, Farson DF. Electrospinning for tissue engineering scaffolds. *Materials Science & Engineering C-Biomimetic and Supramolecular Systems*. 2007 Apr;27(3):504-9.
24. Reneker DH, Yarin AL. Electrospinning jets and polymer nanofibers. *Polymer*. 2008;49(10):2387-425.
25. Frenot A, Chronakis IS. Polymer nanofibers assembled by electrospinning. *Current opinion in colloid & interface science*. 2003;8(1):64-75.

26. Theron S, Zussman E, Yarin A. Experimental investigation of the governing parameters in the electrospinning of polymer solutions. *Polymer*. 2004;45(6):2017-30.
27. McKee MG, Wilkes GL, Colby RH, Long TE. Correlations of solution rheology with electrospun fiber formation of linear and branched polyesters. *Macromolecules*. 2004;37(5):1760-7.
28. Kowalewski T, NSKI S, Barral S. Experiments and modelling of electrospinning process. *Technical Sciences*. 2005;53(4).
29. Huang ZM, Zhang YZ, Kotaki M, Ramakrishna S. A review on polymer nanofibers by electrospinning and their applications in nanocomposites. *Composites Science and Technology*. 2003 Nov;63(15):2223-53.
30. Tripatanasuwan S, Zhong Z, Reneker DH. Effect of evaporation and solidification of the charged jet in electrospinning of poly (ethylene oxide) aqueous solution. *Polymer*. 2007;48(19):5742-6.
31. Huang L, Bui NN, Manickam SS, McCutcheon JR. Controlling electrospun nanofiber morphology and mechanical properties using humidity. *Journal of Polymer Science Part B: Polymer Physics*. 2011;49(24):1734-44.
32. Hardick O, Stevens B, Bracewell DG. Nanofibre fabrication in a temperature and humidity controlled environment for improved fibre consistency. *Journal of Materials Science*. 2011;46(11):3890-8.
33. De Schoenmaker B, Van der Schueren L, Zugle R, Goethals A, Westbroek P, Kiekens P, et al. Effect of the relative humidity on the fibre morphology of polyamide 4.6 and polyamide 6.9 nanofibres. *Journal of Materials Science*. 2013;48(4):1746-54.
34. Icoğlu HI, Ogulata RT. EFFECT OF AMBIENT PARAMETERS ON MORPHOLOGY OF ELECTROSPUN POLYETHERIMIDE (PEI) FIBERS. *TEKSTİL VE KONFEKSİYON*. 2013;23(4):313-8.
35. Fashandi H, Karimi M. Comparative studies on the solvent quality and atmosphere humidity for electrospinning of nanoporous polyetherimide fibers. *Industrial & Engineering Chemistry Research*. 2013;53(1):235-45.
36. Nezarati RM, Eifert MB, Cosgriff-Hernandez E. Effects of humidity and solution viscosity on electrospun fiber morphology. *Tissue Engineering Part C: Methods*. 2013;19(10):810-9.
37. Rýglová Š, Braun M, Suchý T. Collagen and Its Modifications—Crucial Aspects with Concern to Its Processing and Analysis. *Macromolecular Materials and Engineering*. 2017.

38. Delgado LM, Bayon Y, Pandit A, Zeugolis DI. To cross-link or not to cross-link? Cross-linking associated foreign body response of collagen-based devices. *Tissue Engineering Part B: Reviews*. 2015;21(3):298-313.
39. Huang GP, Shanmugasundaram S, Masih P, Pandya D, Amara S, Collins G, et al. An investigation of common crosslinking agents on the stability of electrospun collagen scaffolds. *Journal of Biomedical Materials Research Part A*. 2015;103(2):762-71.
40. Liu T, Teng WK, Chan BP, Chew SY. Photochemical crosslinked electrospun collagen nanofibers: synthesis, characterization and neural stem cell interactions. *Journal of Biomedical Materials Research Part A*. 2010;95(1):276-82.
41. Li Y, Liu J, de Bruyn JR, Wan W. Optimization of the Electrospinning Process for Core-Shell Fiber Preparation. *Journal of Biomaterials and Tissue Engineering*. 2014;4(11):973-80.
42. Dong B, Arnoult O, Smith ME, Wnek GE. Electrospinning of collagen nanofiber scaffolds from benign solvents. *Macromolecular Rapid Communications*. 2009;30(7):539-42.
43. Damodaran VB, Bhatnagar D, Murthy NS. *Biomedical Polymers: An Overview*. *Biomedical Polymers*: Springer; 2016. p. 1-22.
44. Okamoto M, John B. Synthetic biopolymer nanocomposites for tissue engineering scaffolds. *Progress in polymer science*. 2013;38(10):1487-503.
45. Potrč T, Baumgartner S, Roškar R, Planinšek O, Lavrič Z, Kristl J, et al. Electrospun polycaprolactone nanofibers as a potential oromucosal delivery system for poorly water-soluble drugs. *European Journal of Pharmaceutical Sciences*. 2015;75:101-13.
46. Chong LH, Hassan MI, Sultana N, editors. Electrospun polycaprolactone (PCL) and PCL/nano-hydroxyapatite (PCL/nHA)-based nanofibers for bone tissue engineering application. *Control Conference (ASCC), 2015 10th Asian*; 2015: IEEE.
47. Suwantong O. *Biomedical applications of electrospun polycaprolactone fiber mats*. *Polymers for Advanced Technologies*. 2016.
48. Kuzelova Kostakova E, Meszaros L, Maskova G, Blazkova L, Turcsan T, Lukas D. Crystallinity of Electrospun and Centrifugal Spun Polycaprolactone Fibers: A Comparative Study. *Journal of Nanomaterials*. 2017;2017.
49. Baker SR, Banerjee S, Bonin K, Guthold M. Determining the mechanical properties of electrospun poly- ϵ -caprolactone (PCL) nanofibers using AFM and a novel fiber anchoring technique. *Materials Science and Engineering: C*. 2016;59:203-12.

50. Chou S-F, Woodrow KA. Relationships between mechanical properties and drug release from electrospun fibers of PCL and PLGA blends. *Journal of the mechanical behavior of biomedical materials*. 2017;65:724-33.
51. Robinson JJ. Comparative biochemical analysis of sea urchin peristome and rat tail tendon collagen. *Comparative Biochemistry and Physiology Part B: Biochemistry and Molecular Biology*. 1997;117(2):307-13.
52. Silver F, Trelstad R. Type I collagen in solution. Structure and properties of fibril fragments. *Journal of Biological Chemistry*. 1980;255(19):9427-33.
53. Matthews JA, Wnek GE, Simpson DG, Bowlin GL. Electrospinning of collagen nanofibers. *Biomacromolecules*. 2002;3(2):232-8.
54. Mekhail M, Wong KKH, Padavan DT, Wu Y, O'Gorman DB, Wan W. Genipin-cross-linked electrospun collagen fibers. *Journal of Biomaterials Science, Polymer Edition*. 2011;22(17):2241-59.
55. Harrell CR. Collagen compositions and uses for biomaterial implants. Google Patents; 2016.
56. Jiang Q, Reddy N, Zhang S, Roscioli N, Yang Y. Water-stable electrospun collagen fibers from a non-toxic solvent and crosslinking system. *Journal of Biomedical Materials Research Part A*. 2013;101(5):1237-47.
57. Kazanci M. Solvent and temperature effects on folding of electrospun collagen nanofibers. *Materials Letters*. 2014;130:223-6.
58. Liu J, Agrawal SK, Ladak HM, Wan W. Fiber Arrangement in the Rat Tympanic Membrane. *The Anatomical Record*. 2016;299(11):1531-9.
59. Choi Hw, Johnson JK, Nam J, Farson DF, Lannutti J. Structuring electrospun polycaprolactone nanofiber tissue scaffolds by femtosecond laser ablation. *Journal of Laser Applications*. 2007;19(4):225-31.
60. Agrawal A, Lee BH, Irvine SA, An J, Bhuthalingam R, Singh V, et al. Smooth muscle cell alignment and phenotype control by melt spun polycaprolactone fibers for seeding of tissue engineered blood vessels. *International journal of biomaterials*. 2015;2015.
61. Tan S, Inai R, Kotaki M, Ramakrishna S. Systematic parameter study for ultra-fine fiber fabrication via electrospinning process. *Polymer*. 2005;46(16):6128-34.
62. Beachley V, Wen X. Effect of electrospinning parameters on the nanofiber diameter and length. *Materials Science and Engineering: C*. 2009;29(3):663-8.
63. Sun L, Han RP, Wang J, Lim C. Modeling the size-dependent elastic properties of polymeric nanofibers. *Nanotechnology*. 2008;19(45):455706.

64. Gulfam M, Lee JM, Kim J-e, Lim DW, Lee EK, Chung BG. Highly porous core-shell polymeric fiber network. *Langmuir*. 2011;27(17):10993-9.
65. Saunders P. Dilute solution properties of polyamides in formic acid. Part II. The influence of ionic strength. *Journal of Polymer Science Part A: Polymer Chemistry*. 1962;57(165):131-9.
66. Saunders P. Dilute solution properties of polyamides in formic acid. Part I. Repression of polyelectrolyte effects by means of excess counterions. *Journal of Polymer Science Part A: Polymer Chemistry*. 1964;2(8):3755-64.
67. Bulte A, Naafs E, Van Eeten F, Mulder M, Smolders C, Strathmann H. Equilibrium thermodynamics of the ternary membrane-forming system nylon, formic acid and water. *Polymer*. 1996;37(9):1647-55.
68. De Schoenmaker B, Van der Schueren L, Ceylan Ö, De Clerck K. Electrospun polyamide 4.6 nanofibrous nonwovens: parameter study and characterization. *Journal of Nanomaterials*. 2012;2012:14.

Chapter 5

5 Preparation and ion beam stabilization of electrospun rat tail collagen type I fibers

5.1 Introduction

The loss or failure of a tissue or organ is devastating to human health. There are limited options available other than tissue or organ transplantation (2). With the shortage of donors, the gap between supply and demand is increasing. One emerging approach for solution is to engineer and construct living biological substitutes. This approach is known as tissue engineering (33). Among the ingredients necessary for tissue engineering, the design and fabrication of the scaffold is an important factor to ensure its success as it provides the environment for cells to survive and perform the necessary regeneration. The scaffold has to be made of a biocompatible material with the appropriate structure and mechanical properties. Moreover, it should be degradable at a rate that commensurate with the deposition of the natural extracellular matrix. Natural and synthetic polymers that are biocompatible and cell compatible are the materials of choice as many of the required properties can be tailored for specific tissue engineering applications. When suitable synthetic and natural polymers are both available, there is always a tendency to prefer the natural material. This is especially true if it is a component of our own extracellular matrix.

Among the natural polymers available, collagen is probably one of the most attractive biomaterial in tissue engineering applications (134, 135). It is present in nanofiber

form in the extracellular matrix. In many types of tissue their mechanical properties, such as strength, stiffness and toughness are attributed to the presence of the collagen fibers (46). Among the different types of collagen, collagen type I is of particular interest as it provides the structural integrity to the tissue (136).

In the design and construction of a tissue engineering scaffold, the structural aspects would have to also be considered. A porous structure is necessary as it would not only allow for cell migration but would also allow for the transport of oxygen, carbon dioxide, nutrients and metabolites into and out of the three-dimensional scaffold structure. There are two popular approaches to the formation of porous structure. It can either be a sponge like porous structure or the structure can be formed with overlapping fibers. Since collagen nanofiber is already a natural component of the extracellular matrix, a scaffold using collagen type I as the biomaterial in the form of nanofiber would be more closely mimicking the natural extracellular matrix environment (89, 145).

Purified collagen can be converted into the fiber form using the fiber spinning technique. Among the fiber spinning techniques available, electrospinning has emerged to be a favorite method of choice as it can produce fibers with diameter in the nanometers to several micrometers range (149). This technique has been demonstrated to be applicable to the preparation of collagen and many other polymer nanofibers.

The experimental parameters that can influence and control the outcome of the electrospinning process can be broadly classified into three categories. These are the polymer solution parameters, the electrospinning process parameters and the

environmental parameters (63). Among these parameters, the least studied is the effect of humidity. Depending on the water miscibility of the solvent system used, humidity can play an important role in determination the quality and size of the fiber produced as we have demonstrated in Chapter 4.

Collagen fiber in its native state is stable in the aqueous environment. This is due to its unique three-dimension stereochemistry of the native collagen structure. However, collagen nanofibers produced by processes such as electrospinning are not stable in water as the native collagen structure is not conserved in the regeneration process. The regenerated fibers disintegrate readily upon exposure to water or any aqueous media. In order to make use of these fibers in the fabrication of scaffold for tissue engineering, they need to be stabilized.

Several approaches have been used in the stabilization of regenerated protein materials. The commonest approach is to use a chemical approach making use of chemical crosslinking agents such as glutaraldehyde. The first reported electrospun collagen fibers were stabilized using glutaraldehyde vapor. Other chemical crosslinking agents commonly used include genepin and 1-ethyl-3-(3-dimethyl aminopropyl) carbodiimide (EDC) (212, 213) which is sometimes enhanced by N-hydroxysuccinimide (NHS) with the degree of crosslinking of the collagen material controlled by varying the ratio of EDC/NHS used. These chemical agents invariably causes concern of potential toxicity and excessive swelling. For these reasons, the approach of stabilization by physical methods have also been explored (26, 216, 217). Thermal annealing can be used to

impart aqueous stability to electrospun poly(vinyl alcohol) fibers by increasing the crystallinity of the polymer matrix without imparting significant chemical structural changes (29) . In addition, mechanical strength of the electrospun polysulphone fiber membranes, poly(L-lactic acid)(219) and poly(ϵ -caprolactone) (220) fiber mats can be improved by thermal annealing (221).

Ion beam treatment is a unique physical processing technique based on transfer of energy from accelerating ions to the target material. Both inert ion such as helium and reactive ions such as nitrogen can be used. Although the conventional ion implantation process is regarded as a surface treatment technique for bulk materials, its use on nanomaterials such as electrospun fibers is a bulk modification technique as ions penetrate through the fiber cross-section. This method of energy transfer offers the opportunity to be investigated as a new and novel approach to crosslinking of electrospun collagen fibers.

In this study we investigated the use of ion beam to treat the collagen nanofibers prepared by the electrospinning technique under controlled humidity and varying collagen solution concentration conditions as reported in Chapter 4. Broad spectrum helium ion and nitrogen ion beams were used and the effect of ion dosages were studied. Stability of the ion beam treated collagen fibers in both water and cell culture media were tested. The associate chemical changes within the collagen fibers associated with their changing aqueous stability was investigated with high resolution x ray photoelectron spectroscopy.

5.2 Experimental

5.2.1 Materials

Collagen type I derived from rat tail was used in collagen fiber preparation. The crude collagen isolated from rat tails was purified using an established procedure (237, 238). Briefly crude collagen was soaked in 70% aqueous ethanol for 30 minutes and then air dried. It was then sterilized using UV lamp overnight. The sterile crude collagen was purified by digesting in a 0.0175M acetic acid solution at 4°C for 7 days. The resulting solution was centrifuged at 11,000 rpm for 2 hours and the supernatant containing the purified collagen was collected. It was lyophilized to give the purified collagen type I in powder form.

5.2.2 Fiber fabrication

Lyophilized rat tail collagen type I (5 wt%) was dissolved in hexafluoroisopropanol (HFIP). Collagen fibers were produced in a custom built environmental control chamber at a controlled temperature of 21 ± 2 °C. The relative humidity was controlled over the range of 45 ± 5 %. A voltage of 20 kV, (Glassman High Voltage Inc.) and a distance between the syringe needle (22-gauge) and the collector electrode of 20 cm were used. Collagen solution flowrate was controlled by a single syringe pump (KD Scientific Inc.) at 0.15 mL/hr. Electrospun fibers were collected on the collector electrode.

5.2.3 Ion implantation

After fabricating the fibers, we implanted ions on them for aqueous stability. We used the ion implantation facility at the University of Western Ontario. Ion beams are generated using the 1.7 MV Tandem accelerator. Ion beam treatment was performed with the sample mounted vertically and at room temperature in an ultra-high vacuum (10^{-8} Torr) at the energies shown in table 3. Nitrogen (N^+) and Helium (He^+) ion beams are generated and implanted on the collagen fibers deposited on silicon wafers. This entire setup was mounted on the sample holder with 1.0 μ m thick tantalum (Ta) foil (Ta, 99.9% purity, Goodfellow Cambridge Ltd.)

Table 3 Ion beam treatment was performed with these energies

	Nitrogen (N^+)	Helium (He^+)
Energy:	1.7 Mev	520 Kev
Dose (ions/cm²)	8×10^{15}	12×10^{15}

Tantalum (Ta), acts as a diffuser in the set-up. Ta has high atomic mass and thus it is used to reduce the penetrating energy to the nanofibers. This diffuser or filter foil helps in converting the high-energy mono-energetic ions to lower poly-energetic ions. This gives a range of penetration depth for ion deposition with reduced energy-related damage to the

fibers. Only a fraction of N⁺ and He⁺ beam that penetrates the Ta foil is implanted into the fibers. The beam currents of N⁺ and He⁺ were limited to 200 nA.

Simulation results using the software *Stopping and Range of Ions in Matter* (SRIM), were used to guide the ion implantation experiments. SRIM is used to estimate the ion trajectory during implantation experiments. Calculation, for the estimation is organized by using Monte-Carlos (statistical) algorithms. It was used for simulating first layer of Ta foil to our work. *Transport of Ion in Matter* (TRIM), is a software that is included in the SRIM program package. TRIM allows simulation of up to eight layers of different material compositions. TRIM, estimates both the final 3D distribution of the ions and also all kinetic phenomena associated with the ion's energy loss as target damage, sputtering, ionization, and phonon production.

The simulation results indicated that using a 1.0 μm thick Ta foil, the initial ion energies of 1.7 MeV for N⁺ and 520 keV for He⁺ were reduced and diffused into energy distributions ranging from 0 to 300 keV for N⁺ and 0 to 100 keV for He⁺. Table 4 gives the specification of two different ion species used to crosslink the collagen fibers with two different energies and three different dosages.

The beam currents were kept below 200 nA. Ion beam treatment was performed with the sample placed vertically at room temperature in an ultra-high vacuum (10⁻⁸ Torr). An ultra-high vacuum beamline is necessary to keep the beam line free of residual gas. This prevents beam intensity reducing collisions between the ions and the molecules, or the formation of a contamination layer on the sample during the implantation.

5.2.4 Effect of ion implantation

The average diameter of as-spun collagen fiber was calculated as $D_{as-spun}$. Fiber diameter of crosslinked (ion implanted) sample for 100 fibers was measured for n-6, for both the ion species for implantation

(He^+ and N^+) and, for three different ion doses. Average of ion implanted crosslinked collagen fibers, for each condition was measured as $D_{crosslinked}$.

The change in fiber diameter was determined using the following equation:

$$\% \text{ Change in diameter after ion implantation} = 100 \% \times \frac{(D_{crosslinked} - D_{as-spun})}{D_{as-spun}}$$

5.2.5 Effect of exposure to aqueous solutions

Each of the ion implanted, crosslinked collagen nanofiber samples were tested for seven days for aqueous stability using swelling effect as a factor after soaking the sample in water (H_2O) and cell culture media (DMEM) for seven (7) days.

Each (ion implanted) crosslinked sample (for both the ion species for implantation (He^+ and N^+) and, for three different ion dose), were cut in half and one half was placed in

distilled water, while the other half was placed in cell culture media (DMEM) for the seven days.

After exposure to aqueous solutions, the samples were rinsed with water to remove any salt deposition on fiber over time and then imaged using SEM. Average fiber diameter, as D_{final} was calculated for both, water and cell culture media (DMEM).

The percentage of swelling was then calculated using the equation below.

$$\begin{aligned} & \% \text{ Change in diameter after exposure to aqueous solutions} \\ & = 100 \% \times \frac{(D_{\text{final}} - D_{\text{crosslinked}})}{D_{\text{crosslinked}}} \end{aligned}$$

5.2.6 Scanning electron microscopy (SEM)

Collagen fiber size and morphology were determined using a high-resolution scanning electron microscope by using a Leo 1540XB (LEO Electron Microscopy Ltd). The fibers were not sputter coated and an accelerating voltage of 1 kV to 3 kV was used.

5.2.7 Fiber diameters

A Java-based image processing program, Image J (National Institutes of Health) was used to measure the fiber diameter and understand the morphology of the images.

Four SEM images were acquired for each crosslinked collagen nanofibers and, twenty-five fibers were randomly picked from each image and measured. Thus, the total fiber diameters measured were 100 for each image (sample). Each condition was repeated six times to get, approximately 600 + fibers were measured for each of the conditions.

5.2.8 X-ray photoelectron spectroscopy (XPS)

A XPS system from Kratos Axis Ultra with a 210 W Al-K α monochromatic source was used. XPS spectra were acquired for both purified collagen (as control) and the as spun collagen fiber samples.

In addition, spectra for the fiber samples after ion implantation were also acquired. For all samples both the survey scan and high-resolution scans of selected elemental regions were also acquired. For the full scan pass energy of the survey scan was 160 eV and the high-resolution scan was 20 eV. The program CasaXPS (Casa Software Ltd.) was used to construct and curve-fit multiple peaks for the data envelope that appeared in the core-level energy spectra based on the built-in Marquardt-Levenberg (29) optimization algorithm.

5.2.9 Fiber degradation of crosslinked collagen nanofibers

Ninhydrin assay was conducted on each condition after ion implantation. The main objective was to quantify the amount of free primary amine group right after implantation. Although, this assay does not provide any information on the density or nature of crosslinking. But, estimating the free amine group in the given sample right after crosslinking, it will give the rate of the degradation of these ions implanted fiber with respect to the dose delivered. And this, quantification of the free amine group will also provide us with a good indication of the degree of crosslinking of electrospun collagen nanofibers.

Each of my samples for ninhydrin assay, were fabricated by electrospun technique on 1cm by 1cm silicon wafer with same time interval of fifteen (15) minutes. These samples were then ion implanted with respective dose, energy and species. Control (n=3) to this experiment were the as spun electrospun collagen nanofibers.

A ninhydrin solution was prepared according to Starcher et al.(245), however the quantities were different. A 4 N sodium acetate buffer was prepared by dissolving 544 g of sodium acetate trihydrate in 100 ml of glacial acetic acid and 400 ml of distilled water. The solution was left to mix overnight and the final pH was measured to be 5.5. A stannous chloride solution was prepared by adding 100 mg of SnCl₂ to 1 ml of ethylene glycol. The ninhydrin solution was prepared by dissolving 800 mg of ninhydrin in a mixture of 30 ml of ethylene glycol and 10 ml of the 4 N acetate buffer. 1 ml of the

stannous chloride suspension was added and the solution was stirred for one hour. A linear calibration curve was created using different glycine concentrations.

Crosslinked samples were then placed in vials containing 2 ml of distilled water mixed with 1 ml of the ninhydrin solution. The vials were placed in an 80 °C water bath for 15 minutes and then left to cool down. A Beckman DU spectrophotometer was used to measure the optical absorbance at 570 nm, which is the typical absorbance for the purple complex that is formed upon the reaction of ninhydrin with amino acids. After measuring the absorbance, the calibration curve (Refer to Appendix) was used to determine the concentration of free amino acids in solution. Followed by calculating the degree of crosslinking. We used following formula to calculate the degree of crosslinking at different dose and energies.

The degree of crosslinking was determined by the following equation:

$$\text{Degree of crosslinking } \% = \frac{[AC \text{ non - crosslinked} - AC \text{ crosslinked}] * 100}{AC \text{ non - crosslinked}}$$

Where AC is the Amine concentration at different dose.

5.2.10 Statistical analysis

All statistics were performed using OriginPro 8 (OriginLab Corporation). Propagation of error and the overlapping statistical formula were done on the data using Microsoft Excel (Microsoft Corp).

5.3 Results & Discussion

5.4 Physical effect of ion implantation on electrospun collagen fibers

Collagen nanofibers produced by electrospinning are not stable in water. In fact, they disintegrate readily upon exposure to water or any aqueous media due to the inability to regenerate the natural stereochemistry (216, 295). In order to make use of these fibers in the fabrication of scaffold for tissue engineering, they need to be stabilized. Chemical cross-linking is the well-established approach to stabilize collagen fibers. In this study, a novel approach of ion implantation has been used.

The ability to control degradation of the collagen nanofibers in an aqueous environment has been an important aspect of tissue engineering (296). To achieve these optimal conditions for collagen fiber stabilization, we made studied two different ions, helium which is unreactive and nitrogen which readily reacts with the chemical functionalities in collagen. Since the Tendatron only generates monochromatic energy ions at relatively high energy that readily degrades polymer, simulation using the software's Simulation

results using the software *Stopping and Range of Ions in Matter* (SRIM), were used to guide the ion implantation experiments. SRIM is used to estimate the ion trajectory during implantation experiments. Calculation, for the estimation is organized by using Monte-Carlos (statistical) algorithms. It was used for simulating first layer of Ta foil to our work. *Transport of Ion in Matter* (TRIM), is a software that is included in the SRIM program package. TRIM allows simulation of up to eight layers of different material compositions. TRIM, estimates both the final 3D distribution of the ions and also all kinetic phenomena associated with the ion's energy loss as target damage, sputtering, ionization, and phonon production.

The simulation results, presented in the experimental section, indicated that using a 1.0 μm thick Ta foil, the initial ion energies of 1.7 MeV for N^+ and 520 keV for He^+ were reduced and diffused into energy distributions ranging from 0 to 300 keV for N^+ and 0 to 100 keV for He^+ . Table 4, gives the specification of two different ion species used to crosslink the collagen fibers with two different energies and three different dosages.

Table 4 The specification of two different ion species used to crosslink the collagen fibers with two different energies, and three different doses

	Nitrogen (N^+)	Helium (He^+)
Energy:	1.7 Mev	520 Kev
energy with Ta foil	0 to 300 keV	0 to 100 keV
Dose (ions/cm²)	4 x 10 ¹⁵	
Dose (ions/cm²)	8 x 10 ¹⁵	
Dose (ions/cm²)	12 x 10 ¹⁵	

5.5 Effect of ion implantation on fiber diameters

The electrospun collagen nanofibers were ion implanted with the specific ion species using conditions outlined in Table 1. The change in diameter was analyzed using the SEM images. The diameter distribution was determined from 600+ randomly chosen fibers from 6 different sets, on (6x4) 24 captured images. SEM images shown in figure 19 to figure 24 represent the morphologies of the as spun and after ion implanted fibers as a function of ion dose delivered for different ions at different energies. The collagen nanofibers maintained their morphology after ion implantation as shown in figure 19 B, 20 B, 21 B, 22B, 23 B and 24 B . Fiber diameter distribution in the form of histogram for a given sample was also determined and is shown in the appendix The results were best-fits of normal distribution.

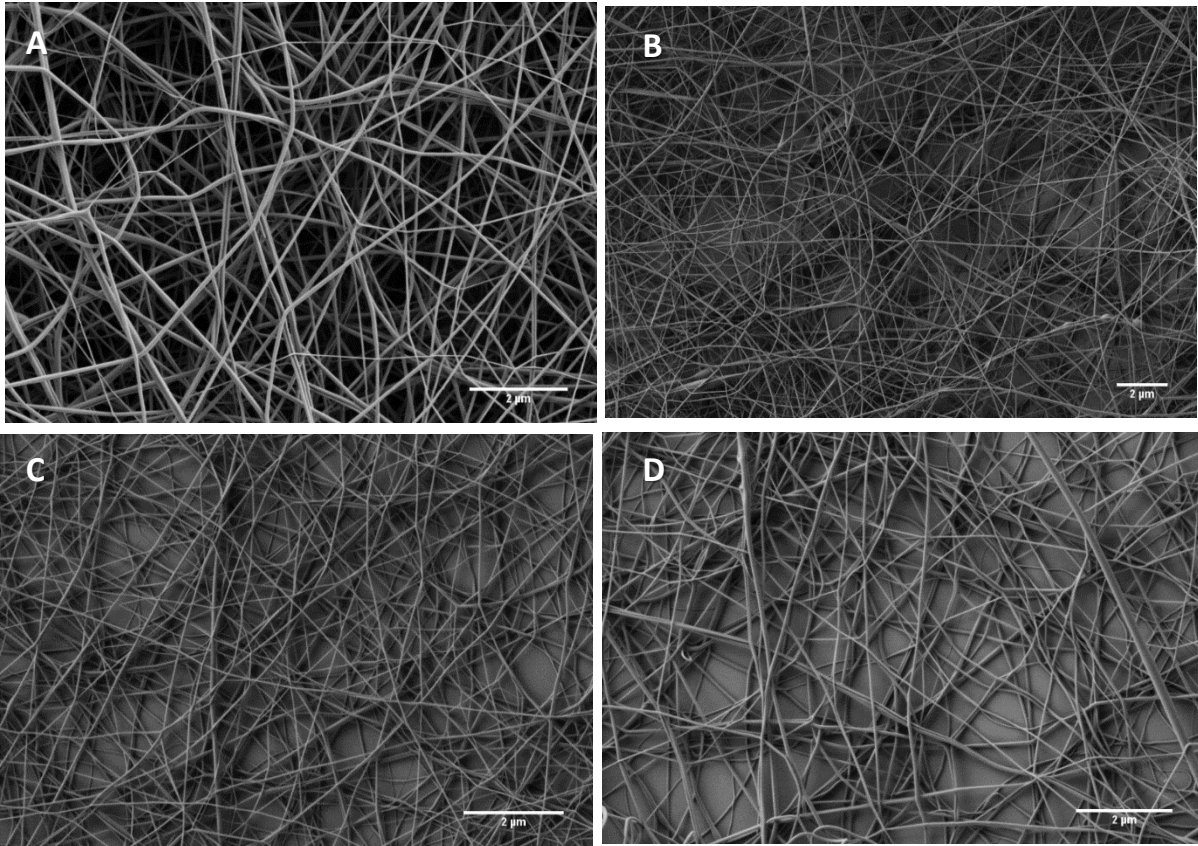


Figure 19 Nitrogen- ion implantation at 4×10^{15} ions/cm² on collagen type-1 nanofibrous scaffold A: Before ion implantation (as- spun fibers) B: After N⁺ ion implantation C: After soaking it in water for seven days D: After soaking it in cell culture media for seven days in cell culture media

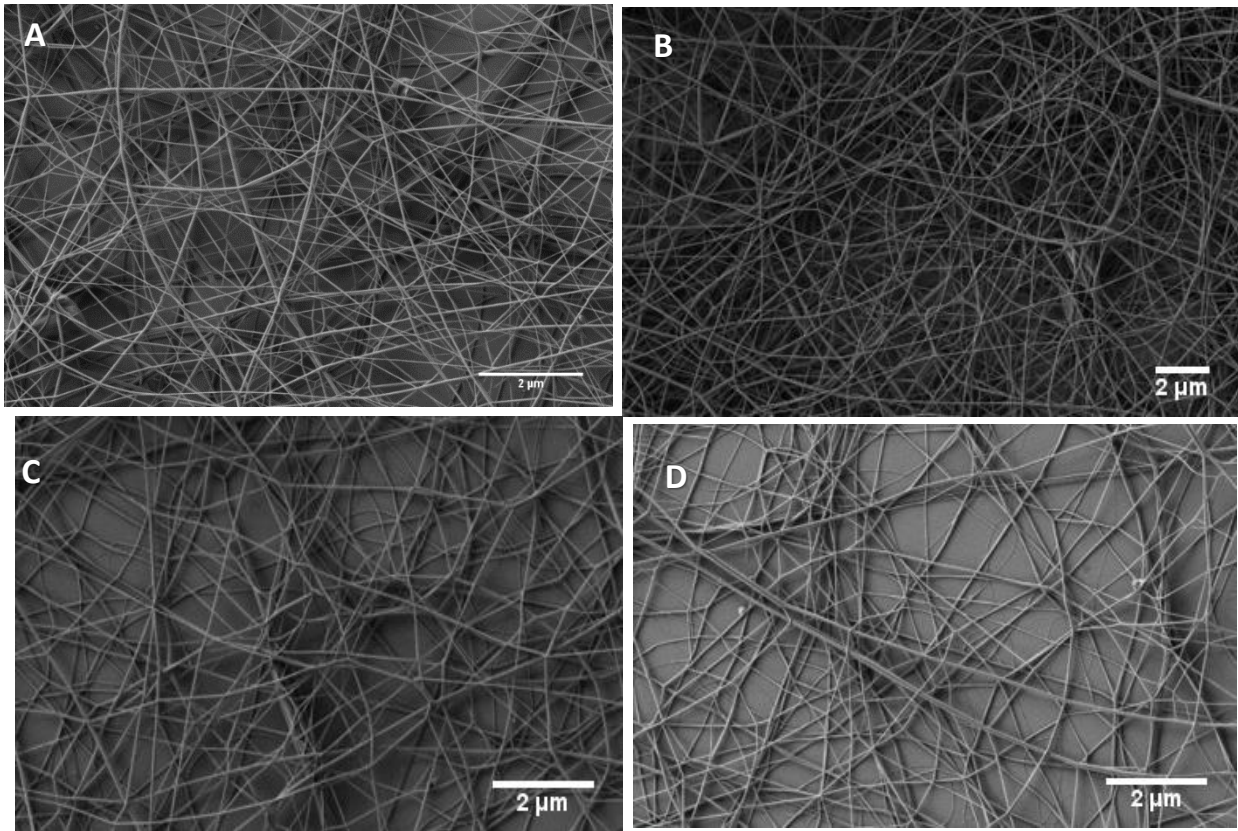


Figure 20 Nitrogen- ion implantation at 8×10^{15} ions/cm² on collagen type-1 nanofibrous scaffold A: Before ion implantation (as- spun fibers) B: After N⁺ ion implantation C: After soaking it in water for seven days D: After soaking it in cell culture media for seven days in cell culture media

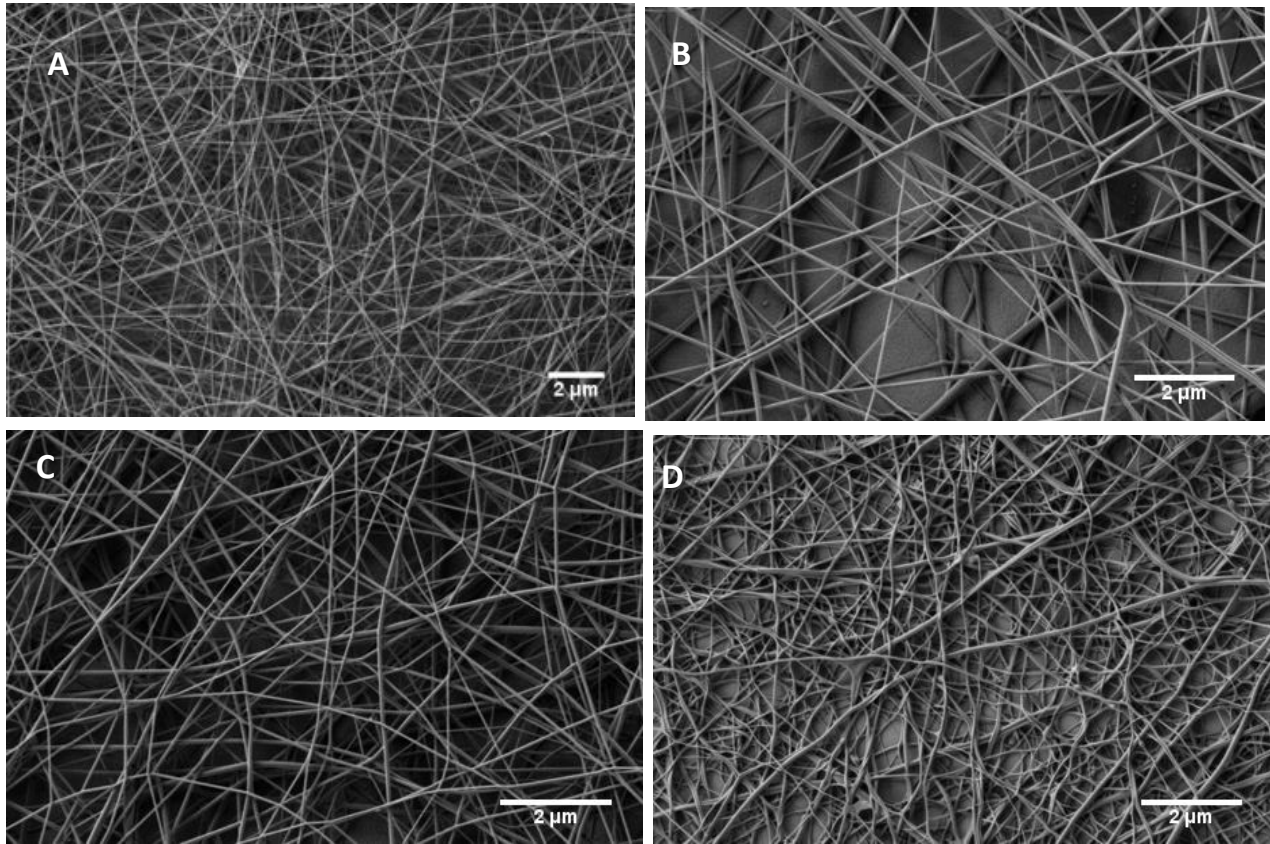


Figure 21 Nitrogen- ion implantation at 12×10^{15} ions/cm² on collagen type-1 nanofibrous scaffold A: Before ion implantation (as- spun fibers) B: After N⁺ ion implantation C: After soaking it in water for seven days D: After soaking it in cell culture media for seven days in cell culture media

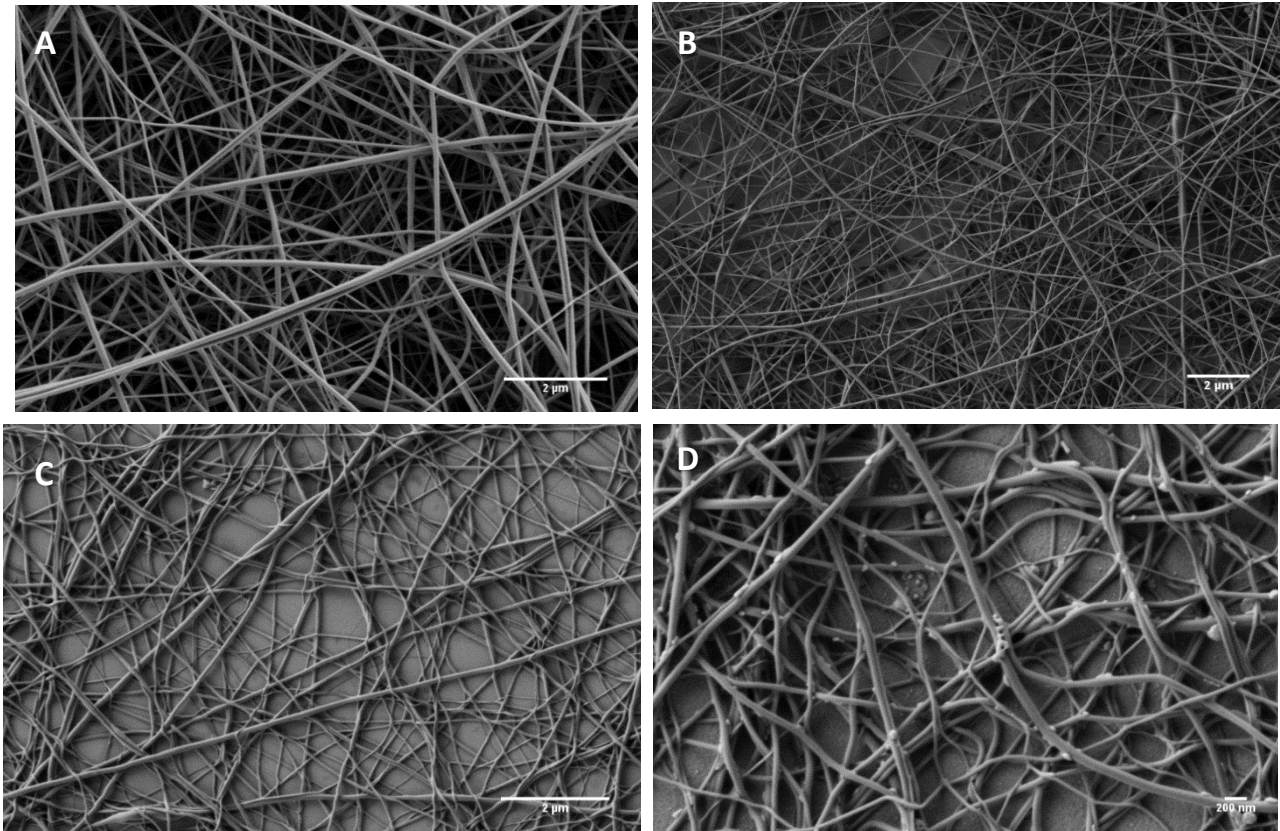


Figure 22 Helium- Ion Implantation at 4×10^{15} ions/cm² on collagen type-1 nanofibrous scaffold A: Before ion implantation (as- spun fibers) B: After He⁺ ion implantation C: After soaking it in water for seven days D: After soaking it in cell culture media for seven days in cell culture media

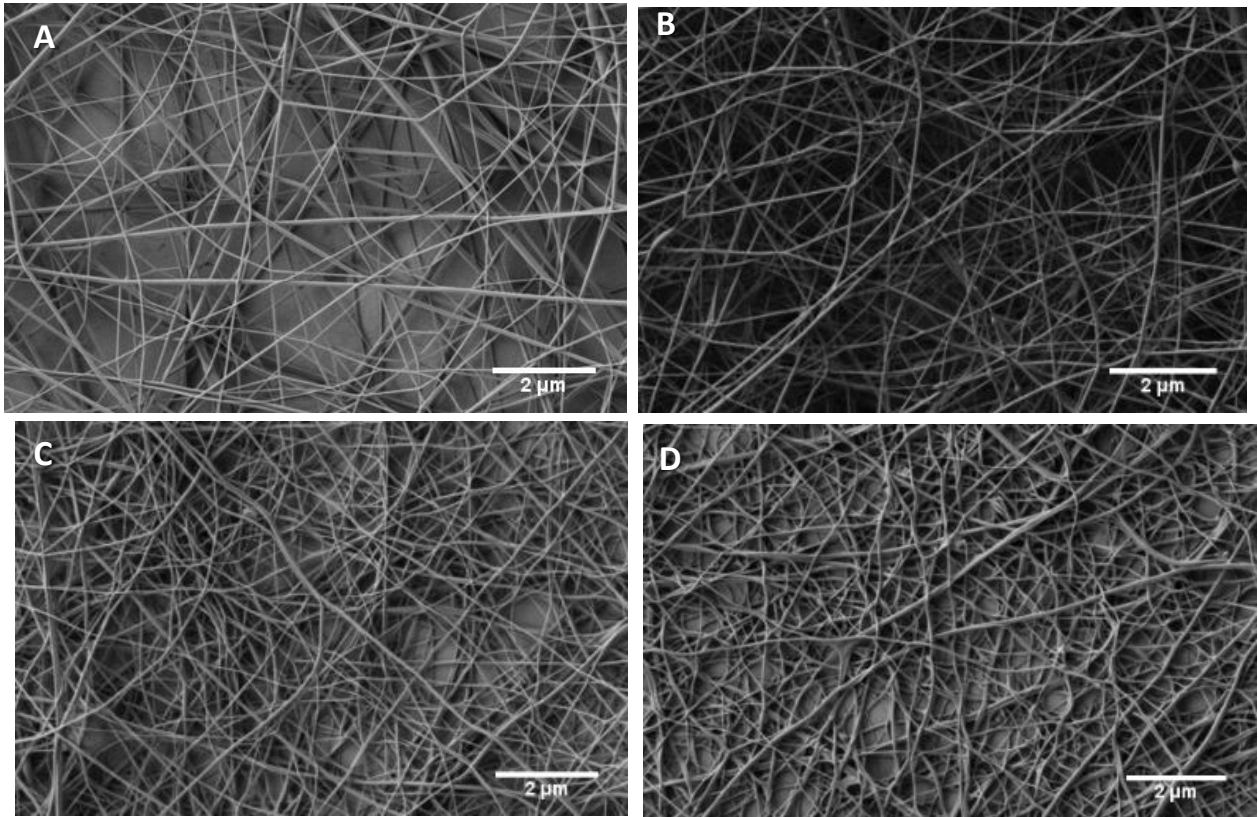


Figure 23 Helium- Ion Implantation at 8×10^{15} ions/cm² on collagen type-1 nanofibrous scaffold on collagen type-1 nanofibrous scaffold

A: Before ion implantation (as- spun fibers) B: After He⁺ ion implantation

C: After soaking it in water for seven days D: After soaking it in cell culture media for seven days in cell culture media

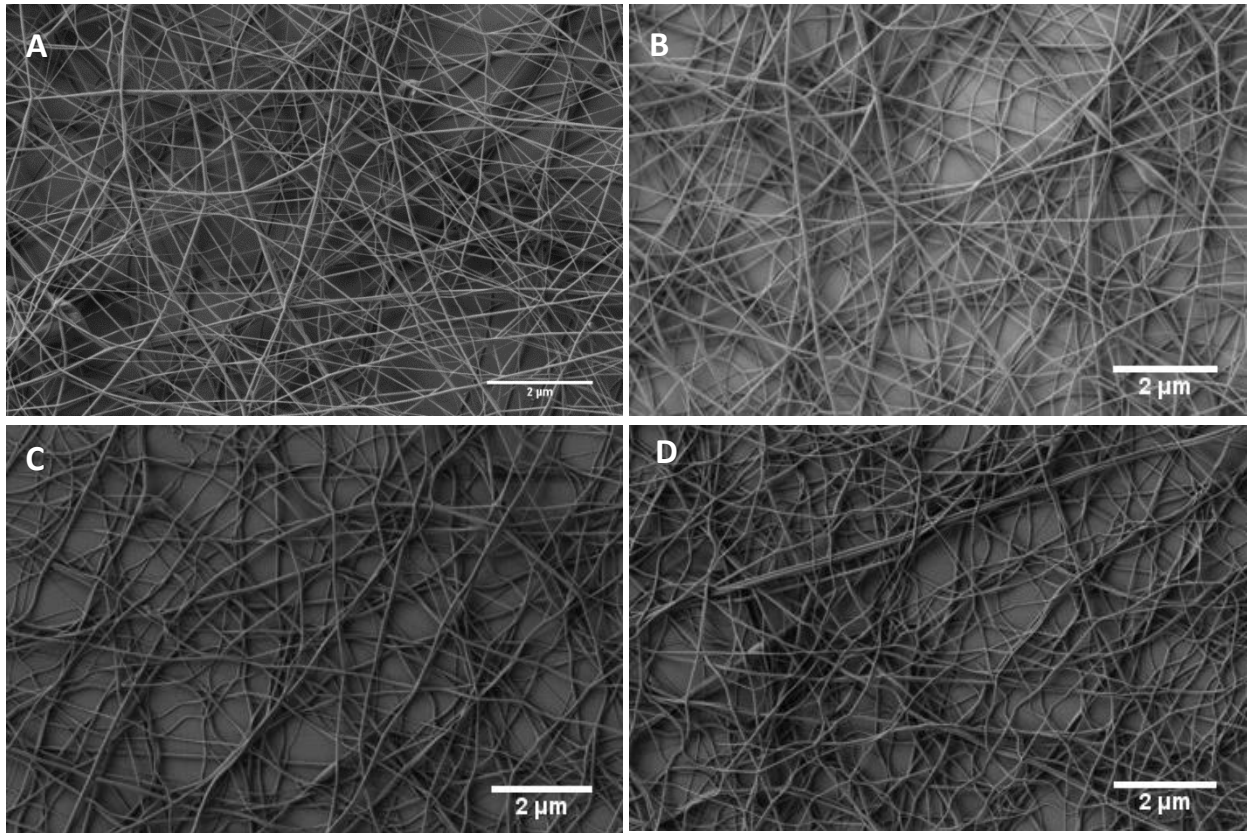


Figure 24 Helium- Ion Implantation at 12×10^{15} ions/cm² on collagen type-1 nanofibrous scaffold A: Before - ion implantation (as- spun fibers) B: After He + ion implantation C: After soaking it in water for seven days D: After soaking it in cell culture media for seven days in cell culture media

The detail quantitative analysis of the diameter changes measured using SEM images of before and after ion implantation for both the ion species are summarized in Table 2. For

each of the dose, the percentage change in diameter is recorded using the formula of the percentage change in the diameter (see the appendix).

From Table 5 below, we found that for helium ion implantation fiber diameter varied proportionally with respect to dose implanted into the collagen nanofiber. As the dose increased the fiber diameter also increased. But a similar trend was not found in nitrogen ion implantation. For nitrogen implantation on these collagen nanofibers, we found these collagen nanofibers diameter reaches maxima at 8×10^{15} ions/cm² of implantation.

Table 4 Diameter change for before and after ion implantation for two different species for all three doses.

Dose (ions/cm ²)	Diameter (nm)	Diameter (nm)	(%) change in the diameter (nm)
Helium	As spun	Post implantation	
4 x 10¹⁵	55 ± 24	42 ± 18	-23 ± 55
8 x 10¹⁵	40 ± 20	34 ± 14	-15 ± 61
12 x 10¹⁵	47 ± 20	56 ± 25	+19 ± 68
Nitrogen			
4 x 10¹⁵	58 ± 23	36 ± 17	-38 ± 50
8 x 10¹⁵	47 ± 20	55 ± 20	+17 ± 60
12 x 10¹⁵	52 ± 26	33 ± 15	-36 ± 58

The figure 25 below, the error propagation displays the opposite trend for both the ion species implanted.

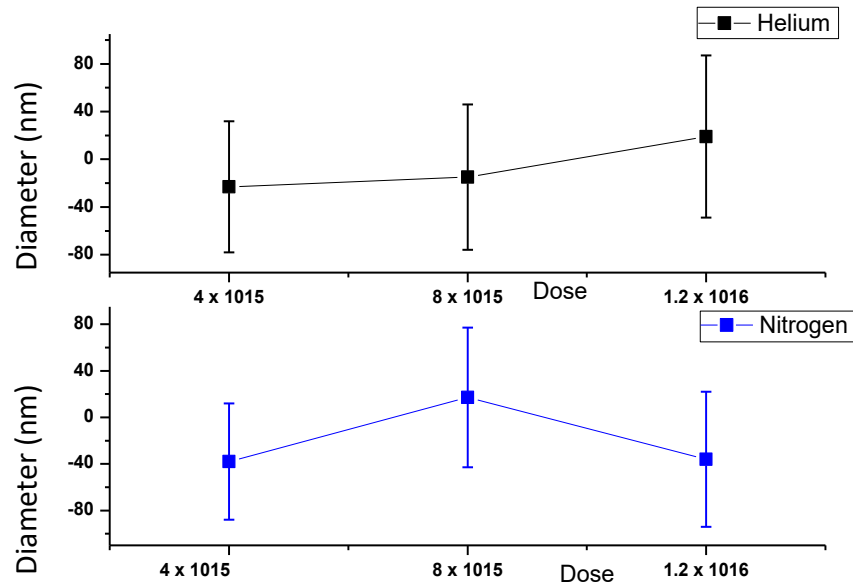


Figure 25 Error propagation on the results of before and after ion implantation on two different species at different energies and doses

To these results, we then applied the overlapping statistical formula, a statistical test to test if the data set at each set is significantly similar to each other.

Following is the formula for the equation we have used in for our data.

Equation 2

$$|A - B| \leq (\delta A + \delta B)$$

If the equation (1) is satisfied, then $A=B$ with in the experimental uncertainties

We substituted the value of nitrogen as A, and helium as B. By doing so, we then substitute the values of each dose point to check $|A - B| \leq (\delta A + \delta B)$ if it states true for each dose applied. Where A, B is the average and δA , δB are the standard error of the values A and B respectively.

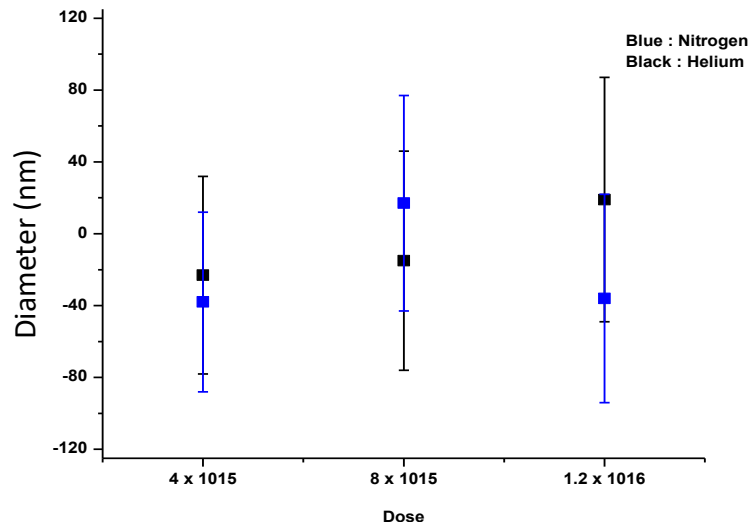


Figure 26 Overlapping formula for Nitrogen ion and Helium ion implant at for after ion implantation for all three doses.

Applying the overlapping statistical formula, for both the ion species. We get that their standard error overlaps on each other as shown in figure 26 above.

Demonstrating that helium ion implant or the nitrogen ion implant, behave similarly on each of the treatment applied to the crosslinked electrospun collagen nanofibers.

Statistically demonstrates that these electrospun collagen nanofibers behave significant to both the ion species, after ion implantation.

5.6 Stability of the ion implanted electrospun collagen fibers in water and DMEM

Aqueous stability test was conducted after the ions were implanted to crosslink the collagen nanofibers. This aqueous stability test was conducted by exposing the ion implanted collagen nanofibers in water and DMEM for seven days.

Morphology of the fibers after ion implantation under various implantation conditions were summarized figure 19 to 24 as images C. The results demonstrated that these crosslinked fibers (for both the ion species at all the different doses) were stable in water and DMEM, maintained their fiber integrity for up to seven days.

5.6.1 Discussion

Several approaches have been used in the stabilization of regenerated protein materials. The commonest approach is to use a chemical approach making use of chemical crosslinking agents such as glutaraldehyde. The first reported electrospun collagen fibers were stabilized using glutaraldehyde vapor. Other chemical crosslinking agents commonly used include genepin and 1-ethyl-3-(3-dimethyl aminopropyl) carbodiimide (EDC) (212, 213) which is sometimes enhanced by N-hydroxysuccinimide (NHS) with the degree of crosslinking of the collagen material controlled by varying the ratio of EDC/NHS used. These chemical agents invariably cause concern of potential toxicity and excessive swelling. For these reasons, the approach of stabilization by physical methods have also been explored (26, 216, 217). Thermal annealing can be used to impart aqueous stability to electrospun poly(vinyl alcohol) fibers by increasing the crystallinity of the polymer matrix without imparting significant chemical structural changes (29) . In addition, mechanical strength of the electrospun polysulphone fiber membranes, poly(L-lactic acid) (219) and poly(ϵ -caprolactone) (220) fiber mats can be improved by thermal annealing (221). Ion beam treatment is a unique physical processing technique based on transfer of energy from accelerating ions to the target material. Both inert ion such as helium and reactive ions such as nitrogen can be used. Although the conventional ion implantation process is regarded as a surface treatment technique for bulk materials, its use on nanomaterials such as electrospun fibers is a bulk modification technique as ions penetrate through the fiber cross-section. This method of energy transfer offers the opportunity to be investigated as a new and novel approach to crosslinking of electrospun collagen fibers.

5.7 Quantify in terms of diameter changes as a proxy for stability – as spun (control) vs. ion implanted

To quantify the differences among the diameter data collected before and after water exposure. The overlapping statistical formula, a statistical test to test if the data set at each set is significantly similar to each other was applied to the data sets as shown in figure 27.

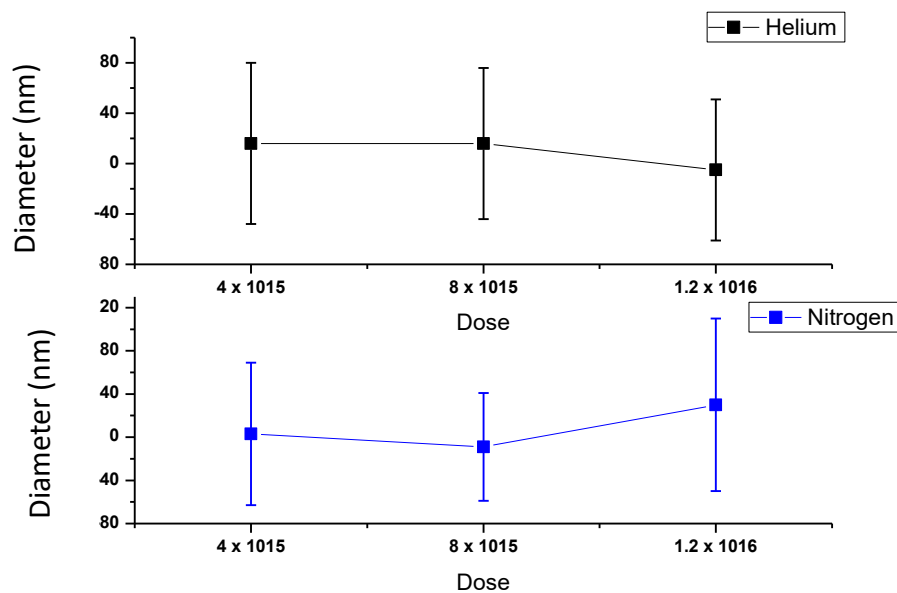


Figure 27 Applying error propagation on water – treatment percentage change on the diameter of crosslinked collagen nanofibers, when soaked in water for seven days (for two different species at different energies and doses).

Following is the formula for the equation we have used in for our data.

$$|A - B| \leq (\delta A + \delta B)$$

Equation 2

If the equation (1) is satisfied, then $A=B$ with in the experimental uncertainties

We substituted the value of nitrogen as A, and helium as B. By doing so, we then substitute the values of each dose point to check $|A - B| \leq (\delta A + \delta B)$ if it states true for each dose applied. Where A, B is the average and δA , δB are the standard error of the values A and B respectively.

Applying the overlapping statistical formula, for both the ion species. We obtained the standard error overlaps on each other as shown in figure 28 below. Demonstrating that helium ion implant or the nitrogen ion implant, behave similarly on each of the treatment applied to the crosslinked electrospun collagen nanofibers. It can be concluded that these electrospun collagen nanofibers behave similarly to both the ion species after ion implantation.

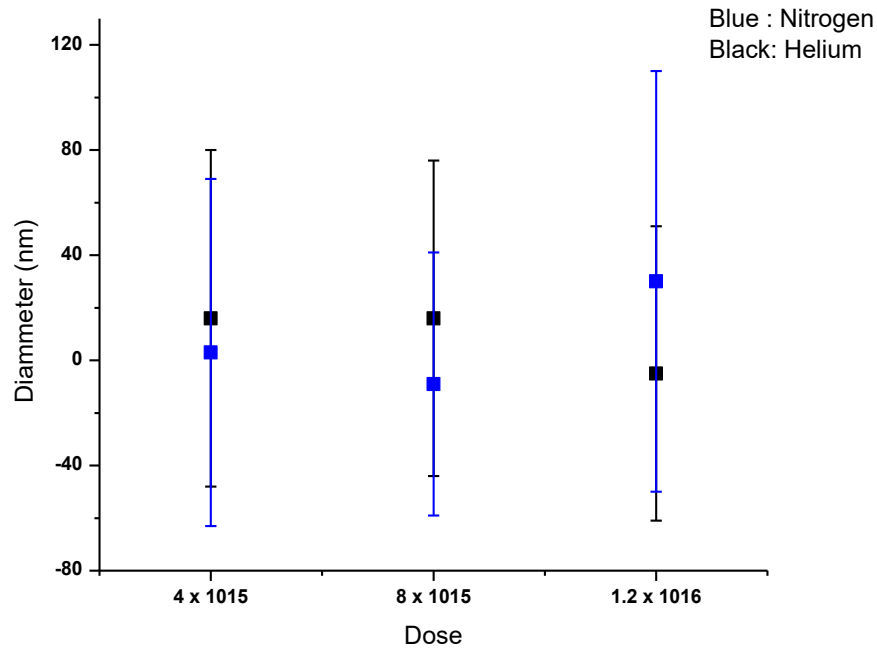


Figure 28 Applying over lapping law on water - treatment of the percentage change in the diameter of crosslinked collagen nanofibers, when soaked in water for seven days (for two different species at different energies and doses).

5.7.1 Physical effect of exposure of the ion implanted electrospun collagen fibers to DMEM

Under realistic tissue engineering conditions, the collagen fiber scaffold will be exposed to cell culture media which contains an appreciable amount of ionic species instead of water. It is therefore important that stability of the ion implanted scaffolds be tested in cell culture media. A series of stability test of the ion implanted collagen scaffold was carried out the cell culture media Dulbecco's Modified Eagle's Medium) (DMEM).

This cell culture media stability test was conducted by immersing the ion implanted electrospun collagen fiber scaffolds in cell culture media (DMEM) for seven days. The series of Image D in figure 19 to 24 summarize the morphology results for both helium and nitrogen ion implanted scaffolds at all doses used.

These images figure 19 to 24, D images demonstrate the ion implanted collagen nanofibers maintained their fiber integrity in the cell culture media used DMEM for both types of ion and for all doses used.

These results from figure 19 to 24, demonstrate thicker fiber diameter as compared to water soaked samples for seven days. These trends of thicker fibers diameter were observed in cell culture media due to the presence of iron. This presence of iron in cell culture media promotes degradation of these collagen nanofibers.

5.7.2 Fiber diameter changes as a measure of fiber stability

The data analysis shown in Figure 5 and table 8, indicated that for helium (He^+) the fiber diameter increased in cell culture media with the largest diameter increase at the lowest ion dose implanted (4×10^{15}). This increase in fiber diameter in cell culture media decreases as for the dose of the ion implantation increased.

We found the reverse effect for nitrogen (N^+) implanted collagen fiber. The fiber diameter increases for N^+ in cell culture media was higher for the highest dose (12×10^{15})

¹⁵). And the fiber diameter decreases in cell culture media as for the dose of the ion implantation decreased.

These trends of indicating the thicker fibers diameter in cell culture media were found due to the presence of iron (297) . This presence of iron in cell culture media promote degradation of these collagen nanofibers (297). A similar trend was not observed in water immersed samples for both He⁺ and N⁺ implanted samples.

Table 5 Diameter change for after soaking in water and cell culture medial DMEM for seven days for two different species for all three doses.

Helium Dose (ions/cm ²)	Post implantation Diameter (nm)	Water	Percentage	DMEM (7days)	Percentage
		(7 days) Diameter (nm)	Change (%)	Diameter (nm)	Change (%)
4 x 10¹⁵	42 ± 18	49 ± 20	+16 ± 65	65 ± 28	+54 ± 85
8 x 10¹⁵	34 ± 14	39 ± 15	+14 ± 61	45 ± 18	+32 ± 70
12 x 10¹⁵	56 ± 25	53 ± 19	-5 ± 56	54 ± 18	-3.5 ± 55
Nitrogen					
4 x 10¹⁵	36 ± 17	37 ± 17	+3 ± 67	39 ± 20	+8 ± 73
8 x 10¹⁵	55 ± 20	50 ± 19	-9 ± 50	50 ± 16	-9 ± 47
12 x 10¹⁵	33 ± 15	43 ± 21	+30 ± 81	65 ± 31	+96 ± 125

To better understand the comparison between these results under the ion implantation conditions used, we applied the overlapping statistical formula (Equation 2) to determine their uncertainties overlap. The results shown in Figure 29 /table 8 demonstrate that implantation of both ion species result in similar trend, even after soaking in cell culture media for seven days. We did observe an increase in fiber diameter after immersion in DMEM as compared to that of fibers soaked in water for the same length of time. And the difference of both the species at different dose after soaking in cell culture media for seven days.

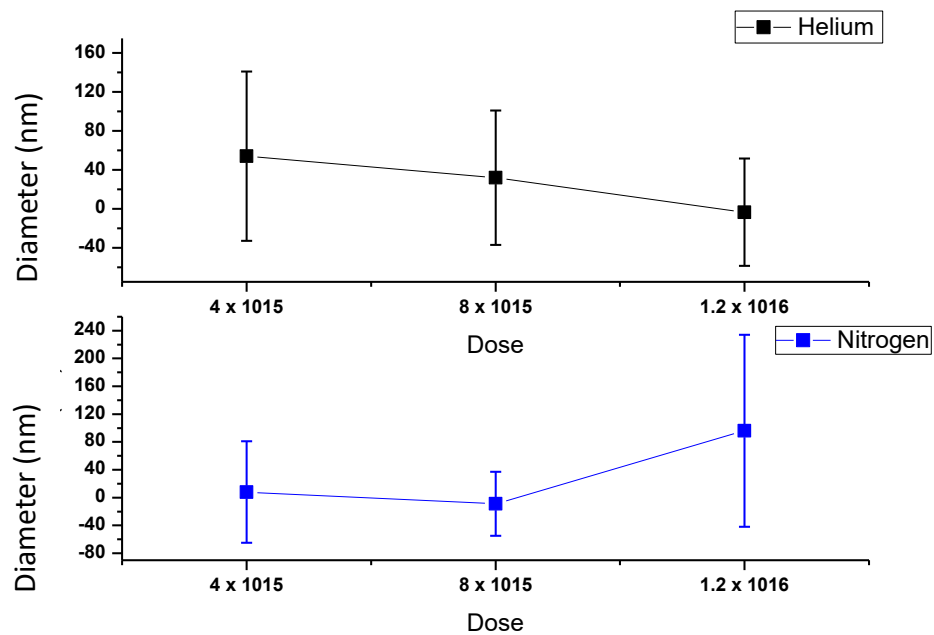


Figure 29 Applying lapping law on cell culture media – treatment of the percentage change in the diameter of crosslinked collagen nanofibers, when soaked in water for seven days (for two different species at different energies and doses).

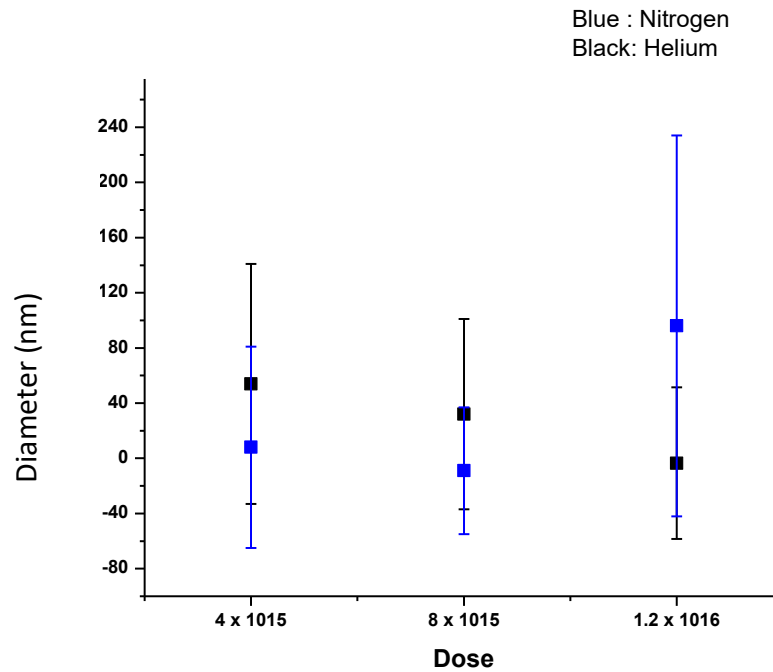


Figure 30 Applying over lapping law on cell culture media - treatment the percentage change in the diameter of crosslinked collagen nanofibers, when soaked in cell culture media for seven days (for two different species at different energies and dose

By applying this formula (Equation 2), we got that their uncertainties overlap on each other as shown in figure 30. Demonstrating that, both the ions species on collagen nanofibers create the similar trend, even after soaking in cell culture media for seven days. Comparing the results of water exposure to that of DMEM immersion, a larger diameter increase was observed for the DMEM exposed samples. This is not a surprise considering the compositional difference between the two solutions. The ionic species present in DMEM can interact with the collagen molecule to promote water ingress into the fiber that could lead to degradation thus leading to the observed increase in fiber diameter.

5.8 Chemical effects of ion implantation on electrospun collagen fibers

Although no chemicals were used in the ion implantation process, this does not necessarily mean that there were no chemical changes taking place during ion implantation. The energy ranges of the ion beams used are undoubtedly large enough to break chemical bonds (for He⁺ and the N⁺, the energy ranges are 0 – 100 kV and 0 – 300 kV respectively). It is therefore reasonable to expect chemical changes to take place in the ion implantation process. X-ray photoelectron spectroscopy (XPS) was used to confirm and delineate any changes in the chemical composition of the ion implanted fibers.

Survey XPS spectra of the as produced electrospun collagen fibers was collected and shown in Figure 31. The untreated collagen showed an elemental composition of (atomic percentage) 13.7 ± 2.0 % of nitrogen, 57 ± 5.4 % of carbon and 21.3 ± 3.8 % of oxygen. This provides the baseline data to allow for tracking changes in the elemental composition of the ion implanted collagen fibers using different ions and at different ion doses.

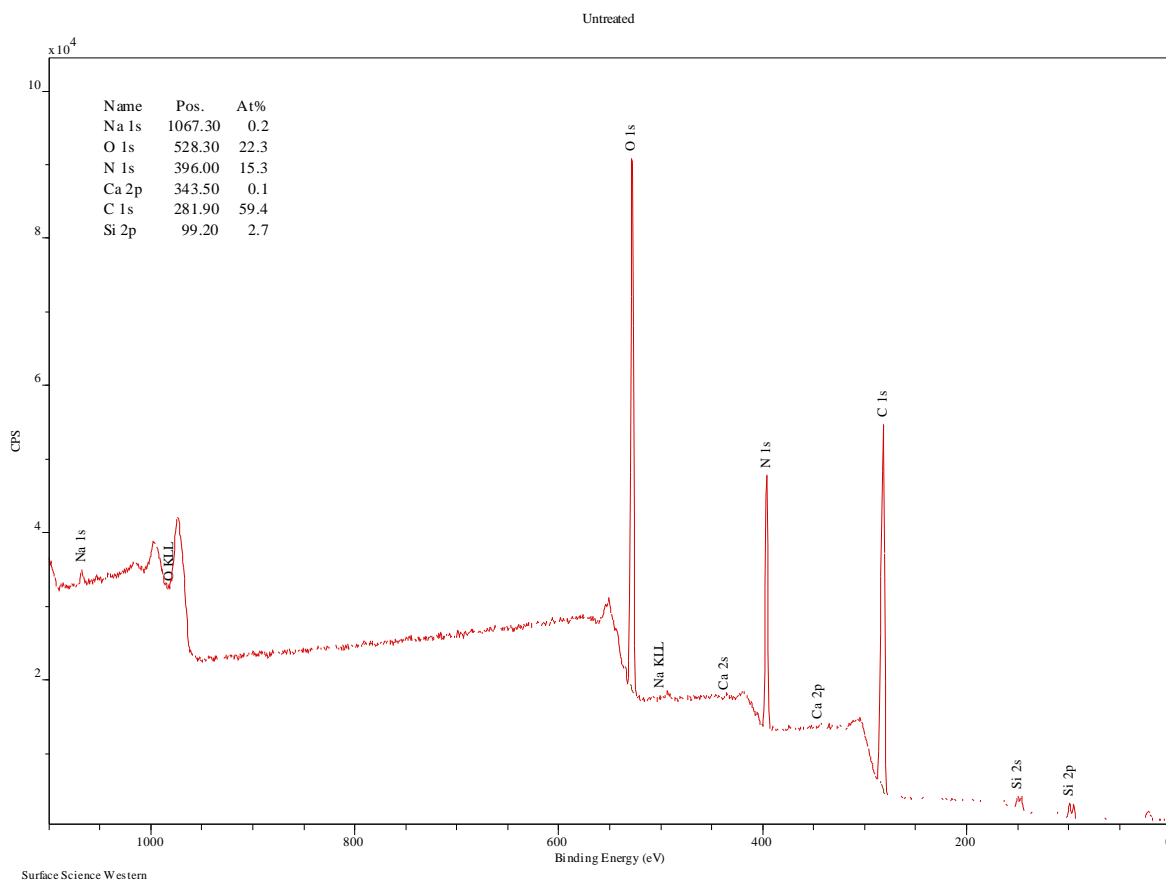


Figure 31 Un-crosslinked collagen sample full scan

Survey XPS spectra of the ion implanted fibers under all the experimental conditions used were collected and shown in Figures 15 - 20 (6 figures as shown in the appendix). The elemental composition of the ion implanted samples using He⁺ and N⁺ ions and at different ion doses as determined from these spectra are summarized in Table 8. It can be seen that although the carbon and oxygen contents varied over a relatively narrow range, there is a much larger change in the nitrogen content. In tissue engineering applications, the nitrogen content is of particular interest as cell adhesion on a substrate depends on the

nitrogen containing peptides (298). The changes in nitrogen contents as a function of ion doses as comparing to that of the non-ion beam treated control sample is shown in Figure 32. The He⁺ implanted samples showed a slightly lower nitrogen content compared to control at the lowest ion dose used (4×10^{15} ions/cm²). As the He⁺ dose of implantation was increased, the nitrogen retained further decreased). Contrast to this trend, nitrogen ion implantation exhibited a lower nitrogen contents relative to He⁺ treatment at doses of 4×10^{15} ions/cm² and 8×10^{15} ions/cm² but as N⁺ dose was further increased to 12×10^{15} ions/cm², the nitrogen content recovered to

higher than that of the He⁺ implanted sample.

Table 6 Amount of nitrogen, carbon and oxygen present in the ion implanted sample for both the species at different doses.

	Nitrogen	Carbon	Oxygen
Control	Average ± SD	Average ±SD	Average ± SD
	13.7 ± 2.0	57 ± 5.4	21.3 ± 3.8
Helium	Average ± SD	Average ±SD	Average ± SD
4 x 10 ¹⁵	12 ± 2.9	56.8 ± 4.7	19.4 ± 1.9
8 x 10 ¹⁵	8.4 ± 1.6	54.1 ± 8.4	21.1 ± 3.7
1.2 x 10 ¹⁶	6.2 ± 0.4	50.6 ± 3.2	25.6 ± 2.4
Nitrogen	Average ± SD	Average ±SD	Average ± SD
4 x 10 ¹⁵	7.0 ± 0.7	54.7 ± 5.9	20.3 ± 1.3
8 x 10 ¹⁵	4.3 ± 0.9	53.6 ± 2.9	24.1 ± 3.2
1.2 x 10 ¹⁶	8.0 ± 0.4	55.1 ± 0.6	19.4 ± 1.1

As helium is undetectable in XPS measurements, the amount of helium remaining in the sample after the ion implantation remains unknown. However, since helium is non-reactive and has a high diffusion coefficient due to its small size. We do not expect any amount of helium remaining in the treated sample.

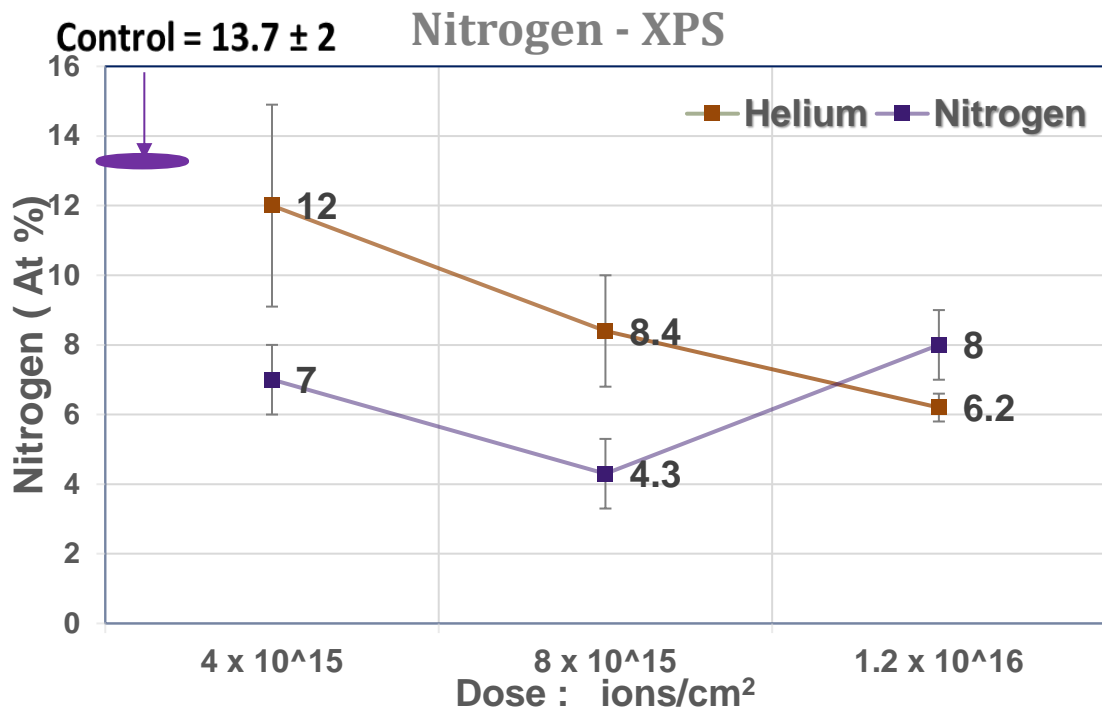


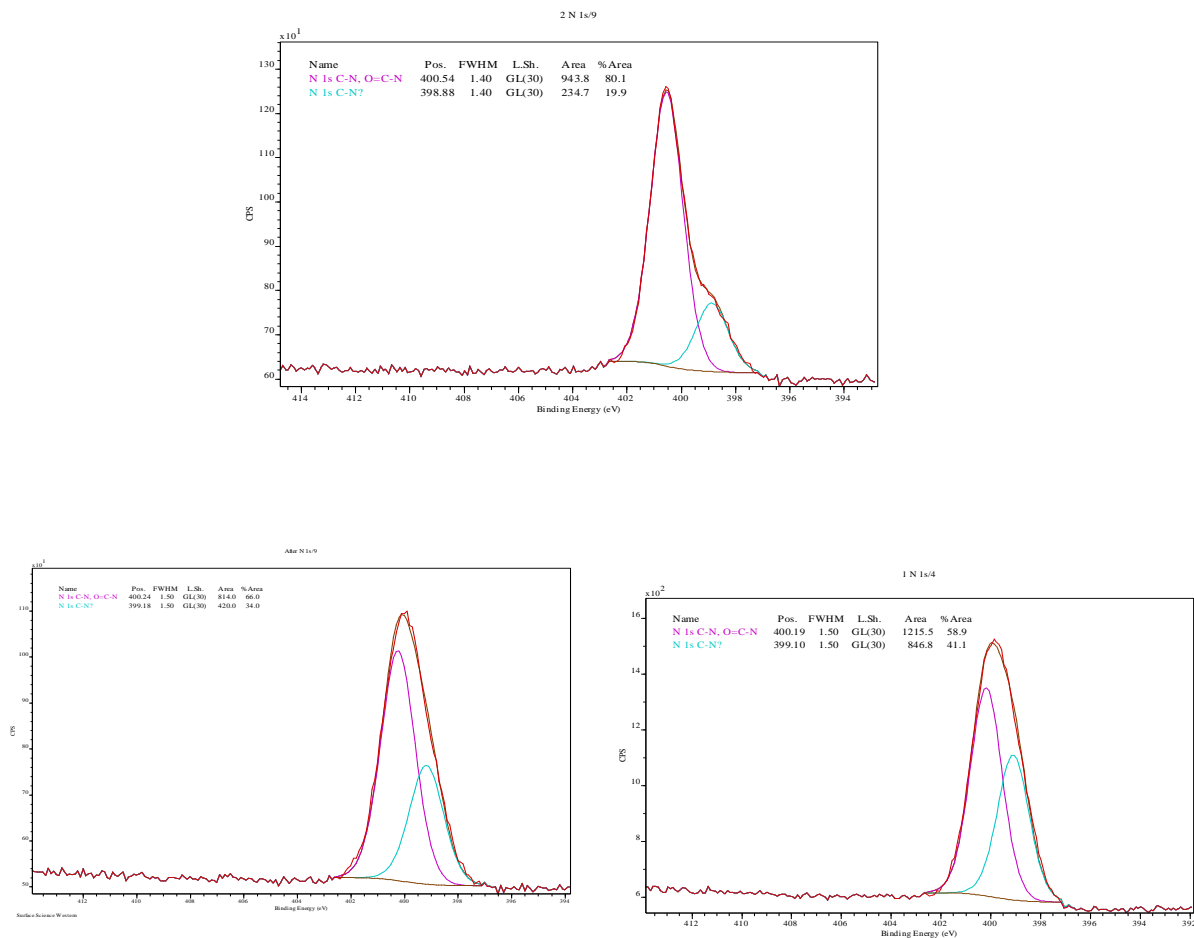
Figure 32 Atomic percentage (at%) of average of nitrogen for both the ion species at different energies and all the different doses. It gives us a comparative edge with the control, which is as spun collagen nanofibers with the helium and nitrogen ion implanted samples at different dose.

The stability tests in water and DMEM presented in the last section indicated that under all implantation conditions used resulted in stable fibers over a period of 7 days. The diameter of the treated collagen fibers exhibited varying degrees of swelling after immersion in water and especially DMEM is an indication that these ion implanted collagen fibers are susceptible to degradation by hydrolysis. This observation is mostly likely related to the detailed chemical structural changes occurring during the ion implantation process.

5.8.1 Effect of Ion Implantation on Chemical Structure

In order to understand the chemical and structural changes taking place in the ion implantation processes that lead to collagen fiber stability, a series of high resolution (15 eV) scans of was performed on the as spun and ion implanted electrospun fibers. This understanding is also important to allow for us to assess the impact of these changes on cell behavior when the scaffolds are to be used in tissue engineering. Among the major elements of C, O and N, the focus is on the nitrogen peak as the nitrogen content undergoes the largest change as a function of ion doses as well as the specific ion used.

A: Original Collagen – Before Implantation



B: N⁺ treated - collagen fibers

C: He⁺ treated - collagen fibers

Figure 33 High resolution scan of nitrogen at the binding energy of 399.9 eV. It displays comparison of as spun sample with helium ion and nitrogen ion implanted sample.

The high-resolution nitrogen XPS spectra for the untreated collagen fiber and those ions implanted with He⁺ and N⁺ at a dose of 12×10^{15} ions/cm² are shown in Figure 33. The results for other ion doses are similar and are collected in Appendix. A cursory comparison confirms that although the envelope peak can be deconvoluted into similar

energy peaks corresponding to different nitrogen containing functionalities, the relative amounts of these functional groups in each sample is different.

Table 7 Amide and amine ratio for helium ion implantation ratio

C-N, N-C=O: C-N	
Untreated sample	92:8
4 x 10¹⁵ ions/cm²	70:30
8 x 10¹⁵ ions/cm²	65:35
12 x 10¹⁵ ions/cm²	48:52

Table 8 Amide and amine ratio for nitrogen ion implantation ratio

C-N, N-C=O: C-N	
Untreated sample	92:8
4 x 10¹⁵ ions/cm²	51:49
8 x 10¹⁵ ions/cm²	54:46
12 x 10¹⁵ ions/cm²	67:33

The nitrogen peak of the untreated collagen nanofibers in the XPS high-resolution scan (Figure 33A) can be deconvoluted into two peaks identified as C–N, N–C=O (amide) and C–N (amine) with binding energies of 400 eV and 398 eV respectively. The area ratio of these two peaks was calculated to be 92:8. This procedure was applied to the high resolution XPS data for all ion doses and to both He⁺ and N⁺ samples. The results are collected in Table 9 for He⁺ implantation and Table 10 for N⁺ implantation.

As shown in Table 9 for helium ion implantation, the ratio of amide to amine decreased as the ion dose increased, an indication that either the amide (peptide) groups were removed or converted into amine groups, most likely tertiary amines, as ion dose was increased. For the lowest dose of helium ion implanted (4×10^{15} ions/cm²) this ratio decreased from 92:8 ratio (untreated) to 70:30. This trend decreased further to 65:35 as He⁺ dose was increased to 8×10^{15} ions/cm² and eventually to 48:52 at the highest experimental dose of helium ion of 12×10^{15} ions/cm². This trend is reasonable as an increase in ions would lead to an increase in amide bond breaking leading to the observed decrease in the ratio of the two peaks. Nevertheless, the He⁺ ions served to transfer energy to break the chemical bonds to allow for crosslinks to be formed. This leads to the observed aqueous stability of the He⁺ implanted collagen nanofibers. However since helium is an inert gas, it would not react with the elements in the collagen fibers and therefore would not be incorporated into the fibers.

Results for nitrogen ion implantation are summarized in Table 10. It can be seen that for implantation with N^+ ions at low doses of 4×10^{15} ions/cm² and 8×10^{15} ions/cm² led to a decrease in the amide to amine ratio from 92:8 to a roughly constant ratio of 50:50 (51:49 and 54:46 respectively). A further increase in N^+ dose to 12×10^{15} ions/cm² resulted in a reverse of the trend to 67:33. These results were quite different from the helium ion implantation results. After a decrease at the two low ion doses, the amide contents increased at the high ion dose. It is quite possible that the N^+ ions serves two different roles in the ion implantation process. It transfer kinetic energy to the amide bonds to break these bonds to create chemical crosslinks but at the same time, nitrogen itself can be incorporated into the crosslinks in the process.

Although both He^+ and N^+ ion implantation resulted in enhanced aqueous stability of the electrospun collagen nanofibers, the difference in nitrogen contents and the amount of amide in the ion implanted fibers can have important implications when being considered for tissue engineering applications. Peptides (amides) such RGD are known to be essential for cell adhesion onto substrates. In the collagen fiber stabilization process, one of the goals would be to maximize the amides (peptides) contents of the crosslinked and stabilized fibers.

Comparing the results of the use of He^+ and N^+ , two possible scenarios emerged. The highest amide contents of He^+ ion stabilized fiber occurred at the lowest He^+ ion dose. For tissue engineering applications, this would be preferred over the higher He^+ doses

treated fibers. However, at this low ion dose, the degree of crosslinking will be the lowest and the fibers are expected to have a faster degradation rate. For the N^+ ion implanted fibers, the highest amide contents occurred at the highest ion dose used. This would also be the conditions for the more stable fibers to be formed. Depending on the specific tissue engineering application, if a scaffold that is needed only for short and medium term, a low dose He^+ ion implanted one would be suitable. On the other hand, if a scaffold is required for the medium to long term, a N^+ ion implanted one would be the choice.

5.9 Fiber degradation

Ninhydrin assay was employed to determine the degree of crosslinking of collagen nanofibers after ion implantation (245). The main objective was to quantify the amount of free primary amine group right after implantation (as shown in figure 34). Glycine was used as the calibration standard as it is the major amino acid present in the collagen type I molecule. The calibration curve is included in Appendix.

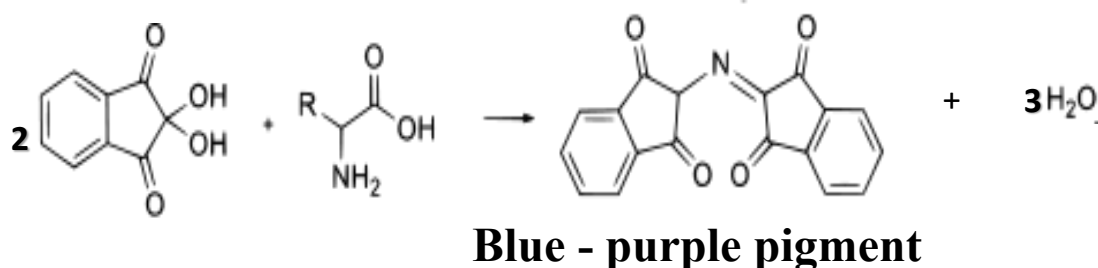


Figure 34 The test reaction will proceed only for a free amino acid

This assay was conducted on each condition after ion implantation. Although, this assay does not provide any direct information on the density or nature of crosslinking.

However, by estimating the free amine group in the given sample immediately after crosslinking, it will give us an idea of the ratio of crosslinking vs. degradation of the ions implanted fiber with respect to the dose delivered. In addition, the quantification of free amine group will also provide us with a good indication of the degree of crosslinking of electrospun collagen nanofibers.

Results of the Ninhydrin assay is shown in Figure 35. The results revealed that the amine concentration after ion implantation is the minimum for the lowest dose for both the ion species implanted on the electrospun collagen nanofibers. This could be interpreted as that we have least amount of degradation due to ion implantation at the lowest dose implanted for both the ion species.

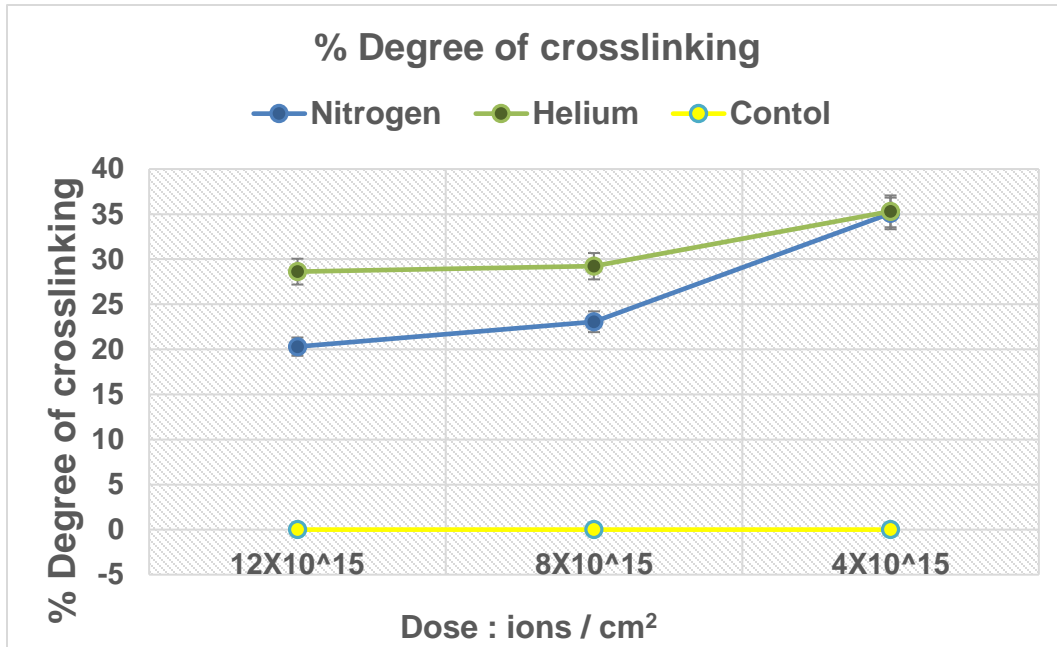


Figure 35 %Degree of crosslinking of the crosslinked samples with respect to the control for all the conditions of crosslinking.

Reference

1. Ikada Y. Challenges in tissue engineering. *Journal of the Royal Society Interface*. 2006;3(10):589-601.
2. Dong C, Lv Y. Application of collagen scaffold in tissue engineering: recent advances and new perspectives. *Polymers*. 2016;8(2):42.
3. Sell SA, McClure MJ, Garg K, Wolfe PS, Bowlin GL. Electrospinning of collagen/biopolymers for regenerative medicine and cardiovascular tissue engineering. *Advanced drug delivery reviews*. 2009;61(12):1007-19.
4. Boekhoven J, Stupp SI. 25th anniversary article: supramolecular materials for regenerative medicine. *Advanced Materials*. 2014;26(11):1642-59.
5. Humphrey JD, Dufresne ER, Schwartz MA. Mechanotransduction and extracellular matrix homeostasis. *Nature reviews Molecular cell biology*. 2014;15(12):802-12.
6. Birk DE, Bruckner P. Collagen suprastructures. *Collagen*. 2005:185-205.
7. Barnes CP, Sell SA, Boland ED, Simpson DG, Bowlin GL. Nanofiber technology: designing the next generation of tissue engineering scaffolds. *Advanced drug delivery reviews*. 2007;59(14):1413-33.
8. Kolacna L, Bakesova J, Varga F, Kostakova E, Planka L, Necas A, et al. Biochemical and biophysical aspects of collagen nanostructure in the extracellular matrix. *Physiological Research*. 2007;56:S51.
9. Albuquerque M, Valera M, Nakashima M, Nör J, Bottino M. Tissue-engineering-based strategies for regenerative endodontics. *Journal of dental research*. 2014;93(12):1222-31.
10. Ramakrishna S. *An introduction to electrospinning and nanofibers*: World Scientific; 2005.
11. Gratzer PF, Lee JM. Control of pH alters the type of cross-linking produced by 1-ethyl-3-(3-dimethylaminopropyl)-carbodiimide (EDC) treatment of acellular matrix vascular grafts. *Journal of Biomedical Materials Research Part A*. 2001;58(2):172-9.
12. Kazenwadel F, Wagner H, Rapp B, Franzreb M. Optimization of enzyme immobilization on magnetic microparticles using 1-ethyl-3-(3-dimethylaminopropyl) carbodiimide (EDC) as a crosslinking agent. *Analytical Methods*. 2015;7(24):10291-8.

13. Huang GP, Shanmugasundaram S, Masih P, Pandya D, Amara S, Collins G, et al. An investigation of common crosslinking agents on the stability of electrospun collagen scaffolds. *Journal of Biomedical Materials Research Part A*. 2015;103(2):762-71.
14. Mekhail M, Wong KKH, Padavan DT, Wu Y, O'Gorman DB, Wan W. Genipin-cross-linked electrospun collagen fibers. *Journal of Biomaterials Science, Polymer Edition*. 2011;22(17):2241-59.
15. Timnak A, Gharebaghi FY, Shariati RP, Bahrami S, Javadian S, Emami SH, et al. Fabrication of nano-structured electrospun collagen scaffold intended for nerve tissue engineering. *Journal of Materials Science: Materials in Medicine*. 2011;22(6):1555-67.
16. Wong KKH, Hutter JL, Zinke-Allmang M, Wan W. Physical properties of ion beam treated electrospun poly (vinyl alcohol) nanofibers. *European Polymer Journal*. 2009;45(5):1349-58.
17. Huda MS, Drzal LT, Mohanty AK, Misra M. Effect of fiber surface-treatments on the properties of laminated biocomposites from poly (lactic acid)(PLA) and kenaf fibers. *Composites science and technology*. 2008;68(2):424-32.
18. Lee SJ, Oh SH, Liu J, Soker S, Atala A, Yoo JJ. The use of thermal treatments to enhance the mechanical properties of electrospun poly (ϵ -caprolactone) scaffolds. *Biomaterials*. 2008;29(10):1422-30.
19. Tan EP, Lim C. Effects of annealing on the structural and mechanical properties of electrospun polymeric nanofibres. *Nanotechnology*. 2006;17(10):2649.
20. Robinson JJ. Comparative biochemical analysis of sea urchin peristome and rat tail tendon collagen. *Comparative Biochemistry and Physiology Part B: Biochemistry and Molecular Biology*. 1997;117(2):307-13.
21. Silver F, Trelstad R. Type I collagen in solution. Structure and properties of fibril fragments. *Journal of Biological Chemistry*. 1980;255(19):9427-33.
22. Starcher B. A ninhydrin-based assay to quantitate the total protein content of tissue samples. *Analytical biochemistry*. 2001;292(1):125-9.
23. Babitha S, Rachita L, Karthikeyan K, Shoba E, Janani I, Poornima B, et al. Electrospun protein nanofibers in healthcare: A review. *International journal of pharmaceutics*. 2017.
24. Rath G, Hussain T, Chauhan G, Garg T, Goyal AK. Collagen nanofiber containing silver nanoparticles for improved wound-healing applications. *Journal of drug targeting*. 2016;24(6):520-9.
25. Sridharan R, Cameron AR, Kelly DJ, Kearney CJ, O'Brien FJ. Biomaterial based modulation of macrophage polarization: a review and suggested design principles. *Materials today*. 2015;18(6):313-25.

26. Tugulu S, Silacci P, Stergiopoulos N, Klok H-A. RGD—Functionalized polymer brushes as substrates for the integrin specific adhesion of human umbilical vein endothelial cells. *Biomaterials*. 2007;28(16):2536-46.

Chapter 6

6 Conclusions

Collagen is an important component of the extracellular matrix, and desirable for tissue engineering application. To fabricate collagen nanofibrous 3D scaffold, we have achieved the following.

Rat tail collagen type I fibers were successfully produced by electrospinning process using a collagen in HFIP solution and the effect of environmental humidity on fiber morphology and fiber diameter were demonstrated.

Being unstable in aqueous solutions, the as spun collagen fibers were implanted with He^+ and N^+ ion. Ion implantation conditions investigated were 0 – 100 MeV of He^+ and 0 – 300 MeV for N^+ and A broadband ion beam of energies of 0 – 300 MeV and 0 – 100 MeV of N^+ (nitrogen) ion and doses of 4×10^{15} ions /cm² - 12×10^{15} ions/cm² at room temperature. Over the range of ion energies and doses investigated, stable collagen fibers were found to be stable in both water and DMEM over a 7 day period. The current results demonstrated that it was possible to induce aqueous stability into electrospun collagen fibers via ion implantation indicating this is an effective crosslinking method for collagen.

XPS results demonstrated that at the lowest dose of helium ion, implant retained higher nitrogen retain at other helium or nitrogen dose implanted. Results from ninhydrin assay demonstrated that higher degree of crosslinking was found at the lowest dose for both the ion species (He^+ and N^+).

6.1 Application

Results of this work may be employed for a wide range of applications, such as tissue engineering (299), cosmetic injections for wrinkle removal (300), and compositions for articular cartilage repair in joints. Additionally, collagen fibers cross-linked with the ion implantation may be used in a method for treating skin or lip related anomalies (301).

Whereas in this methods for modulating the rate of release include increasing or decreasing loading of the pharmaceutically active agent incorporated within or between the fibers treated with ion implantation, selecting polymers to produce the polymeric fibers which degrade at varying rates, varying polymeric concentration of the polymeric fibers and/or varying diameter of the polymeric fibers. Pharmaceutically active agents that can be modulated in accordance with the present invention include: silver nanoparticles (for wound healing applications) (302), growth factors (to control cell proliferation and differentiation in tissue engineering applications) (303, 304), genes (for gene delivery applications), anti-cancer agents, such as paclitaxel, and anticoagulants (drug-eluting stents) (305).

6.2 Future work

Research presented in this thesis lays the groundwork for a wide range of possibilities in the fields of tissue engineering application. One outstanding aspect of characterization is the mechanical properties of the collagen nanofibers using atomic force microscopy. Prior research has demonstrated that different cell types needed respond to different substrate stiffness (306). These results would give us a picture of the appropriate matching between cell type and stiffness of the ion implanted fibrous substrate. Degradation of the fibers should also be studied as a function of ion implantation conditions. in order to better predict the rate and degree of degradation in the tissue engineering environment. Cell proliferation rate on these crosslinked fibers would also need to be quantified.

Reference:

1. Nair LS, Laurencin CT. Biodegradable polymers as biomaterials. *Progress in Polymer Science*. 2007;32(8):762-98.
2. Fertala A, D Shah M, A Hoffman R, V Arnold W. Designing Recombinant Collagens for Biomedical Applications. *Current Tissue Engineering*. 2016;5(2):73-84.
3. McKay E. Assessing the effectiveness of massage therapy for bilateral cleft lip reconstruction scars. *International journal of therapeutic massage & bodywork*. 2014;7(2):3.
4. Ramalingam M, Ramakrishna S. Introduction to nanofiber composites. *Nanofiber Composites for Biomedical Applications*. 2017:1.
5. Cao H, Chen M-M, Liu Y, Liu Y-Y, Huang Y-Q, Wang J-H, et al. Fish collagen-based scaffold containing PLGA microspheres for controlled growth factor delivery in skin tissue engineering. *Colloids and Surfaces B: Biointerfaces*. 2015;136:1098-106.
6. Loh QL, Choong C. Three-dimensional scaffolds for tissue engineering applications: role of porosity and pore size. *Tissue Engineering Part B: Reviews*. 2013;19(6):485-502.
7. Goonoo N, Jeetah R, Bhaw-Luximon A, Jhurry D. Polydioxanone-based biomaterials for tissue engineering and drug/gene delivery applications. *European Journal of Pharmaceutics and Biopharmaceutics*. 2015;97:371-91.
8. Discher DE, Janmey P, Wang Y-l. Tissue cells feel and respond to the stiffness of their substrate. *Science*. 2005;310(5751):1139-43.

Appendices

Isolation of Type I Collagen from Rat Tails:

- 1) Thaw frozen rats tails in 70% ethanol for 1 hour
- 2) Use scalpel to cut off skin of tail and expose white collagen fibres. Using forceps pull out collagen fibres from tail and place in separate sterile dish.
- 3) Continue cutting rat tail in segments, exposing and pulling out fibres, ensuring to clean fibres of contaminating tissue.
- 4) At this point, fibres can be stored at -20 °C or proceed to collagen solution.
- 5) Weigh out 4 g/L of fibres (approximately 5 tails) and soak in 200 mL of 70% ethanol for 30 minutes with forceps.
- 6) Place fibres in sterile Petri dish and leave overnight in a tissue culture hood with UV light on to sterilize fibres.
- 7) Prepare acetic acid solution (1 mL of concentrated acetic acid in 1 L of distilled water) and filter sterilize.
- 8) Add 900 mL of acetic acid solution to collagen fibres in an autoclaved 1 litre flask with sterile stir bar. Place on stirrer in cold room (at 4 °C) for 4-7 days to dissolve collagen.

- 9) Centrifuge the solution at 11, 000 rpm (10, 000 g) for 2 hours at 4 °C with brakes on.
- 10) Collect supernatant in a sterile bottle and measure protein concentration using Sircol Collagen Assay (should be 1-3 mg/mL)
- 11) Collagen solution can be stored at this point at 4 °C.
- 12) To obtain collagen protein powder, freeze small samples (~10-15 ml) overnight in a -20 °C freezer and lyophilize for 1-2 days.

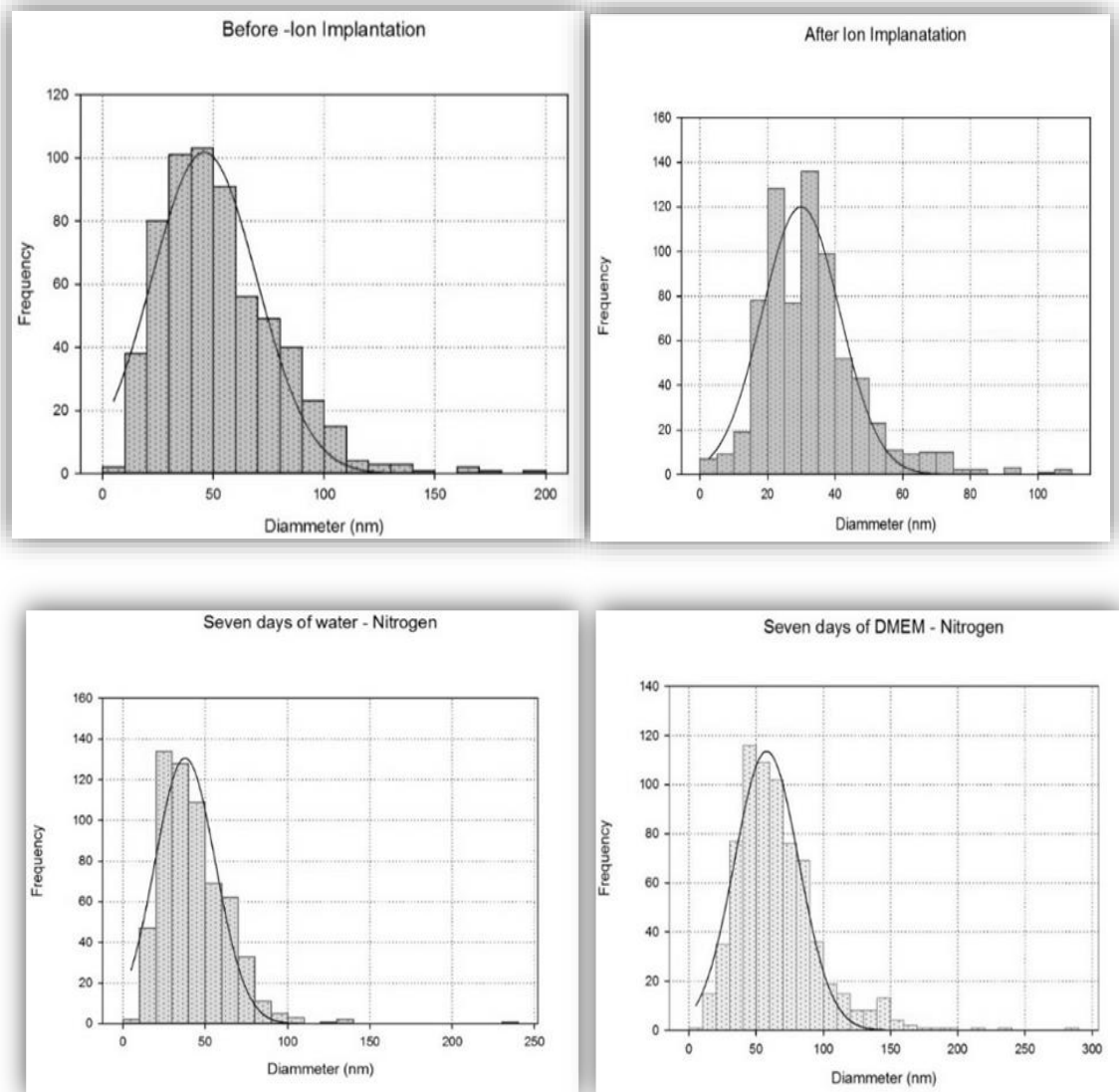


Figure 36 Histogram of $N^+ 1.2 \times 10^{15}$ ions/cm²

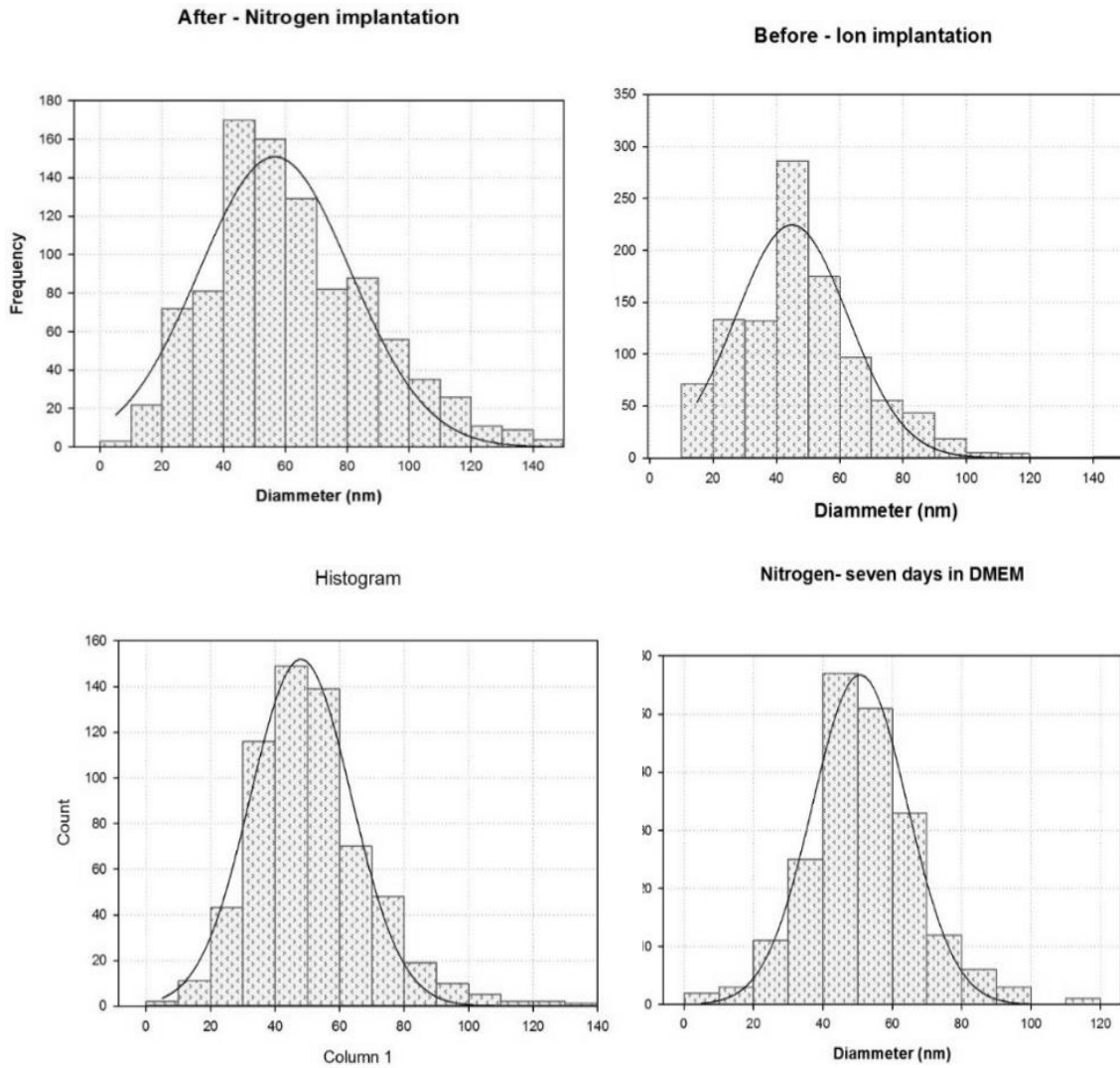


Figure 37 Histogram of $N^+ 8 \times 10^{15}$ ions/cm²

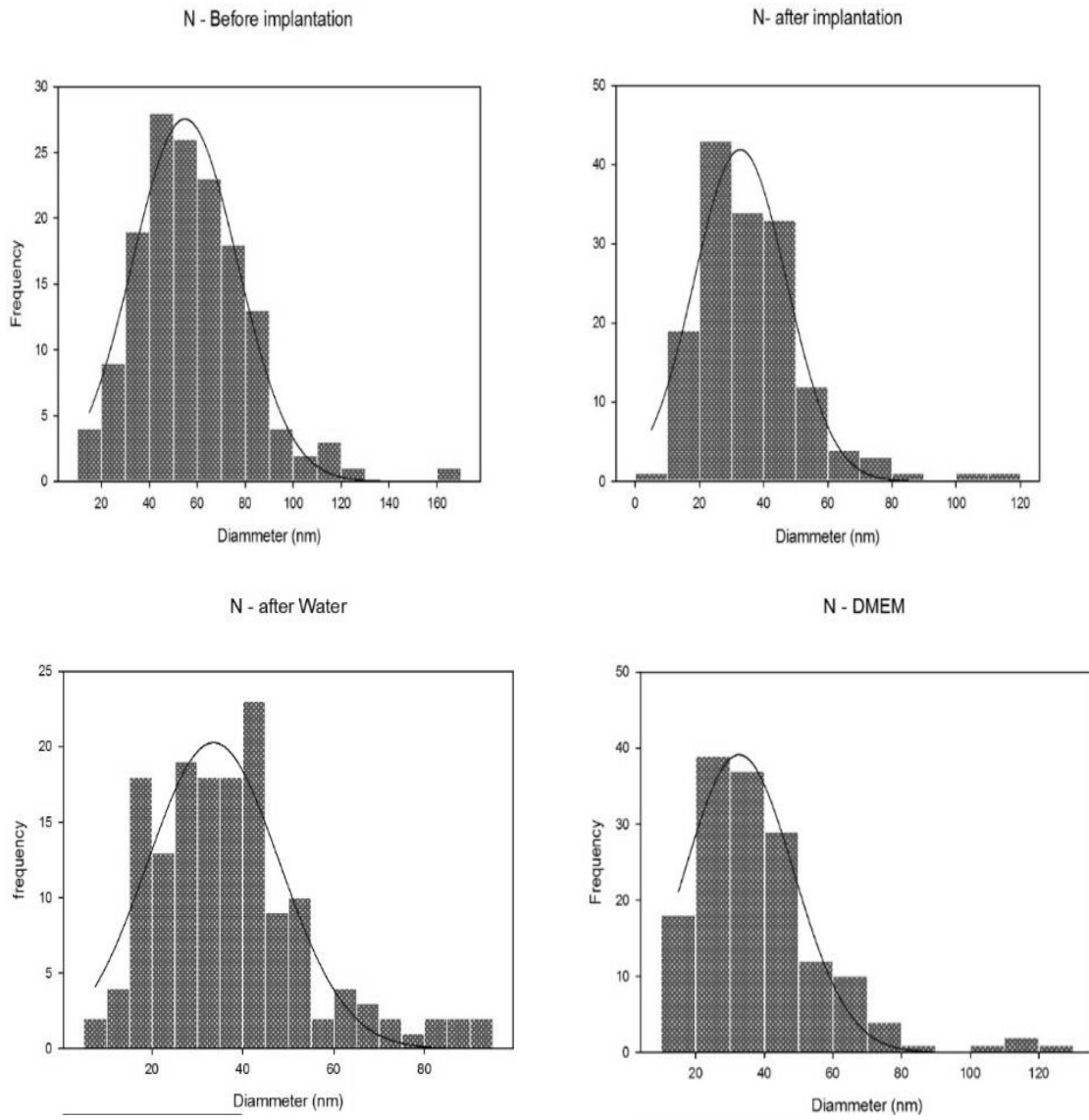


Figure 38 Histogram of $N^+ 4 \times 10^{15}$ ions/cm²

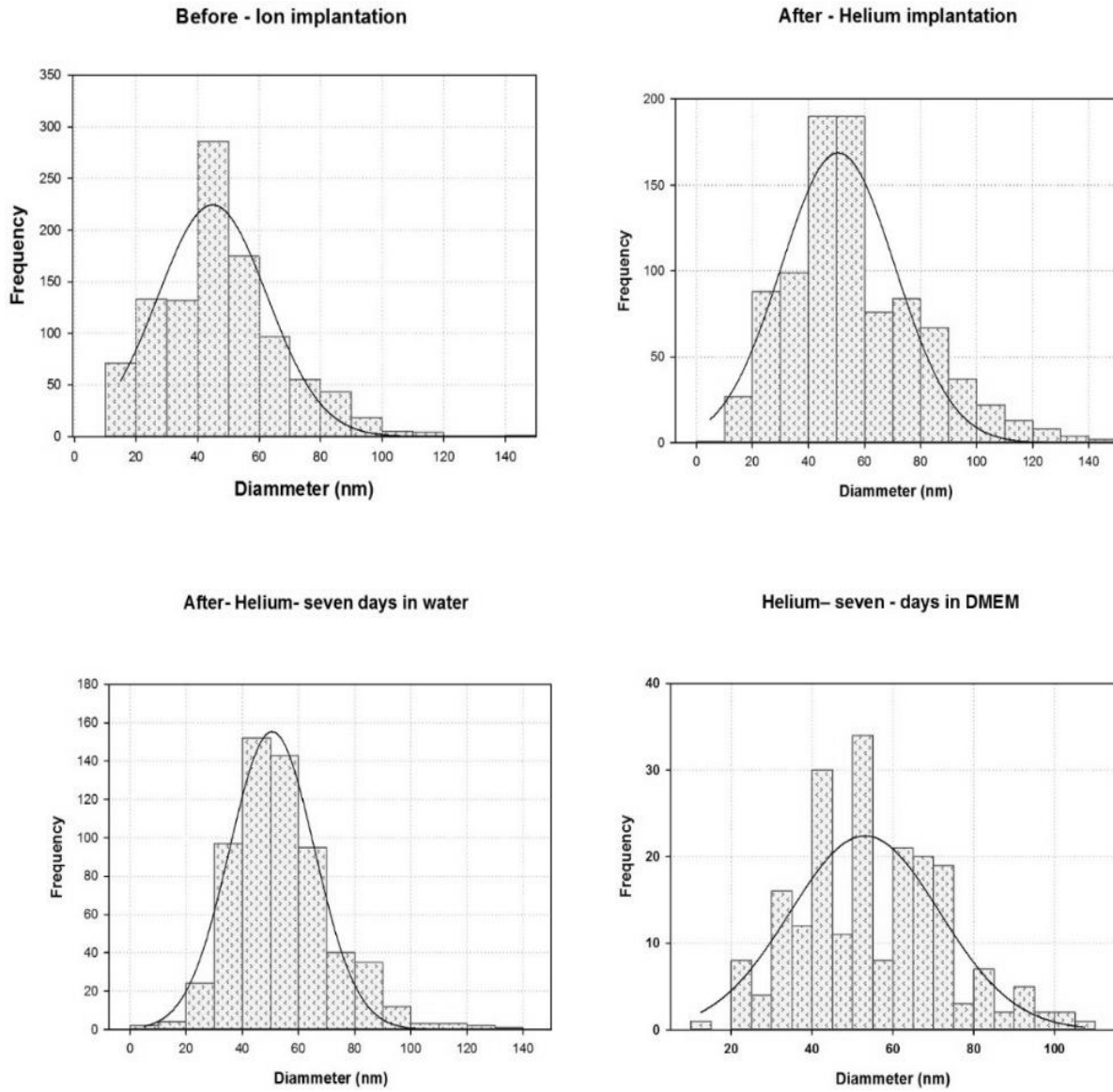


Figure 39 Histogram of helium 1.2×10^{16} ions/cm²

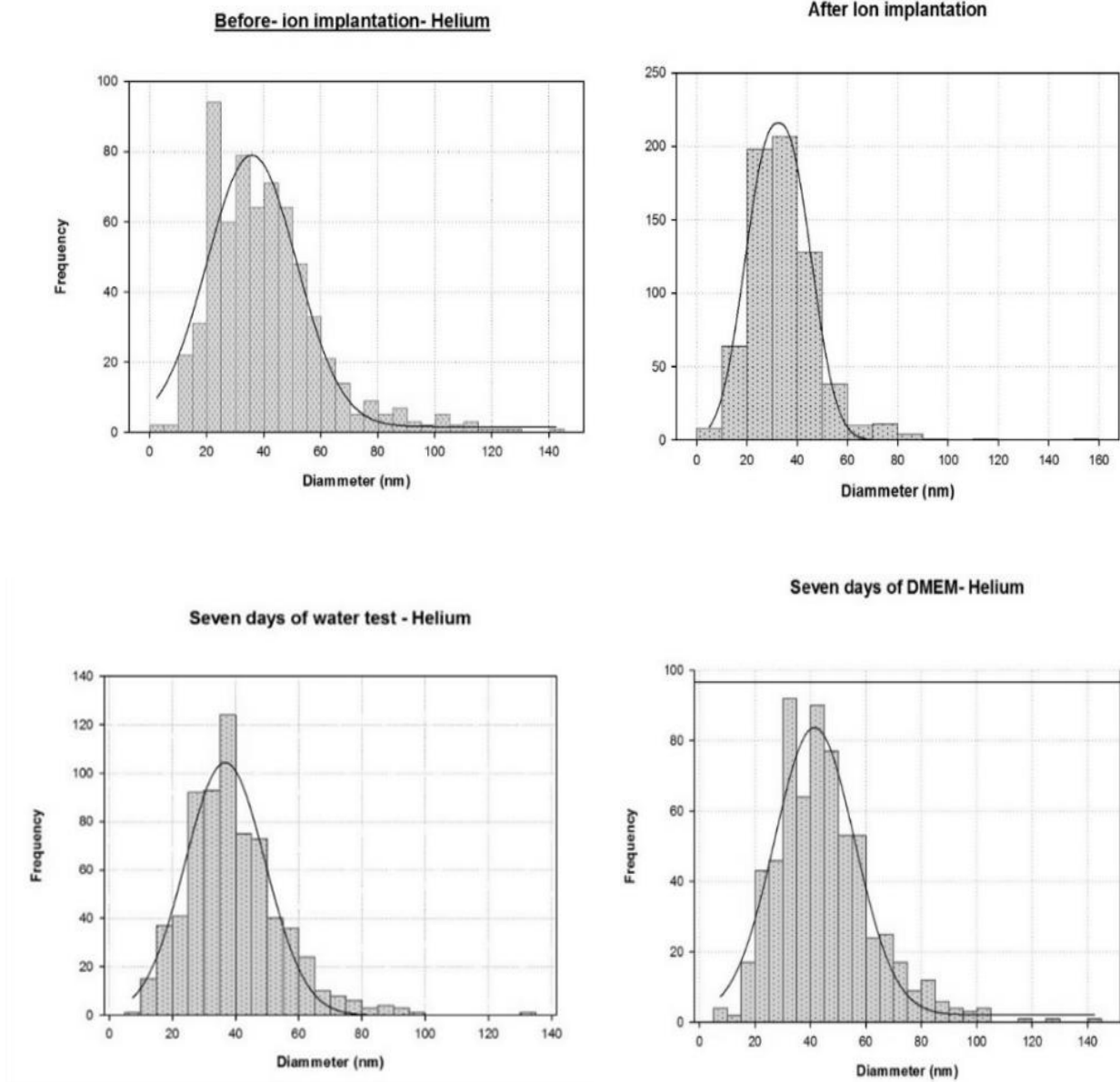


Figure 40 Histogram of helium 8×10^{16} ions/cm²

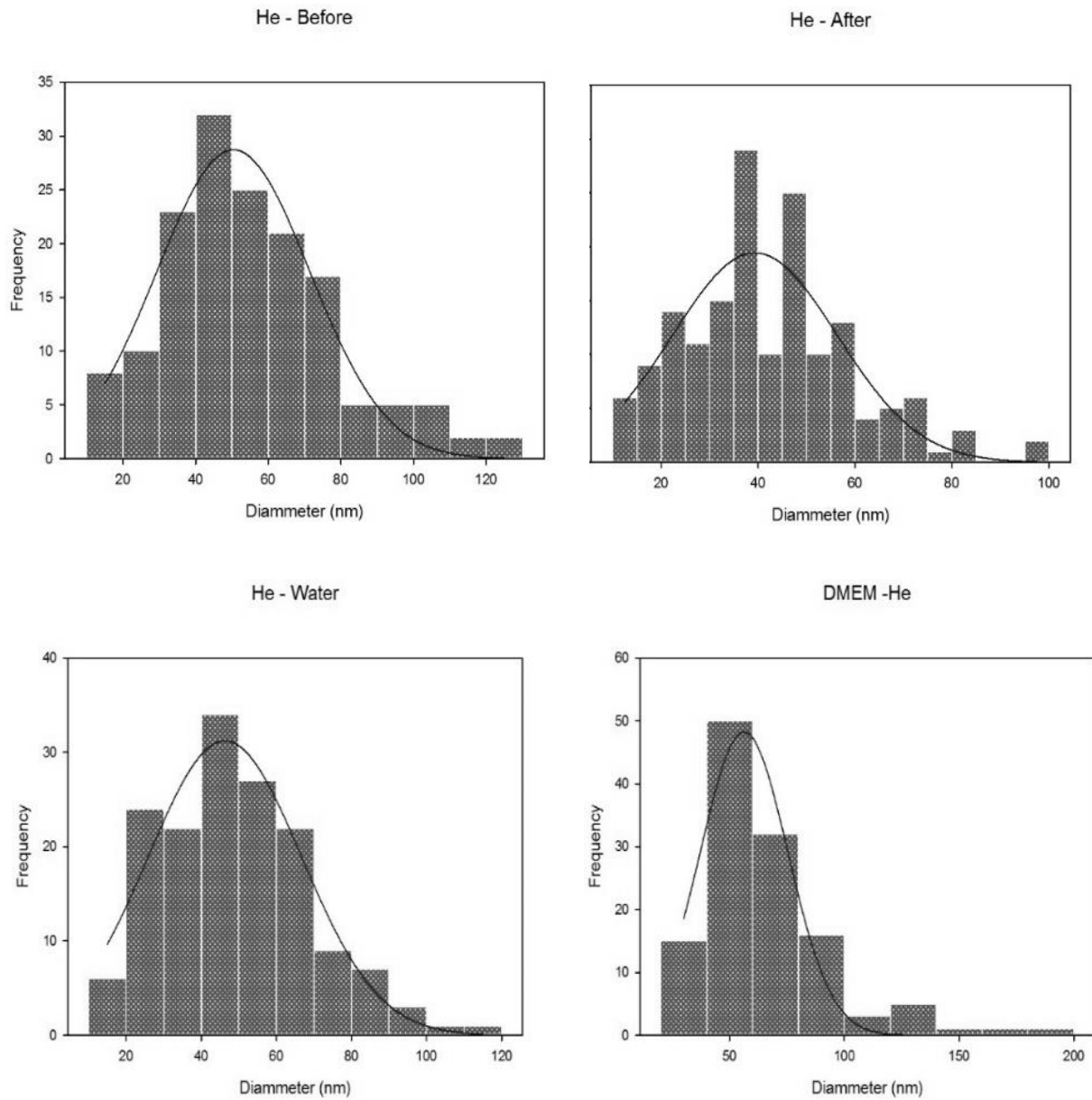
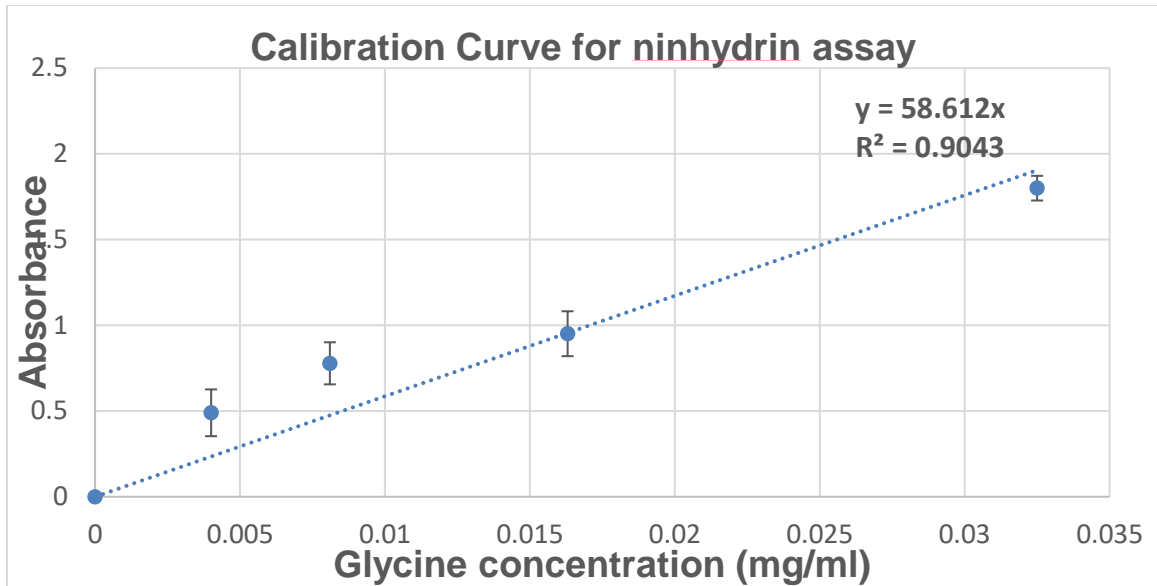


Figure 41 Histogram of helium 4×10^{16} ions/cm²

Calibration curve for the ninhydrin assay

Glycine was chosen to calibrate the ninhydrin assay, as mentioned in the literature (245).

A 10 ml stock solution of glycine in distilled water (0.13 mg/ml) was first prepared. Five vials containing 5 ml of distilled water were also prepared. 5 ml of the stock solution was then transferred to the first vial and mixed well, thus reducing the glycine concentration by half (i.e. 0.065 mg/ml). 5 ml from first vial was then transferred to the second vial, diluting the concentration further; this process was repeated until the fifth vial (where 5 ml are disposed). 1 ml of the ninhydrin solution was added to 2 ml of each of the five glycine concentrations and heated at 80°C for 15 minutes. The vials were then left to cool for 10 minutes and the absorbance was measured at 570 nm, using a UV spectrophotometer (Beckman DU series).



Formula(s):

The % Change quantify the change from one number to another and express the change as an increase or decrease. Percentage change equals the change in value divided by the absolute value of the original value, multiplied by 100. %

$$\text{change} = ((V2 - V1) / |V1|) * 100$$

- (crosslinked nanofibers – as spun nanofibers) /as spun nanofibers * 100
- (crosslinked nanofibers soaked in water for 7 days – Crosslinked nanofibers) / Crosslinked nanofibers *100

- (crosslinked nanofibers soaked in cell culture media for 7 days – Crosslinked nanofibers) / Crosslinked nanofibers *100

Process	Value	Uncertainty
Average	$\bar{x} = \frac{x_1 + x_2 + x_3 + \dots + x_N}{N}$	$\sigma_x = \sqrt{\frac{(x_1 - \bar{x})^2 + (x_2 - \bar{x})^2 + \dots + (x_N - \bar{x})^2}{N-1}}$
Addition	$z = \bar{x} + \bar{y}$	$\sigma_z = \sqrt{(\sigma_x)^2 + (\sigma_y)^2}$
Subtraction	$z = \bar{x} - \bar{y}$	$\sigma_z = \sqrt{(\sigma_x)^2 + (\sigma_y)^2}$
Multiplication	$z = \bar{x} * \bar{y}$	$\sigma_z = z * \sqrt{\left(\frac{\sigma_x}{\bar{x}}\right)^2 + \left(\frac{\sigma_y}{\bar{y}}\right)^2}$
Division	$z = \bar{x} \div \bar{y}$	$\sigma_z = z * \sqrt{\left(\frac{\sigma_x}{\bar{x}}\right)^2 + \left(\frac{\sigma_y}{\bar{y}}\right)^2}$

The link is been aborted from the following website:

<http://www.clemson.edu/ces/phoenix/tutorials/err>

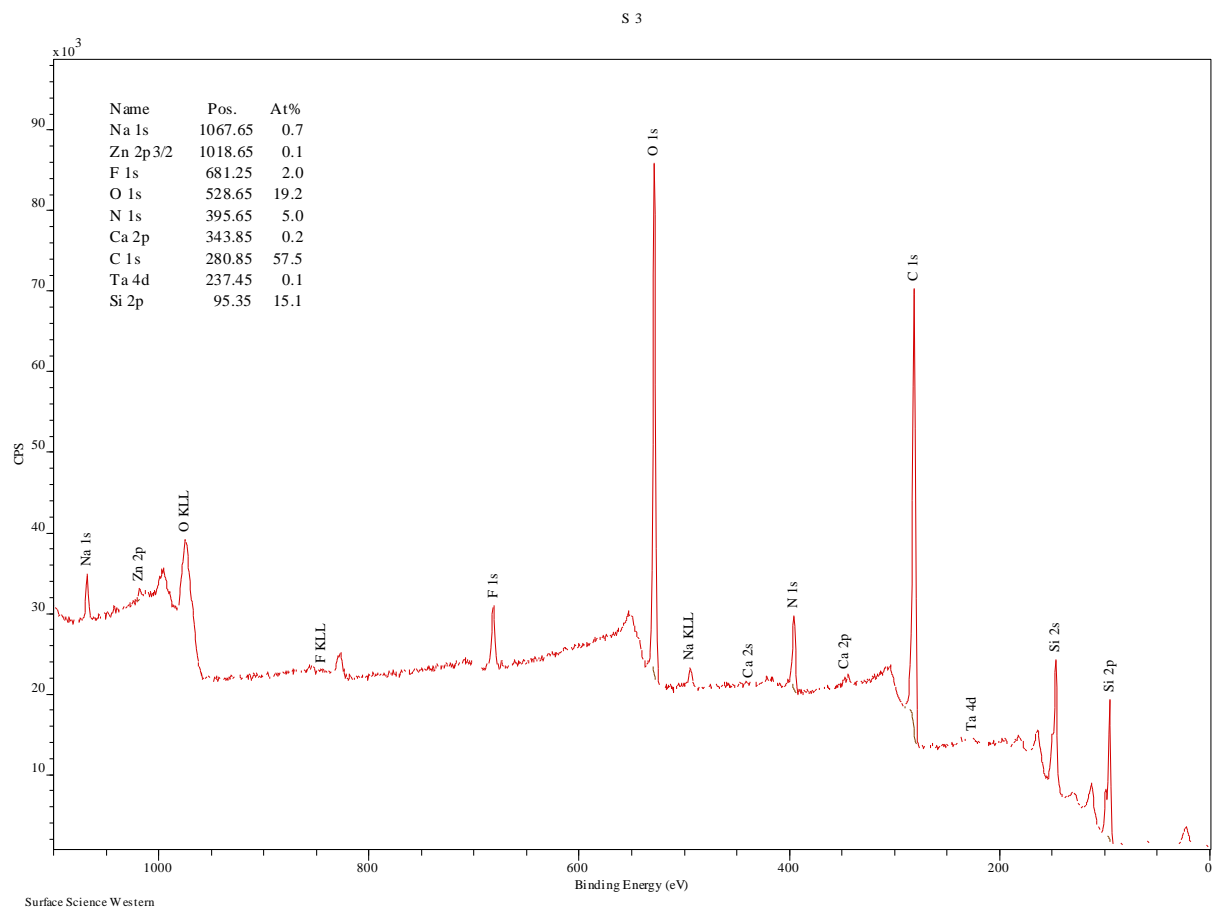


Figure 42 plots a full X-ray photoelectron spectroscopy scan that was after nitrogen ion implantation with a dose at 8×10^{15} ions per cm^2 .

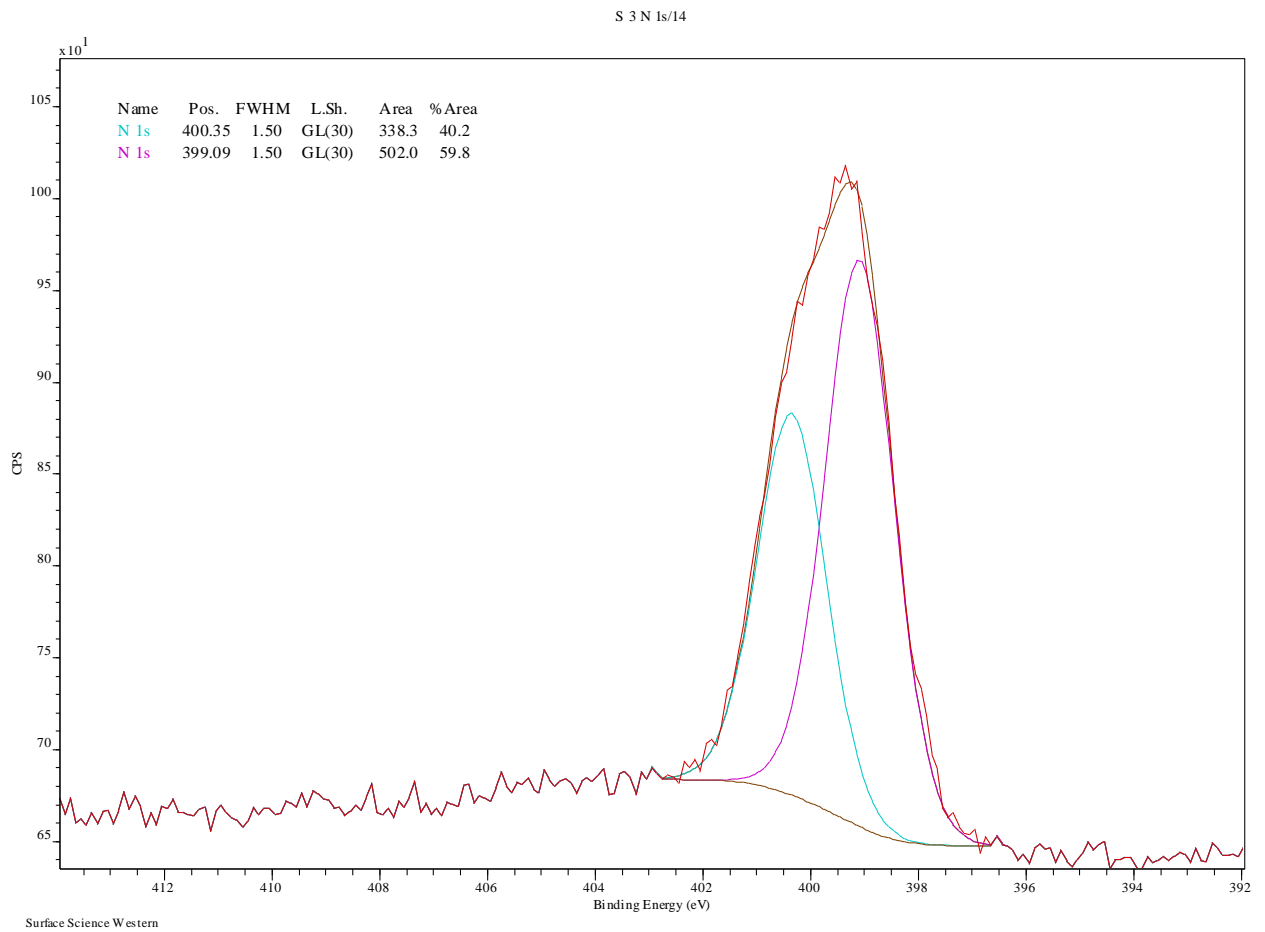


Figure 43 high resolution nitrogen scan that was after nitrogen ion implantation with a dose of at 8×10^{15} ions per cm^2 .

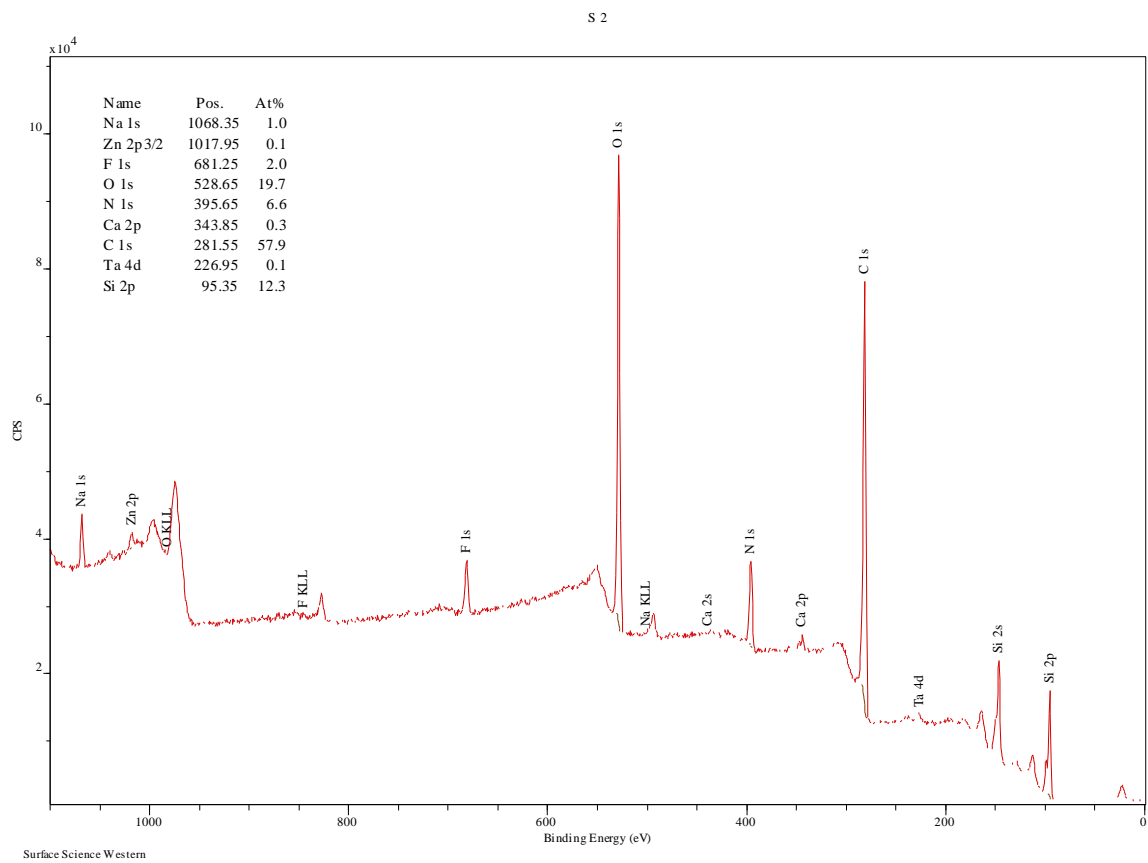


Figure 44 plots a full X-ray photoelectron spectroscopy scan that was after helium ion implantation with a dose of 12×10^{15} ions per cm^2 .

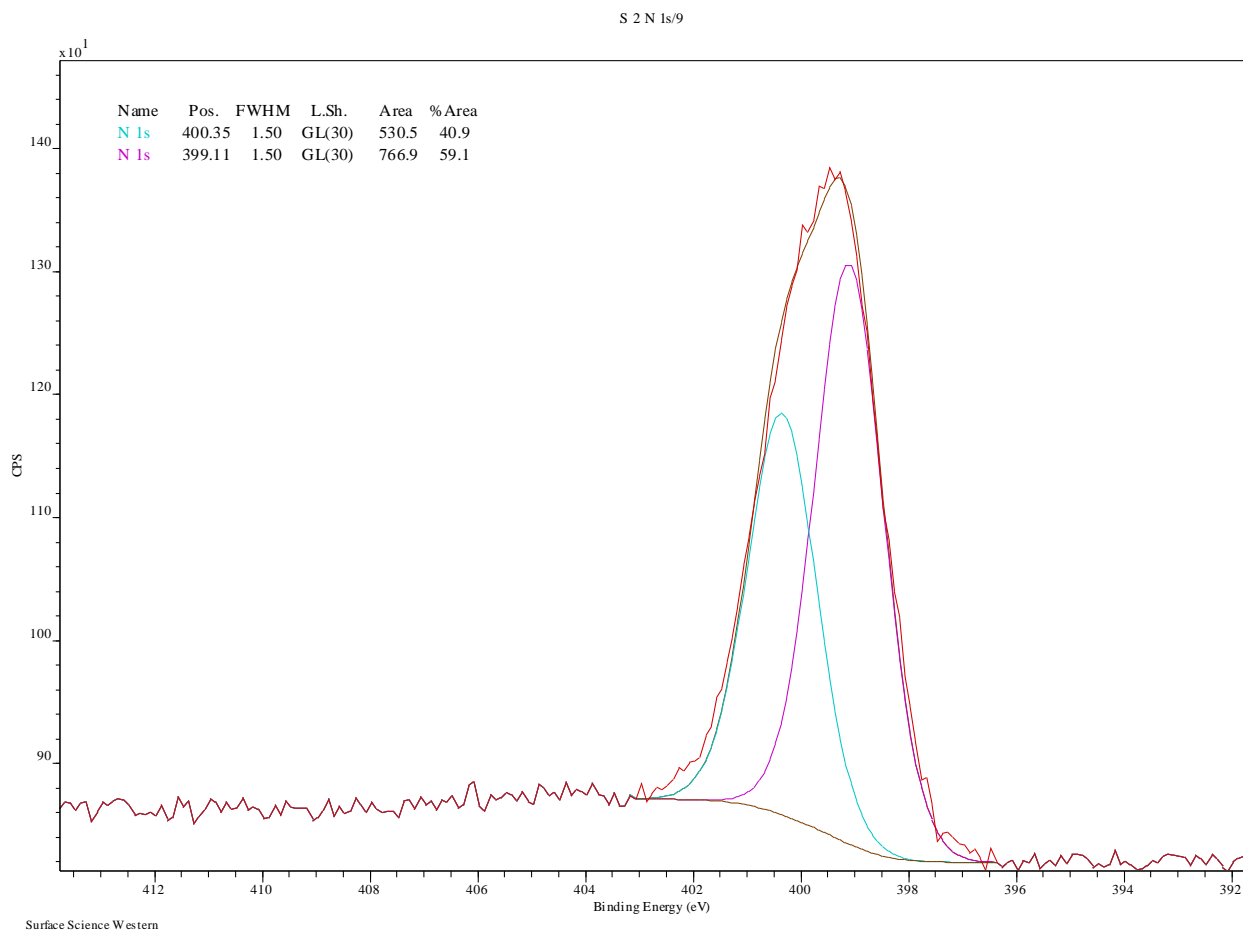


Figure 45 high resolution scan of nitrogen that was after helium ion implantation with a dose of 12×10^{15} ions per cm^2 .

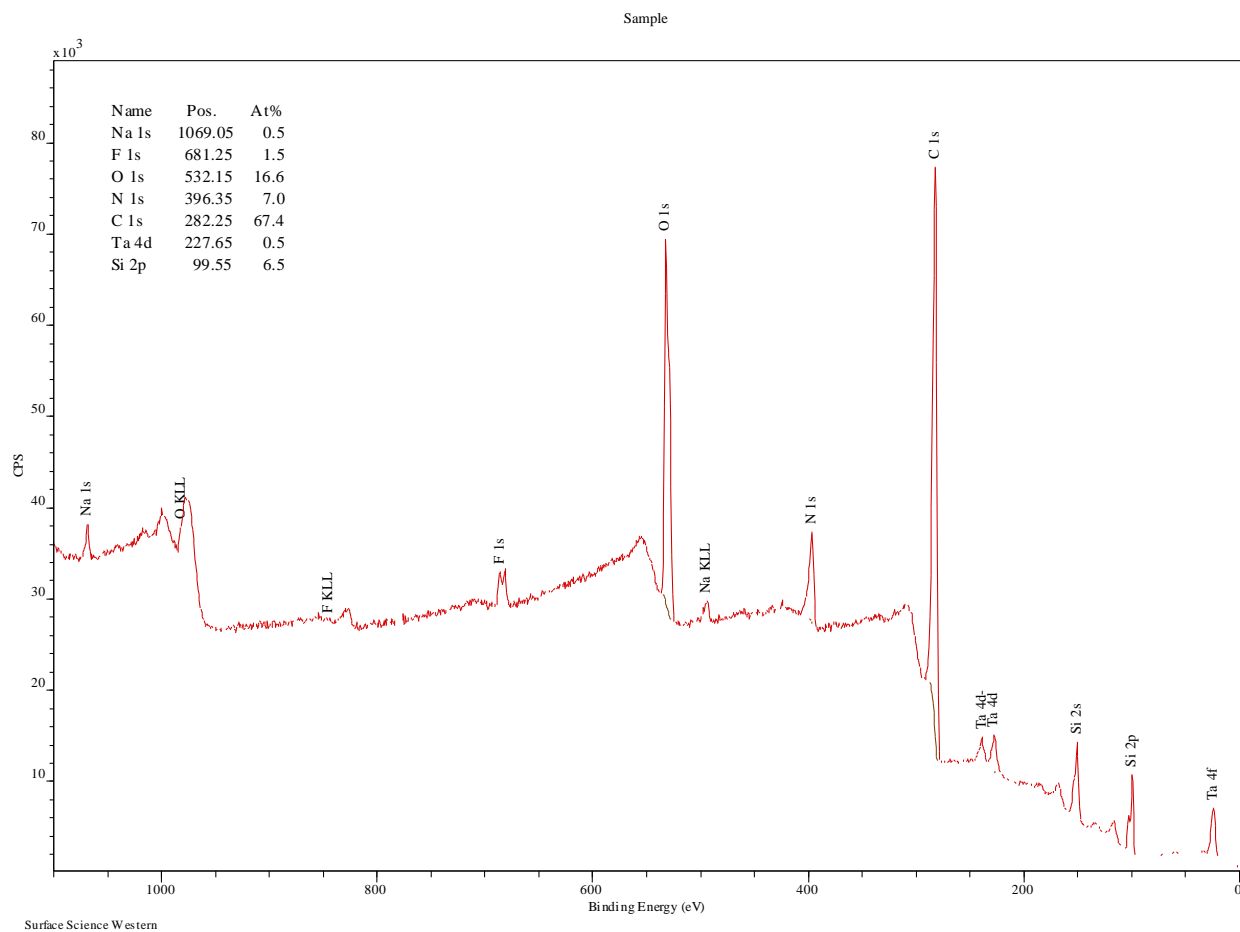


Figure 46 plots a full X-ray photoelectron spectroscopy scan that was after nitrogen (N⁺) ion implantation with a dose of 4×10^{15} ions per cm².

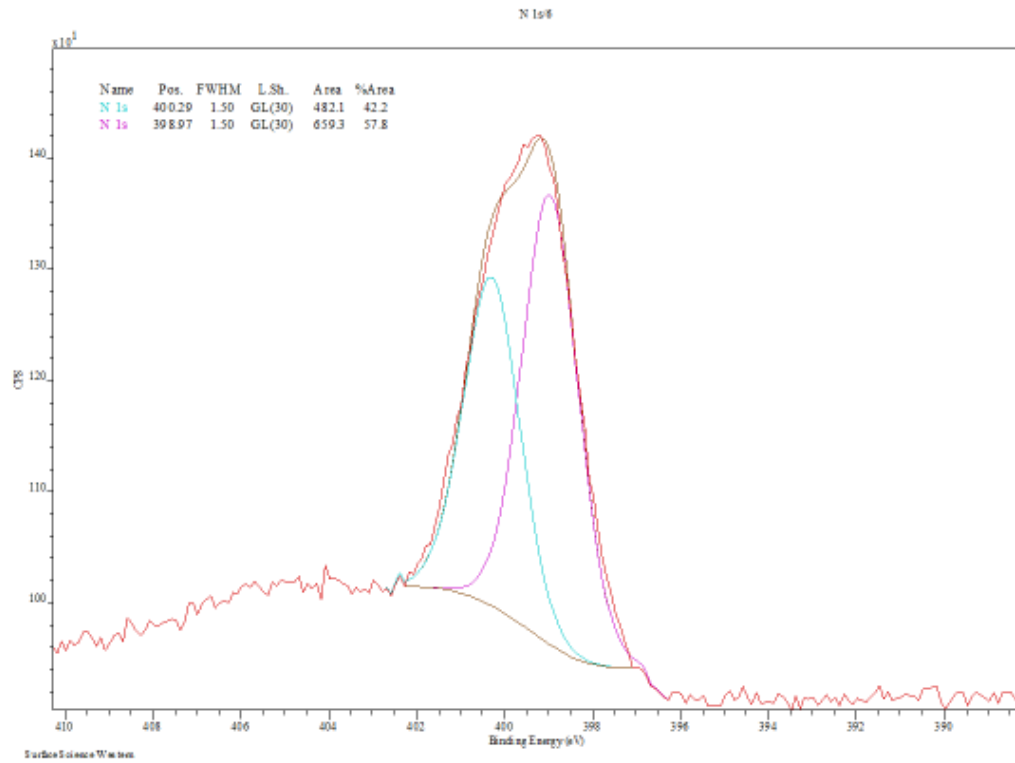


Figure 47 high resolution scan of nitrogen that was after nitrogen (N+) ion implantation with a dose of 4×10^{15} ions per cm^2 .

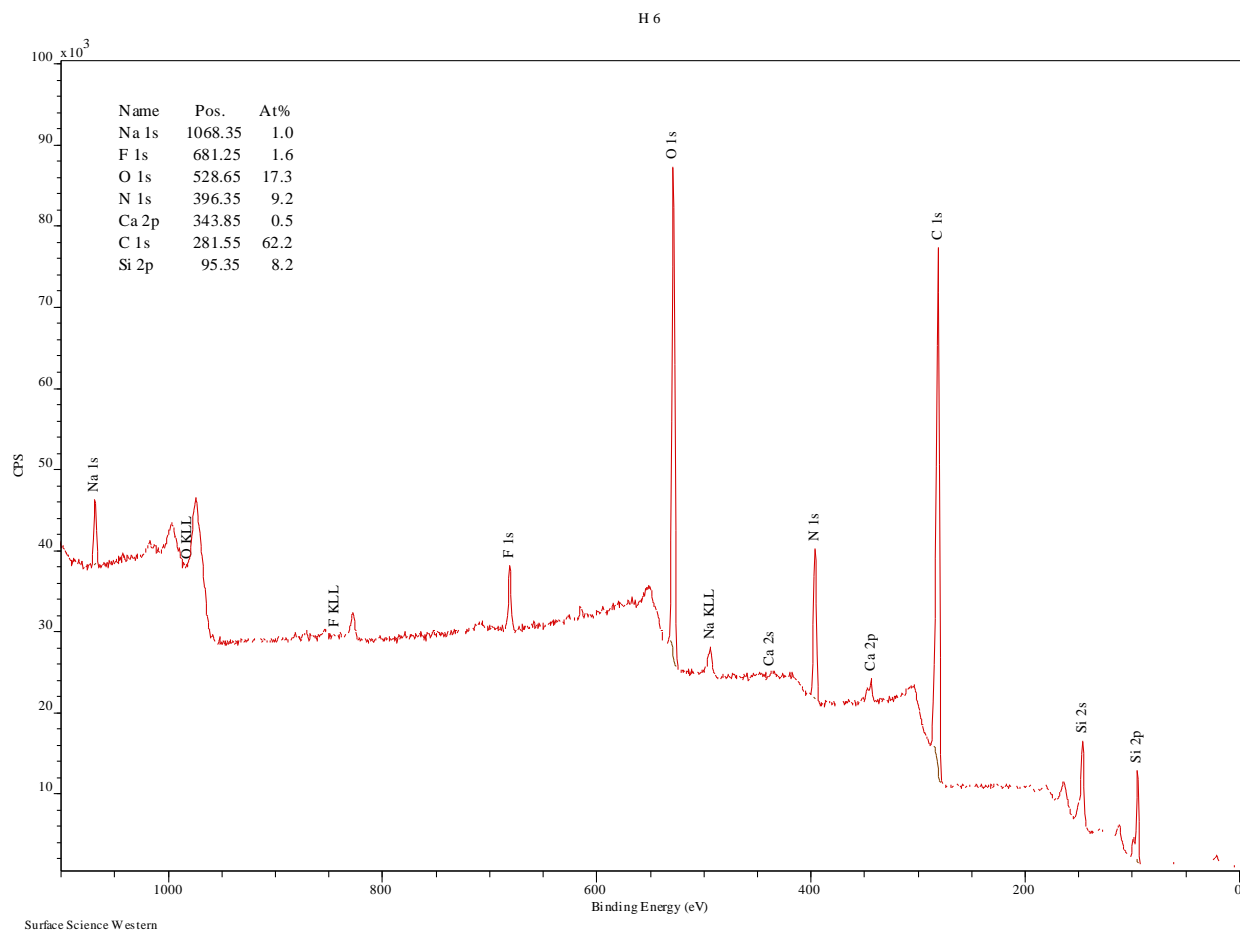


Figure 48 plots a full X-ray photoelectron spectroscopy scan that was after helium ion implantation with a dose of 8×10^{15} ions per cm^2 .

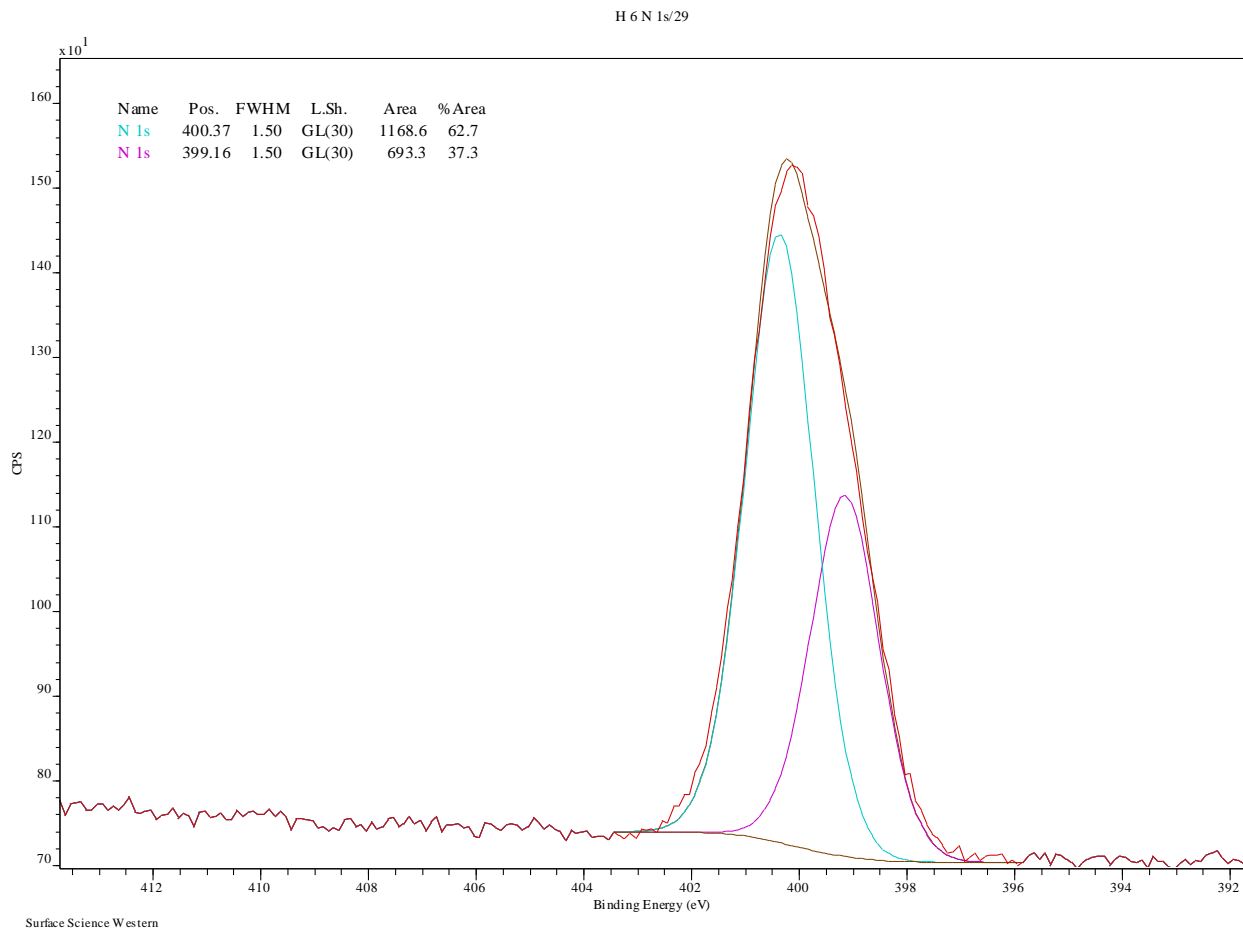


Figure 49 high resolution scan of nitrogen that was after helium ion implantation with a dose of 8×10^{15} ions per cm^2 .

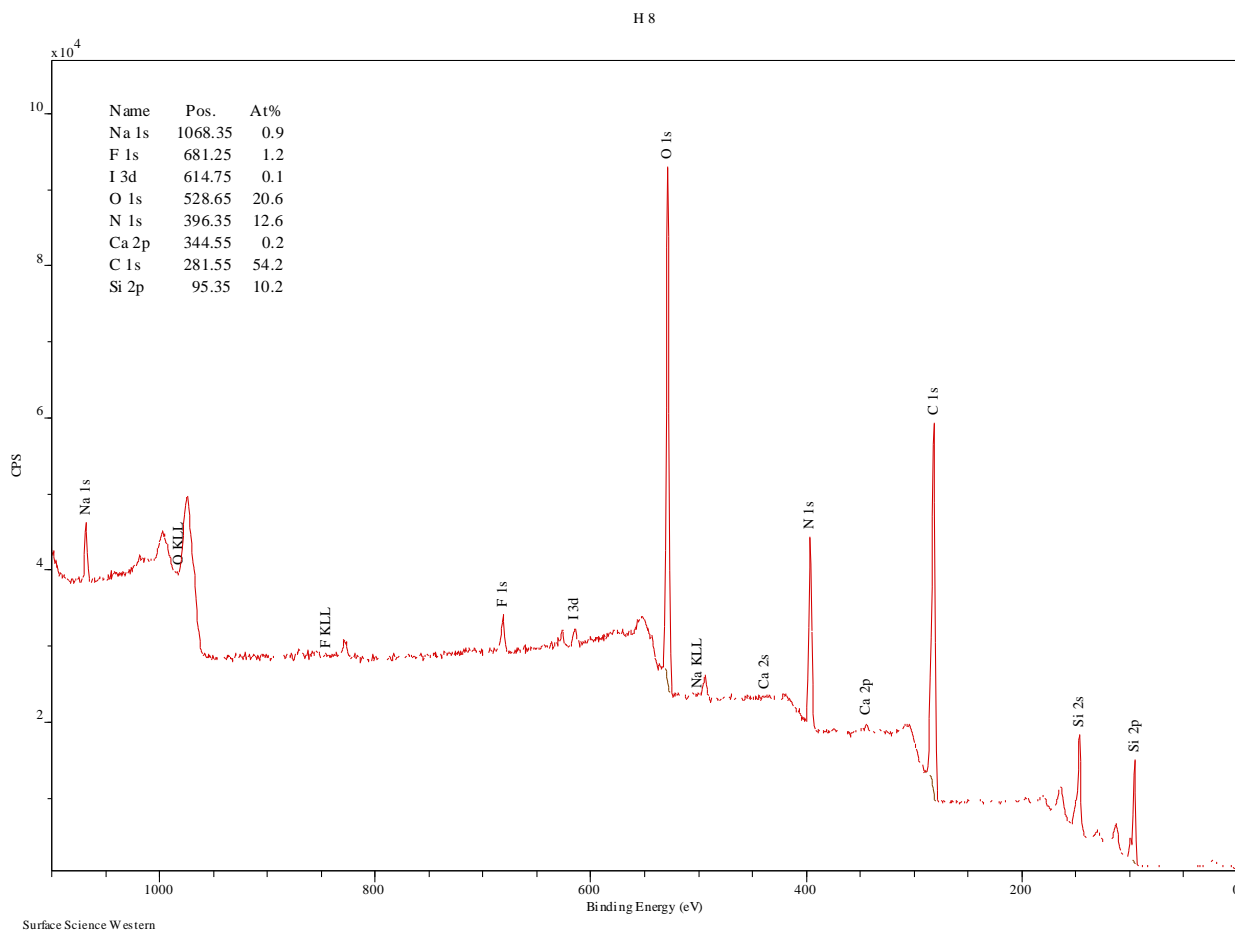


Figure 50 plots a full X-ray photoelectron spectroscopy scan that was after helium ion implantation with a dose of 4×10^{15} ions per cm^2 .

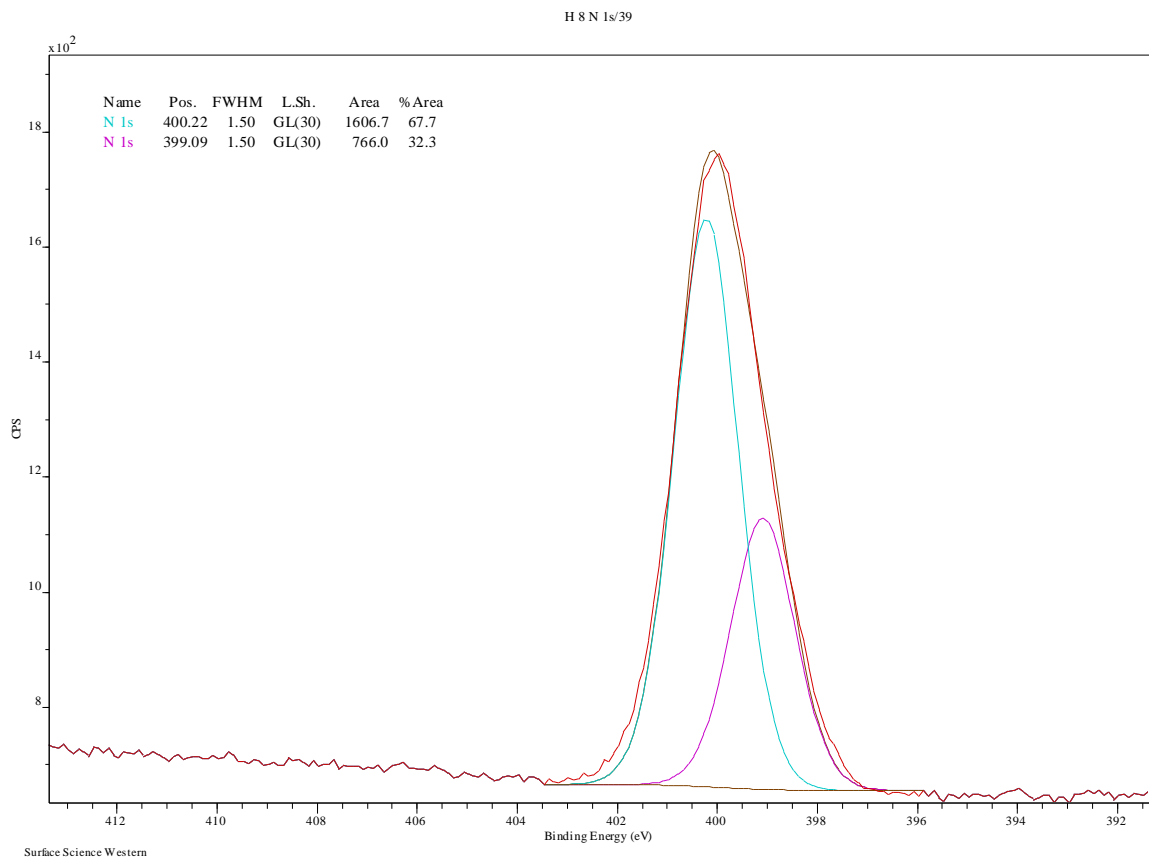


Figure 51 high resolution scan of nitrogen that was after helium ion implantation with a dose of 4×10^{15} ions per cm^2 .

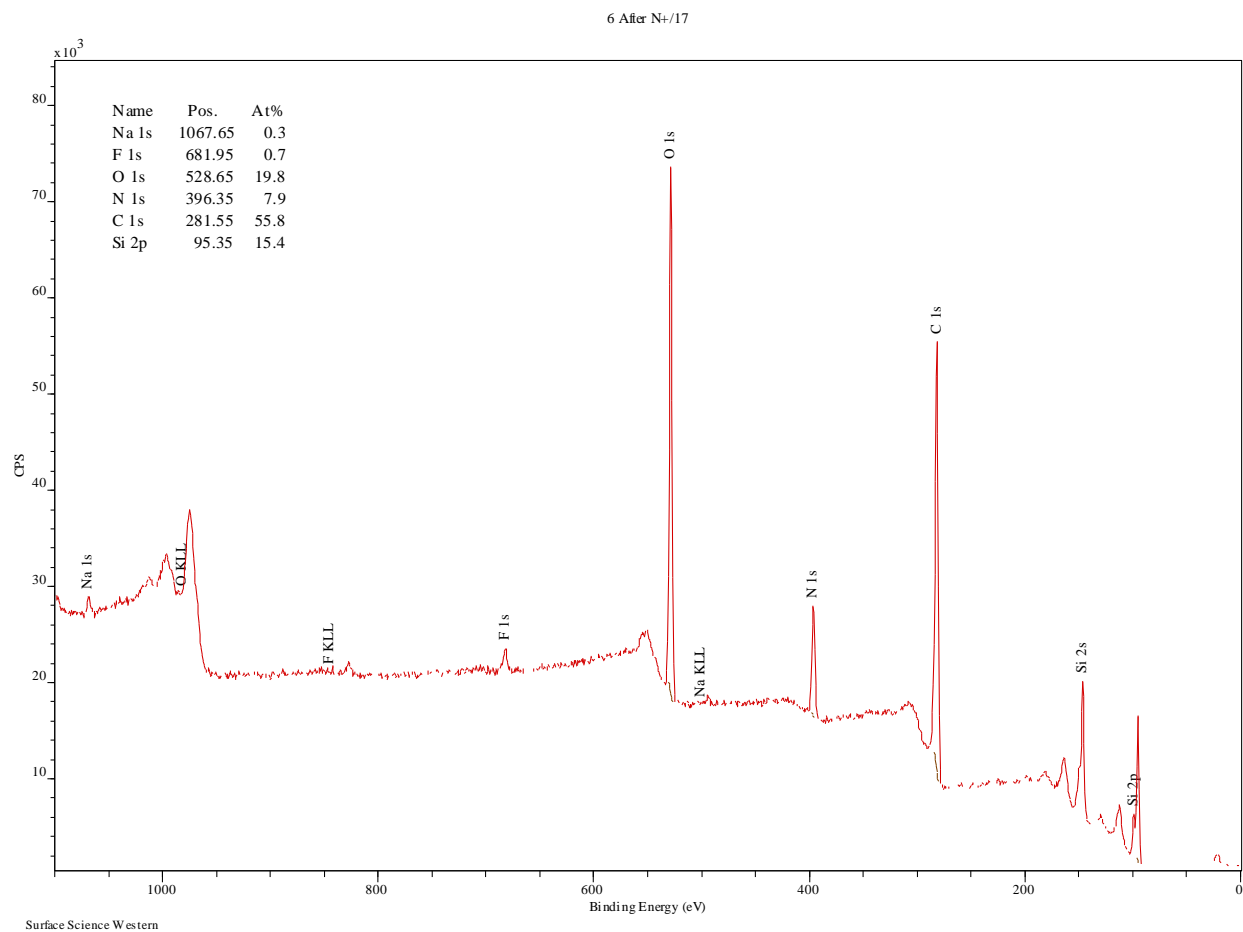


Figure 52 plots a full X-ray photoelectron spectroscopy scan that was after nitrogen ion implantation with a dose of 4×10^{15} ions per cm^2 .

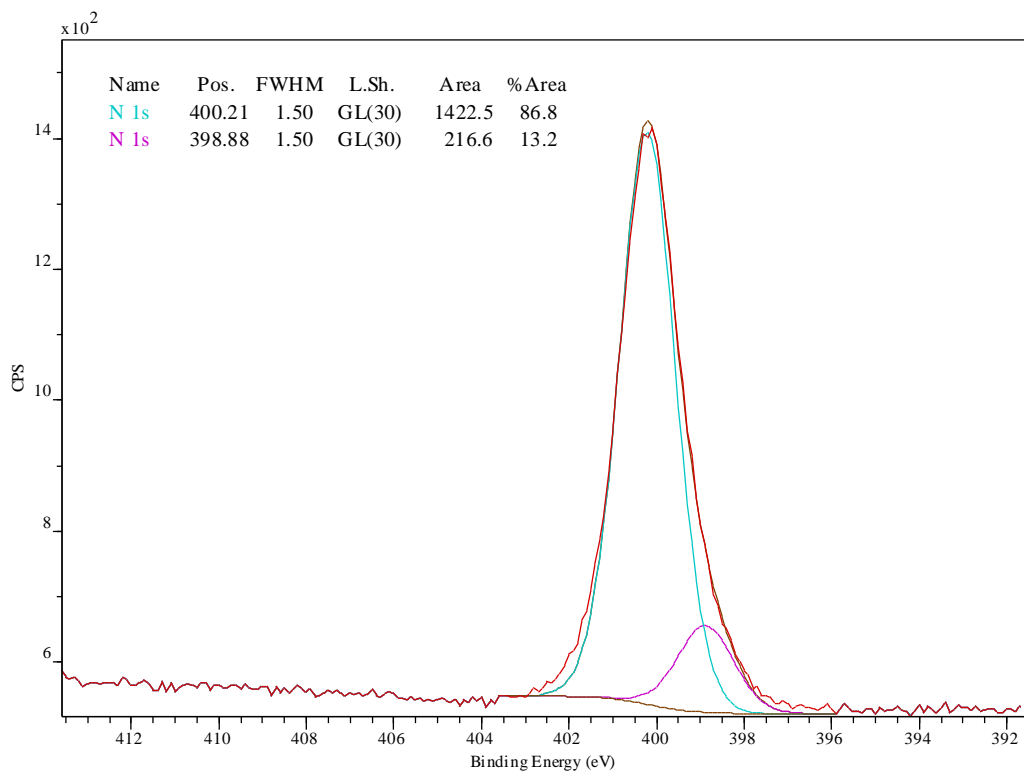


Figure 53 high resolution scan of X-ray photoelectron spectroscopy scan that was after nitrogen ion implantation with a dose of 4×10^{15} ions per cm^2 .

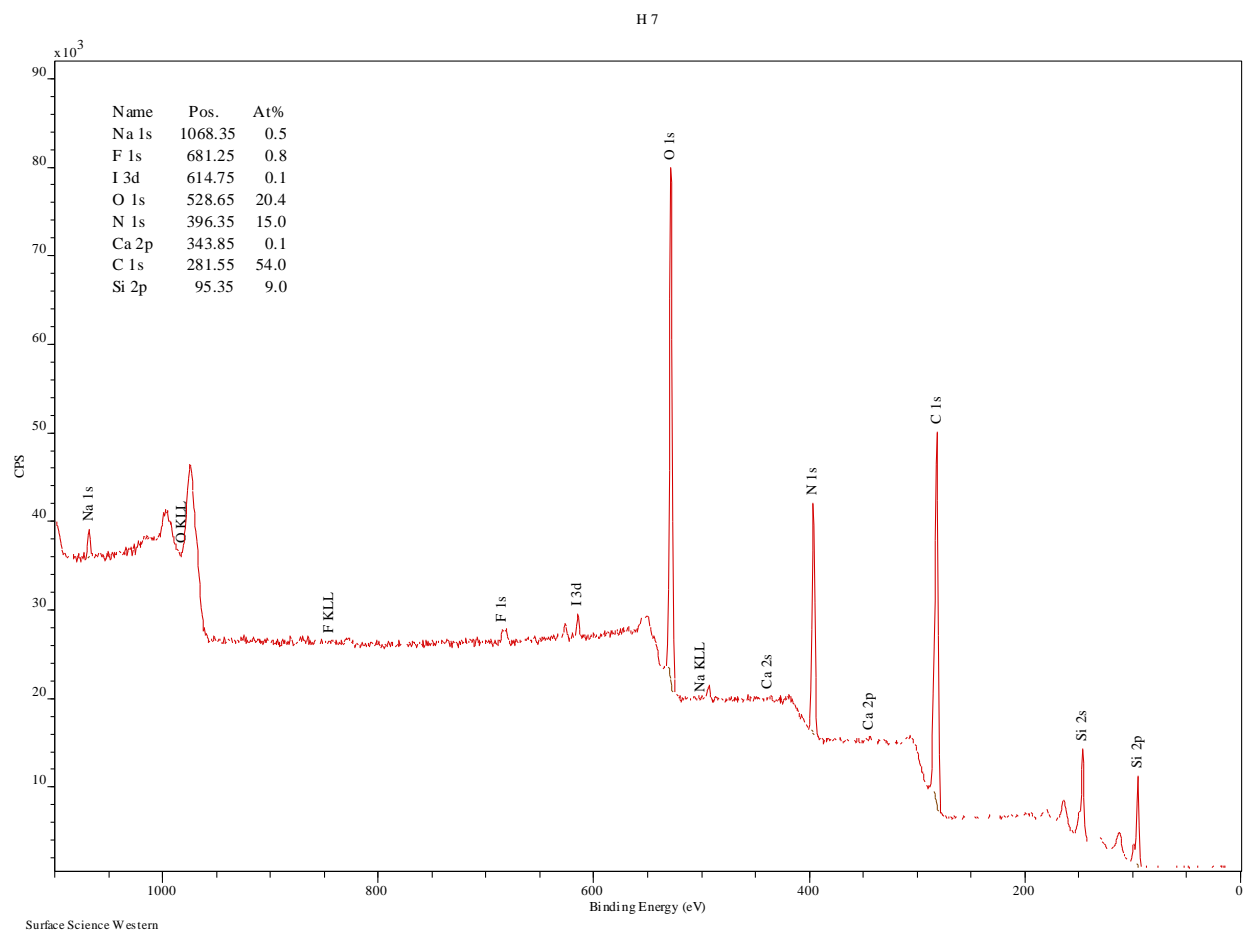


Figure 54 plots a full X-ray photoelectron spectroscopy scan of an implantation as control

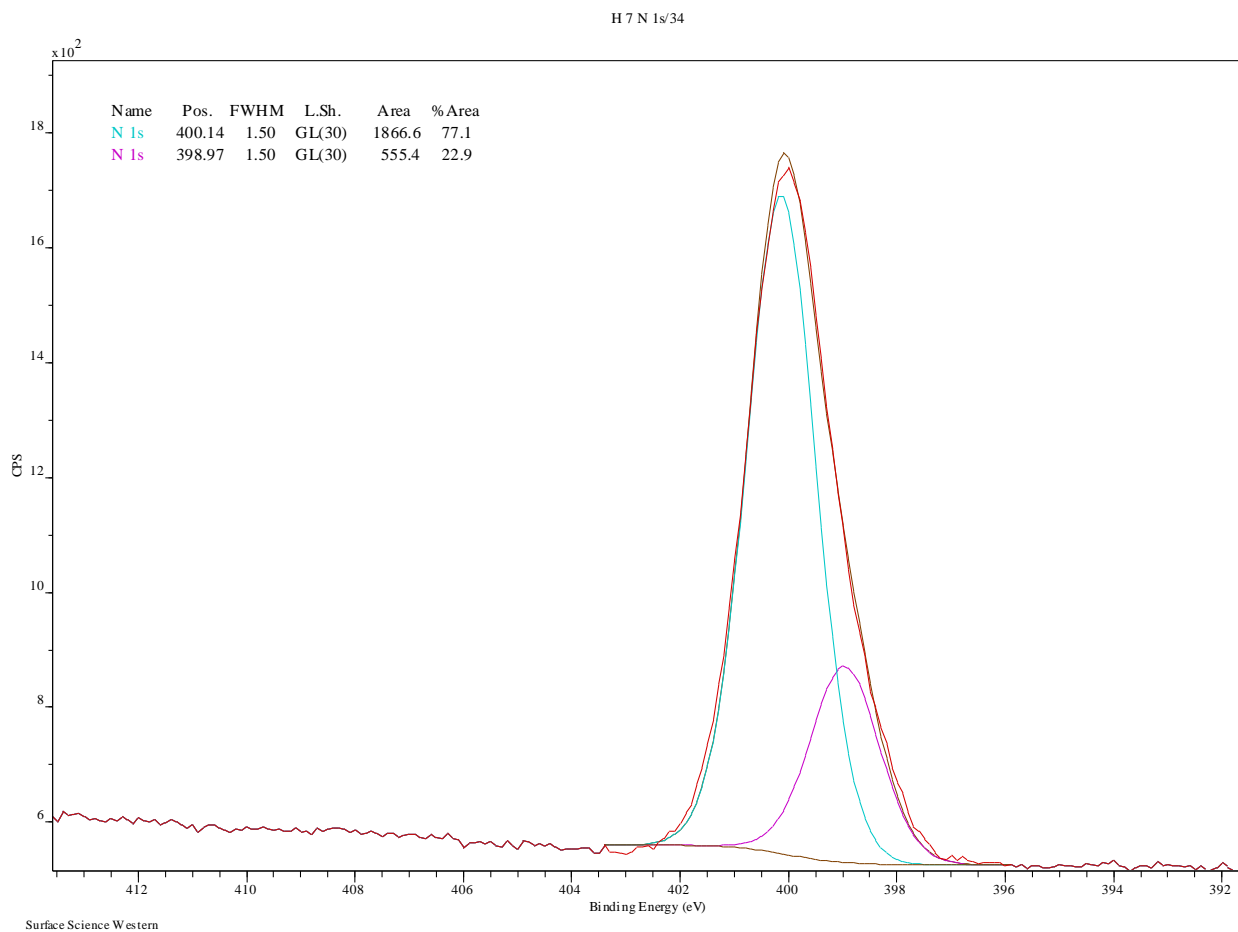


Figure 55 high resolution scan of nitrogen of an implantation as control

Curriculum Vitae

Summary:

Biomedical Engineer, Ph.D. in Biomaterial from Western University, Canada. I carry multidisciplinary educational background, with many years of experience in teaching and research. My expertise is developing curriculum, training university graduate students, and delivering knowledge to elderly students.

Education:

PhD in Biomedical engineering

University of western, Canada
2011 – 2017

Masters in Information Technology

Kent State University, USA.
(G.P.A.3.88/4.0) 2003 - 2005

Masters of Science in Physics

Mumbai University, India
1 997 - 1999

Bachelors of Science in Physics

Mumbai University, India
1993 – 1997

Patent:

Title: ION-IMPLANTATION OF PROTEIN BIOPOLYMER NANOFIBER SCAFFOLD
Inventors: Wankie Wan, Nisha Sharma and Jian Liu

Professional Work History:

Teaching Experience as graduate teaching assistant at university of western:

- Web-site designing: September 2011 – December 2011
- Engineering communication-2211: January 2012 – April 2012
- Programming fundamentals for engineers: September 2012 – December 2012
- Programming fundamentals for engineers: January 2013 – April 2013
- Engineering communication-2211: September 2013 – December,2013
- CBE 2224 Chemical Engineering Thermodynamics: January 2014 – April 2014
- Programming fundamentals for engineers: September 2014 – December 2014
- CBE 2224 Chemical Engineering Thermodynamics: January 2015 – April 2015
- CBE 4415 Chemical engineering project: September 2016 – April 2016

Instructor

Alpha Logic Career College,

London, *ON Canada* (July 2006-March 2009)

- Lead instructor for web-designing, designed the course work, and introduced new materials and tools (with software) for the new course work.
- Trained programming students to get certified with Microsoft Certification Solution Developer (MCSD)
- Taught Microsoft office suite.
- Taught courses for Grade 12

Help-Desk**TeleTech,**

London, ON Canada (Sep 2005–Aug 2006)

- Worked as **Supervisor** of the technical support (Level-3) personals that provide the software and hardware support for Verizon DSL Customers.

Technical Support & System Administrator**Curtis software Inc.**

Ohio, USA (Jan 2004–May 2005)

Technical Support Person (Level -3)**Helpdesk-Kent State University**

Ohio, USA (Aug 2002–Aug 2004)

Instructor**Kent State University (Upper ward Bond)**

Ohio, USA (May 2003–May 2004)

- ◆ Taught and tutored a 15-student classroom on Roller Coaster Physics.
- ◆ successfully displayed live project at Kent State University.
- ◆ Conducted exams, graded papers and coordinated research projects

Instructor**Kent State University (SBC Ameritech)**

Ohio, USA (Aug 2002–Aug 2003)

- ◆ Taught class of 30 students and provided individual coaching on:

- Microsoft Office PowerPoint, Paint Shop, and Photoshop programs.
- Website creation for presentations utilizing HTML.

Instructor

Chate Technical Institute

Mumbai, India (Jun 1999–Jun 2002)

- Taught Classes in Physics, Mathematics; Calculus I and II, Geometry, and Analytical

Calculus and Computer Science

Scholarships:

- **The CIHR Strategic Training Program in Vascular Research:**
The University of Western Ontario: Sep 2013 - Aug 2015
- **The Ontario Graduate Scholarship (OGS):**
The University of Western Ontario: Sep 2013 - Aug 2015
- **Natural Sciences and Engineering Research Council of Canada (NSERC)**
The University of Western Ontario: Sep 2011 - Aug 2013
- **Translational Breast Cancer Research Unit**
London Regional Cancer Program: Sep 2010 - Aug 2011
- **Schulich Graduate Scholarship**
The University of Western Ontario: Sep 2009 - Aug 2013
- **Research Scholar**
Kent State University: Jan 2004 - May 2005
- **Research Award**
University of Mumbai: Jun 1997 - May 1999
- **ISA-Event Holder**
Kent State University: Oct 2004 - Oct 2005
- **Sport Championship (Kabbadi)**
Mumbai, India: Jun 1994 - Jun 1999

- **Winner of Debate competition**
Mumbai, India: Jun 1991 - Jun 1992

Achievements:

- First Place, Winner of Platform Competition, at the Lawson Research Day
March 22, 2011
- Certificate for participating as a finalist of Platform presentation, at the Lawson Research Day March 23, 2010
- Student Committee of Biomedical Engineering:
Social representative position for three years (2012 – 2015) working on diverse exciting projects.

Proceedings Articles:

- **Sharma, N.**, Jian Liu, Boughner, D., & Wan, W. Comparison of different dosage of Ion implantation on electrospun collagen fibers to improve aqueous stability- **World Congress conference 2015**
June 2015
- **Sharma, N.**, Jian Liu, Boughner, D., & Wan, W. Effect of ion implantation on electrospun collagen fiber properties– **Canadian biomaterials conference 2015** May 2015
- **Sharma, N.**, Boughner, D., & Wan, W. Fabrication of nanofibre scaffold in a controlled environment for tissue engineering – **Proc ICNFA'13 (2013)**
- **Sharma, N.**, Kim, E., Belton, M., & J.J.L. Carson. Depth and extent of gold nanorod photothermal conversion in tissue-mimicking phantoms. **Proc SPIE 7750: 775007 (2010)**
- **Sharma, N.**, Chamson-Reig, A., Al-Aabed, H., & J.J.L. Carson. Depth and extent of gold nanorod photothermal conversion in tissue-like phantoms that contain hemoglobin. **Proc. SPIE 7754: 77541D (2010)**

Journal Papers:

- **Nisha Sharma**, Ying Li and Wankei Wan “Effect of humidity on electrospun polymer fibers” (Submitted)
- **Nisha Sharma** and Wankei Wan “Ion implantation on electrospun solid collagen fibers to improve aqueous stability” (*In correction*)

Conference Talks:

- **Sharma, N.**, Jian Liu, Boughner, D., & Wan, W. Comparison of different dosage of Ion implantation on electrospun collagen fibers to improve aqueous stability- **World Congress conference 2015**, June 2015
- **Sharma, N.**, Jian Liu, Boughner, D., & Wan, W. Effect of ion implantation on electrospun collagen fiber properties – **Canadian biomaterials conference 2015**, May 2015
- **Sharma, N.**, Boughner, D., & Wan, W. Fabrication of nanofibre scaffold in a controlled environment for tissue engineering – **ICNFA’13, University of Toronto, August 2013**
- **Sharma, N.**, Boughner, D., & Wan, W. Comparative Study of the Morphology of Natural and Synthetic Nano-Fiber Scaffolds by Controlling Ambient Parameters for Tissue Engineering – **CAMBR, University of western, November 2013**
- **Sharma, N.**, Jian L., Kenneth Kar Ho Wong & Wankei Wan “Ion beam modification of electrospun poly (vinyl alcohol) fibrillar scaffolds for cell compatibility”. **9th World Biomaterials Congress, China, June 2011**
- Makaremi, S., **Sharma, N.**, & W. Wan “Mechanical Characterization of Electrospun Polycaprolactone (PCL) Nanofibres using Atomic Force Microscopy” **NanoOntario 2011, McMaster University, Innovation Park, Hamilton, October 2011**
- **Sharma, N.**, Chamson-Reig, A., Al-Aabed, H., & J.J.L. Carson. “Depth and extent of gold nanorod photothermal conversion in tissue-like phantoms that contain hemoglobin.” **Lawson Research Day, London, March 2011**
- **Sharma, N.**, Kim, E., & J.J.L. Carson. “Depth and extent of gold nanorod photothermal conversion in tissue-mimicking phantoms”. **Lawson Research Day, London, March 2010**

- **Sharma, N.**, Kim, E., & J.J.L. Carson. "Depth and extent of gold nanorod photothermal conversion in tissue-mimicking phantoms". ***Photonics North 2010, Niagara Falls, June 2010***
- **Sharma, N.**, Kim, E., & J.J.L. Carson. "Depth and extent of gold nanorod photothermal conversion in tissue-like phantoms that contain hemoglobin." ***SPIE San Diego, August 2010***

Conference Poster Presentations:

- **Sharma, N.**, Jian Liu, Boughner, D & Wankei Wan. "Ion implantation to improve aqueous stability of electrospun collagen fibers". **London Research Day, London, April 2015.**
- **Sharma, N.**, Jian Liu, Boughner, D & Wankei Wan. "Ion beam implantation onto 3D rat tail collagen type 1 nano-fibrous scaffolds the first step towards the regulate the aqueous stability". **London Research Day, London, March 2014.**
- **Sharma, N.**, Boughner, D & Wankei Wan. "Comparative study on the morphology of nano-fiber scaffold by controlling ambient parameters for tissue engineering applications". **London Imaging Discovery Day 2013, London, June 2013.**
- **Sharma, N.**, Boughner, D & Wankei Wan. "Fabrication of nanofibre scaffold in a controlled environment for tissue engineering applications". **London Research Day, London, March 2013.**
- **Sharma, N.**, & WankeiWan. "Fabrication of Nanofibre Scaffold in a controlled environment for tissue engineering applications". **Canadian Materials Science Conference, UWO, June 2012.**
- **Sharma, N.**, & WankeiWan. "Fabrication of Nanofibre Scaffold in a controlled environment for tissue engineering applications". **London Research Day, London, March 2012.**
- **Sharma, N.**, Kenneth Kar HoWong & WankeiWan. "Cell compatibility of ion beam modified of electrospun poly (vinyl alcohol) fibrillar scaffolds". **NanoOntario 2011, McMaster University, Innovation Park, Hamilton, October 2011**

- **Sharma, N.**, Chamson-Reig, A., Al-Abed, H., & J.J.L. Carson. Depth and extent of gold nanorod photothermal conversion in tissue-like phantoms that contain haemoglobin. **9th ImNO Symposium Toronto**, January 2011.
- **Sharma, N.**, Kim, E., & J.J.L. Carson. "Depth and extent of gold nanorod photothermal conversion in tissue-mimicking phantoms". **Research & Education Day 2010, London**, June 2010
- **Sharma, N.**, Kim, E., & J.J.L. Carson. "Depth and extent of gold nanorod photothermal conversion in tissue-mimicking phantoms". **London Imaging Discovery Day, London**, June,2010
- **Sharma, N.**, Kim, E., & J.J.L. Carson. "Depth and extent of gold nanorod photothermal conversion in tissue-mimicking phantoms". **NanoOntario 2010, UWO, London**, May 2010.

- Kim, E., **Sharma, N.**, & J.J.L. Carson. Preparation of phantoms and gold nanorod spheres for exposure. **2010 Lawson Research Day, London**, March 2010.

- **Sharma, N.**, Kim, E., & J.J.L. Carson. "Depth and extent of gold nanorod photothermal conversion in tissue-mimicking phantoms". **ImNO 2010, Symposium, U of T, Toronto**, February 2010